

# Eigenvalues and Eigenfunctions of the Scalar Laplace Operator on Calabi-Yau Manifolds

Volker Braun<sup>1</sup>, Tamaz Brelidze<sup>1</sup>, Michael R. Douglas<sup>2</sup>, and  
Burt A. Ovrut<sup>1</sup>

<sup>1</sup> Department of Physics, University of Pennsylvania,  
209 S. 33rd Street, Philadelphia, PA 19104-6395, USA

<sup>2</sup> Rutgers University, Department of Physics and Astronomy,  
136 Frelinghuysen Rd., Piscataway, NJ 08854-8019, USA

## Abstract

A numerical algorithm for explicitly computing the spectrum of the Laplace-Beltrami operator on Calabi-Yau threefolds is presented. The requisite Ricci-flat metrics are calculated using a method introduced in previous papers. To illustrate our algorithm, the eigenvalues and eigenfunctions of the Laplacian are computed numerically on two different quintic hypersurfaces, some  $\mathbb{Z}_5 \times \mathbb{Z}_5$  quotients of quintics, and the Calabi-Yau threefold with  $\mathbb{Z}_3 \times \mathbb{Z}_3$  fundamental group of a heterotic standard model. The multiplicities of the eigenvalues are explained in detail in terms of the irreducible representations of the finite isometry groups of the threefolds.

# Contents

<b>1</b>	<b>Introduction</b>	<b>2</b>
<b>2</b>	<b>Solving the Laplace Equation</b>	<b>4</b>
<b>3</b>	<b>The Spectrum of <math>\Delta</math> on <math>\mathbb{P}^3</math></b>	<b>7</b>
3.1	Analytic Results . . . . .	7
3.2	Numerical Results . . . . .	11
3.3	Asymptotic Behaviour . . . . .	15
<b>4</b>	<b>Quintic Calabi-Yau Threefolds</b>	<b>15</b>
4.1	Non-Symmetric Quintic . . . . .	18
4.2	Fermat Quintic . . . . .	22
4.3	Symmetry Considerations . . . . .	29
4.4	Donaldson's Method . . . . .	30
<b>5</b>	<b><math>\mathbb{Z}_5 \times \mathbb{Z}_5</math> Quotients of Quintics</b>	<b>35</b>
5.1	$\mathbb{Z}_5 \times \mathbb{Z}_5$ Symmetric Quintics and their Metrics . . . . .	35
5.2	The Laplacian on the Quotient . . . . .	38
5.3	Quotient of the Fermat Quintic . . . . .	40
5.4	Group Theory and the Quotient Eigenmodes . . . . .	42
5.5	Varying the Complex Structure . . . . .	44
5.6	Branching Rules . . . . .	46
5.7	Another Family . . . . .	48
<b>6</b>	<b>A Heterotic Standard Model Manifold</b>	<b>49</b>
6.1	The Spectrum of the Laplacian on $X$ . . . . .	51
<b>7</b>	<b>The Sound of Space-Time</b>	<b>54</b>
7.1	Kaluza-Klein Modes of the Graviton . . . . .	54
7.2	Spectral Gap . . . . .	57
<b>A</b>	<b>Spectrum of the Laplacian on Projective Space</b>	<b>58</b>
<b>B</b>	<b>Semidirect Products</b>	<b>59</b>
<b>C</b>	<b>Notes on Donaldson's Algorithm on Quotients</b>	<b>60</b>
	<b>Bibliography</b>	<b>62</b>

# 1 Introduction

A central problem of string theory is to find compactifications whose low-energy effective action reproduces the standard model of elementary particle physics. One of the most promising candidates for this task is the compactification of heterotic string theory on a Calabi-Yau manifold [1]. In particular, the so-called “non-standard embedding” of  $E_8 \times E_8$  heterotic strings has been a very fruitful approach to string phenomenology [2, 3, 4, 5, 6, 7, 8].

For a number of reasons, the most successful models of this type to date are based on non-simply connected Calabi-Yau threefolds. These manifolds admit discrete Wilson lines which, together with a non-flat vector bundle, play an important role in breaking the heterotic  $E_8$  gauge theory down to the standard model [9, 10, 11, 12, 13, 14, 15, 16]. In addition, they project out many unwanted fields which would otherwise give rise to exotic matter representations and/or additional replicas of standard model fields. In particular, one can use this mechanism to solve the doublet-triplet splitting problem [17, 18]. Finally, the non-simply connected threefolds have many fewer moduli as compared to their simply connected covering spaces [19]. In recent work [20, 21, 22, 23], three generation models with a variety of desirable features were introduced. These are based on a certain quotients of a Schoen Calabi-Yau threefold, yielding a non-simply connected Calabi-Yau manifold.

The ultimate goal is to compute all of the observable quantities of particle physics, in particular gauge and Yukawa couplings, from the microscopic physics of string theory [24, 25, 26, 27]. There are many issues which must be addressed to achieve this goal. Physical Yukawa couplings, for example, depend on both coefficients in the superpotential and the explicit form of the Kähler potential. In a very limited number of specific geometries [24, 28, 29, 30], the former can be computed using sophisticated methods of algebraic geometry, topological string theory and the like. For the latter, one is usually limited to the qualitative statement that a coefficient is “expected to be of order one”. Improving our computational abilities and extending these calculations to non-standard embedding has been an outstanding problem [1].

Recently [31, 32], a plan has been outlined to analyze these problems numerically, at least in the classical limit. The essential point is that, today, there are good enough algorithms and fast enough computers to calculate Ricci-flat metrics and to solve the hermitian Yang-Mills equation for the gauge connection directly. Given this data, one can then find the correctly normalized zero modes of fields, determine the coefficients in the superpotential and compute the explicit form of the Kähler potential. Some progress in this direction was made in [31, 32, 33, 34, 35] and also [36, 37, 38]. Making effective use of symmetries [39, 40], one can significantly improve the computational procedure to find Calabi-Yau metrics and further extend it to non-simply connected manifolds. In this work, we take one step further in the numerical approach to string theory compactification and present an explicit algorithm to numerically solve for the eigenvalues and eigenfunctions of the scalar Laplace operator. We use as one of the

inputs the Calabi-Yau metrics computed using the techniques developed in [40].

We start, in Section 3, by discussing the general idea of the method and list the key steps of our algorithm. This algorithm is then applied to the simplest compact threefold, the projective space  $\mathbb{P}^3$ . This threefold is, of course, not a Calabi-Yau manifold. However, it has the advantage of being one of the few manifolds where the Laplace equation can be solved analytically. We compare the numerical results of this computation with the analytical solution in order to verify that our implementation is correct and to understand the sources of numerical errors. We note that the multiplicities of the approximate eigenvalues are determined by the dimensions of corresponding irreducible representations of the symmetry group of the projective space, as expected from the analytical solution. We conclude the section by investigating the asymptotic behavior of the numerical solution and comparing it with Weyl's formula.

Having gone through this illustrative example, we apply our numerical procedure to Calabi-Yau quintic threefolds in Section 4. The eigenvalues and eigenfunctions are explicitly computed for both a quintic at a random point in moduli space as well as for the Fermat quintic. We can again explain the multiplicities of eigenvalues on the Fermat quintic as arising from its enhanced symmetry; here, however, being a finite isometry group. The asymptotics of the numerical solution is verified using Weyl's formula. Note that the eigenvalues and eigenfunctions are not known analytically in the Calabi-Yau case, so our numerical algorithm is essential for their calculation. Recently, Donaldson has proposed a different algorithm to solve for the spectrum<sup>1</sup> of the scalar Laplacian. At the end of the section, we use it to numerically compute the eigenvalues and eigenfunctions on a random quintic and on the Fermat quintic and compare these to our results. In Section 5, we consider non-simply connected Calabi-Yau manifolds, namely  $\mathbb{Z}_5 \times \mathbb{Z}_5$  quotients of certain quintic threefolds. The eigenvalues and eigenfunctions of the Laplacian are numerically computed using our algorithm, exploiting the Hironaka decomposition discussed in our previous paper [40]. In this case, the multiplicities of the eigenvalues are determined by finite "pseudo-symmetries" [41]. We work out the necessary representation theory and again find perfect agreement with the multiplicities predicted by our numerical computation of the eigenvalues. We conclude this section by studying the moduli dependence of the eigenvalues for a one-parameter families of quintic quotients.

In Section 6, we apply this machinery to the case of a certain  $\mathbb{Z}_3 \times \mathbb{Z}_3$  quotient of a Schoen threefold [42, 43]. This is the Calabi-Yau threefold underlying the heterotic standard model constructed in [21, 22, 23]. The essential new feature is the existence of non-trivial Kähler moduli, not just the overall volume of the threefold as in all previous sections. As an explicit example, we numerically compute the eigenvalues of the Laplacian at two different points in the Kähler moduli space, corresponding to distinct "angular" directions in the Kähler cone. The group representation theory associated with the covering space and the quotient is discussed.

---

<sup>1</sup>The spectrum of an operator is the set of eigenvalues.

We conclude in Section 7 by considering some physical applications of the eigenvalues of the scalar Laplacian on a Calabi-Yau threefold. In particular, we consider string compactifications on these backgrounds and study the effect of the massive Kaluza-Klein modes on the static gravitational potential in four-dimensions. We compute this potential in the case of the Fermat quintic, and explicitly show how the potential changes as the radial distance approaches, and passes through, the compactification scale. We then give a geometrical interpretation to the eigenvalue of the first excited state in terms of the diameter of the Calabi-Yau manifold. Inverting this relationship allows us to calculate the “shape” of the Calabi-Yau threefold from the numerical knowledge of its first non-trivial eigenvalue.

Additional information is provided in three appendices. We explicitly determine the first massive eigenvalue for the Laplacian  $\mathbb{P}^3$  in Appendix A. Some technical aspects of semidirect products, which are useful in understanding Section 4, are discussed in Appendix B. Finally, in Appendix C, we explain a modification of Donaldson’s algorithm for the numerical computation of Calabi-Yau metrics on quotients, which is used Section 5.

## 2 Solving the Laplace Equation

Consider any  $d$ -dimensional, real manifold  $X$ . We will only be interested in closed manifolds; that is, compact and without boundary. Given a Riemannian metric<sup>2</sup>  $g_{\mu\nu}$  on  $X$ , the Laplace-Beltrami operator  $\Delta$  is defined as

$$\Delta = -\frac{1}{\sqrt{g}}\partial_{\mu}(g^{\mu\nu}\sqrt{g}\partial_{\nu}) = -\delta d = - * d * d, \quad (1)$$

where  $g = \det g_{\mu\nu}$ . Since this acts on functions,  $\Delta$  is also called the scalar Laplace operator. We will always consider the functions to be complex-valued. Since  $\Delta$  commutes with complex conjugation, the scalar Laplacian acting on real functions would essentially be the same.

An important question is to determine the corresponding eigenvalues  $\lambda$  and the eigenfunctions  $\phi$  defined by

$$\Delta\phi = \lambda\phi. \quad (2)$$

As is well-known, the Laplace operator is hermitian. Due to the last equality in eq. (1), all eigenvalues are real and non-negative. The goal of this paper is to find the eigenvalues and eigenfunctions of the scalar Laplace operator on specific manifolds  $X$  with metrics  $g_{\mu\nu}$ .

Since  $X$  is compact, the eigenvalues of the Laplace operator will be discrete. Let us specify the  $n$ -th eigenvalue by  $\lambda_n$ . Symmetries of the underlying manifold will, in general, cause  $\lambda_n$  to be degenerate; that is, to have multiple eigenfunctions. We denote

---

<sup>2</sup>We denote the real coordinate indices by  $\mu, \nu, \dots$

by  $\mu_n$  the multiplicity at level  $n$ . Each eigenvalue depends on the total volume of the manifold. To see this, consider a linear rescaling of distances; that is, let  $g_{\mu\nu} \mapsto \rho^2 g_{\mu\nu}$ . Clearly,

$$\text{Vol}(\rho^2 g_{\mu\nu}) = \rho^d \text{Vol}(g_{\mu\nu}), \quad \lambda_n(\rho^2 g_{\mu\nu}) = \rho^{-2} \lambda_n(g_{\mu\nu}). \quad (3)$$

Therefore, each eigenvalue scales as

$$\lambda_n \sim \text{Vol}^{-\frac{2}{d}}. \quad (4)$$

In the following, we will always normalize the volume to unity when computing eigenvalues.

Now consider the linear space of complex-valued functions on  $X$  and define an inner product by

$$\langle e|f \rangle = \int_X \bar{e} f \sqrt{g} \, d^d x, \quad e, f \in C^\infty(X, \mathbb{C}). \quad (5)$$

Let  $\{f_a\}$  be an arbitrary basis of the space of complex functions. For reasons to become clear later on, we will primarily be working with bases that are not orthonormal with respect to the inner product eq. (5). Be that as it may, for any complex function  $e$  one can always find a function  $\tilde{e}$  so that

$$e = \sum_a f_a \langle f_a|\tilde{e} \rangle. \quad (6)$$

Given the basis of functions  $\{f_a\}$ , the matrix elements  $\Delta_{ab}$  of the Laplace operator are

$$\begin{aligned} \Delta_{ab} &= \langle f_a|\Delta|f_b \rangle = \int_X \bar{f}_a \Delta f_b \sqrt{g} \, d^d x = - \int_X \bar{f}_a \, d^* df_b = \int_X \langle df_a|df_b \rangle \\ &= \int_X g^{\mu\nu} (\partial_\mu \bar{f}_a) (\partial_\nu f_b) \sqrt{g} \, d^d x. \end{aligned} \quad (7)$$

Thus far, we have considered arbitrary  $d$ -dimensional, real manifolds  $X$  and any Riemannian metric  $g_{\mu\nu}$ . Henceforth, however, we restrict our attention to even dimensional manifolds that admit a complex structure preserved by the metric. That is, we will assume that  $X$  is a  $D = \frac{d}{2}$ -dimensional complex manifold with an hermitian<sup>3</sup> metric<sup>4</sup>  $g_{i\bar{j}}$  defined by

$$g_{\mu\nu} \, dx^\mu \otimes dx^\nu = \frac{1}{2} g_{i\bar{j}} (dz^i \otimes dz^{\bar{j}} + dz^{\bar{j}} \otimes dz^i). \quad (8)$$

With  $X$  so restricted, it follows that

$$g^{\mu\nu} \partial_\mu \bar{f}_a \partial_\nu f_b = 2g^{\bar{i}j} (\bar{\partial}_{\bar{i}} \bar{f}_a \partial_j f_b + \partial_j \bar{f}_a \bar{\partial}_{\bar{i}} f_b) \quad (9)$$

---

<sup>3</sup>In particular, Kähler metrics are hermitian.

<sup>4</sup>We denote the holomorphic and anti-holomorphic indices by  $i, \bar{i}, j, \bar{j}, \dots$

and, hence,

$$\Delta_{ab} = 2 \int_X g^{\bar{i}j} \left( \bar{\partial}_{\bar{i}} \bar{f}_a \partial_j f_b + \partial_j \bar{f}_a \bar{\partial}_{\bar{i}} f_b \right) \det(g) \left( \frac{i}{2} \right)^D \prod_{r=1}^D dz^r \wedge d\bar{z}^{\bar{r}}. \quad (10)$$

Using this and eq. (6) for each eigenfunction  $\phi_{n,i}$ , eq. (2) becomes

$$\sum_b \langle f_a | \Delta | f_b \rangle \langle f_b | \tilde{\phi}_{n,i} \rangle = \sum_b \lambda_n \langle f_a | f_b \rangle \langle f_b | \tilde{\phi}_{n,i} \rangle, \quad i = 1, \dots, \mu_n. \quad (11)$$

Thus, in the basis  $\{f_a\}$ , solving the Laplace eigenvalue equation is equivalent to the generalized eigenvalue problem for the infinite dimensional matrix  $\Delta_{ab}$ , where the matrix  $\langle f_a | f_b \rangle$  indicates the “non-orthogonality” of our basis with respect to inner product eq. (5).

In general, very little known about the exact eigenvalues and eigenfunctions of the scalar Laplace operator on a closed Riemannian manifold  $X$ , including those that are complex manifolds with hermitian metrics. The universal exception are the zero modes, where the multiplicity has a cohomological interpretation. Specifically, the solutions to  $\Delta\phi = 0$  are precisely the locally constant functions and, hence, the multiplicity of the zero eigenvalue is

$$\mu_0(X) = h^0(X, \mathbb{C}) = |\pi_0(X)|, \quad (12)$$

the number of connected components of  $X$ . Furthermore, on symmetric spaces  $G/H$  one can completely determine the spectrum of the Laplace operator in terms of the representation theory of the Lie groups  $G$  and  $H$ . Indeed, in the next section we will discuss one such example in detail. However, in general, and certainly for proper Calabi-Yau threefolds, exact solutions of  $\Delta\phi = \lambda\phi$  are unknown and one must employ numerical methods to determine the eigenvalues and eigenfunctions. The purpose of this paper is to present such a numerical method, and to use it to determine the spectrum of  $\Delta$  on physically relevant complex manifolds. Loosely speaking, the algorithm is as follows.

First, we specify the complex manifold  $X$  of interest as well as an explicit hermitian metric. For Kähler manifolds, the Fubini-Study metric can always be constructed. However, this metric is never Ricci-flat. To calculate the Ricci-flat Calabi-Yau metric, one can use the algorithm presented in [31, 33] and extended in [40]. This allows a numerical computation of the Calabi-Yau metric to any desired accuracy. Giving the explicit metric completely determines the Laplace operator  $\Delta$ . Having done that, we specify a countably infinite set  $\{f_a\}$  that spans the space of complex functions. One can now calculate any matrix element  $\Delta_{ab} = \langle f_a | \Delta | f_b \rangle$  and coefficient  $\langle f_a | f_b \rangle$  using the scalar product specified in eq. (5) and evaluated using numerical integration over  $X$ . As mentioned above, the most convenient basis of functions  $\{f_a\}$  will not be orthonormal. Clearly, calculating the infinite dimensional matrices  $\Delta_{ab}$  and  $\langle f_a | f_b \rangle$ ,

let alone solving for the infinite number of eigenvalues and eigenfunctions, is not possible. Instead, we greatly simplify the problem by choosing a finite subset of slowly-varying functions as an approximate basis. For simplicity of notation, let us take  $\{f_a|a = 1, \dots, k\}$  to be our approximating basis. The  $k \times k$  matrices  $(\Delta_{ab})_{1 \leq a, b \leq k}$  and  $\langle f_a | f_b \rangle_{1 \leq a, b \leq k}$  are then finite dimensional and one can numerically solve eq. (11) for the approximate eigenvalues and eigenfunctions. It is important to note that this procedure generically violates any underlying symmetries of the manifold and, hence, each eigenvalue will be non-degenerate. Finally, we successively improve the accuracy of the approximation in two ways: 1) for fixed  $k$  the numerical integration of the matrix elements is improved by summing over more points and 2) we increase the dimension  $k$  of the truncated space of functions. In the limit where both the numerical integration becomes exact and where  $k \rightarrow \infty$ , the approximate eigenvalues  $\lambda_n$  and eigenfunctions  $\phi_n$  converge to the exact eigenvalues  $\hat{\lambda}_m$  and eigenfunctions  $\phi_{m,i}$  with multiplicity  $\mu_m$ . Inspired by our work on Calabi-Yau threefolds, this algorithm to compute the spectrum of the Laplacian was recently applied to elliptic curves in [44].

### 3 The Spectrum of $\Delta$ on $\mathbb{P}^3$

In this section, we use our numerical method to compute the eigenvalues and eigenfunctions of  $\Delta$  on the complex projective threefold

$$\mathbb{P}^3 = S^7/U(1) = SU(4)/S(U(3) \times U(1)) \quad (13)$$

with a Kähler metric proportional to the Fubini-Study metric, rescaled so that the total volume is unity. As mentioned above, since this is a symmetric space of the form  $G/H$ , the equation  $\Delta\phi = \lambda\phi$  can be solved analytically. The results were presented in [45]. Therefore, although  $\mathbb{P}^3$  is not a phenomenologically realistic string vacuum, it is an instructive first example since we can check our numerical algorithm against the exact eigenvalues and eigenfunctions. Note that, in this case, the metric is known analytically and does not need to be determined numerically.

#### 3.1 Analytic Results

Let us begin by reviewing the known analytic results [45]. First, recall the Fubini-Study metric is given by  $g_{i\bar{j}}^{\text{FS}} = \partial_i \bar{\partial}_{\bar{j}} K_{\text{FS}}$  with

$$K_{\text{FS}}(z, \bar{z}) = \frac{1}{\pi} \ln \left( |z_0|^2 + |z_1|^2 + |z_2|^2 + |z_3|^2 \right). \quad (14)$$

With respect to this metric the volume of  $\mathbb{P}^3$  is

$$\text{Vol}_{\text{FS}}(\mathbb{P}^3) = \int_{\mathbb{P}^3} \det(g_{i\bar{j}}) d^6x = \int_{\mathbb{P}^3} \frac{\omega_{\text{FS}}^3}{3!} = \frac{1}{6}, \quad (15)$$



where  $\omega_{\text{FS}}$  is the associated Kähler (1, 1)-form. However, as discussed above, we find it convenient to choose the metric so as to give  $\mathbb{P}^3$  unit volume. It follows from eq. (14) and (15) that one must rescale the Kähler potential to be

$$K(z, \bar{z}) = \sqrt[3]{6} K_{\text{FS}}(z, \bar{z}) = \frac{\sqrt[3]{6}}{\pi} \ln \left( |z_0|^2 + |z_1|^2 + |z_2|^2 + |z_3|^2 \right). \quad (16)$$

Then

$$\text{Vol}_K(\mathbb{P}^3) = 1, \quad (17)$$

as desired.

The complete set of eigenvalues of  $\Delta$  on  $\mathbb{P}^3$  were found to be [45]

$$\hat{\lambda}_m = \frac{4\pi}{\sqrt[3]{6}} m(m+3), \quad m = 0, 1, 2, \dots, \quad (18)$$

where we determine the numerical coefficient, corresponding to our volume normalization, in Appendix A. Furthermore, it was shown in [45] that the multiplicity of the  $m$ -th eigenvalue is

$$\mu_m = \binom{m+3}{m}^2 - \binom{m+2}{m-1}^2 = \frac{1}{12} (m+1)^2 (m+2)^2 (2m+3). \quad (19)$$

This result for the multiplicity has a straightforward interpretation. As is evident from the description of  $\mathbb{P}^3$  in eq. (13), one can define an  $SU(4)$  action on our projective space. Thus the eigenstates of the Laplace operator eq. (2) carry representations of  $SU(4)$ . In general, any representation of  $SU(4)$  is characterized by a three dimensional weight lattice. In particular, for each irreducible representation there exists a highest weight

$$w = m_1 w_1 + m_2 w_2 + m_3 w_3, \quad (20)$$

where  $w_1, w_2,$  and  $w_3$  are the fundamental weights and  $m_1, m_2, m_3 \in \mathbb{Z}_{\geq 0}$ . Starting with the highest weight, one can generate all the states of the irreducible representation. It turns out that multiplicity eq. (19) is precisely the dimension of the irreducible representation of  $SU(4)$  generated by the highest weight  $m(w_1 + w_3) = (m, 0, m)$ . Hence, the eigenspace associated with the  $m$ -th eigenvalue  $\hat{\lambda}_m$  carries the irreducible representation  $(m, 0, m)$  of  $SU(4)$  for each non-negative integer  $m$ . For convenience, we list the low-lying eigenvalues and their corresponding multiplicities in Table 1.

The eigenfunctions of  $\Delta$  on  $\mathbb{P}^3 = S^7/U(1)$  are the  $U(1)$ -invariant spherical harmonics on  $S^7$ . In terms of homogeneous coordinates  $[z_0 : z_1 : z_2 : z_3]$  on  $\mathbb{P}^3$ , the eigenfunctions can be realized as finite linear combinations of functions of the form<sup>5</sup>

$$\frac{\left( \text{degree } k_\phi \text{ monomial} \right) \overline{\left( \text{degree } k_\phi \text{ monomial} \right)}}{\left( |z_0|^2 + |z_1|^2 + |z_2|^2 + |z_3|^2 \right)^{k_\phi}}. \quad (21)$$

---

<sup>5</sup>We label the degree of the monomials here by  $k_\phi$  to distinguish it from the degree  $k_h$  of polynomials in Donaldson's algorithm.

$m$	$\mu_m$	$\hat{\lambda}_m$
0	1	0
1	15	$\frac{16\pi}{\sqrt[3]{6}} \simeq 27.662$
2	84	$\frac{40\pi}{\sqrt[3]{6}} \simeq 69.155$
3	300	$\frac{72\pi}{\sqrt[3]{6}} \simeq 124.48$
4	825	$\frac{112\pi}{\sqrt[3]{6}} \simeq 193.64$
5	1911	$\frac{160\pi}{\sqrt[3]{6}} \simeq 276.62$
6	3920	$\frac{216\pi}{\sqrt[3]{6}} \simeq 373.44$
7	7344	$\frac{280\pi}{\sqrt[3]{6}} \simeq 484.09$

**Table 1:** Eigenvalues of  $\Delta$  on  $\mathbb{P}^3$ . Each eigenvalue is listed with its multiplicity.

One can show this as follows. Let  $\underline{\mathbf{4}}$  and  $\overline{\underline{\mathbf{4}}}$  be the fundamental representations of  $SU(4)$ . Algebraically, one can show that

$$\text{Sym}^{k_\phi} \underline{\mathbf{4}} \otimes \text{Sym}^{k_\phi} \overline{\underline{\mathbf{4}}} = \bigoplus_{m=0}^{k_\phi} (m, 0, m), \quad (22)$$

where  $(m, 0, m)$  are the irreducible representations of  $SU(4)$  defined above. Now note that  $\mathbb{C}[\vec{z}]_{k_\phi}$ , the complex linear space of degree- $k_\phi$  homogeneous polynomials in  $z_0, z_1, z_2, z_3$ , naturally carries the  $\text{Sym}^{k_\phi} \underline{\mathbf{4}}$  reducible representation of  $SU(4)$ . Similarly,  $\mathbb{C}[\vec{\bar{z}}]_{k_\phi}$  carries the  $\text{Sym}^{k_\phi} \overline{\underline{\mathbf{4}}}$  representation. Defining

$$\mathcal{F}_{k_\phi} = \frac{\mathbb{C}[z_0, z_1, z_2, z_3]_{k_\phi} \otimes \mathbb{C}[\bar{z}_0, \bar{z}_1, \bar{z}_2, \bar{z}_3]_{k_\phi}}{\left(\sum_{j=0}^3 |z_j|^2\right)^{k_\phi}} \quad (23)$$

to be the space of functions spanned by the degree  $k_\phi$  monomials, then it follows from eq. (22) that one must have the decomposition

$$\mathcal{F}_{k_\phi} = \bigoplus_{m=0}^{k_\phi} \text{span} \{ \phi_{m,1}, \dots, \phi_{m,\mu_m} \}, \quad (24)$$

where  $\mu_m = \dim(m, 0, m)$ . Note the importance of the  $SU(4)$ -invariant denominator, which ensures that the whole fraction is of homogeneous degree zero, that is, a function on  $\mathbb{P}^3$ .

To illustrate this decomposition, first consider the trivial case where  $k_\phi = 0$ . Noting that  $\mu_0 = 1$ , eq. (24) yields

$$\phi_{0,1} = 1, \quad (25)$$

corresponding to the trivial representation  $\mathbf{1}$  of  $SU(4)$  and the lowest eigenvalue  $\lambda_0 = 0$ . Now, let  $k_\phi = 1$ . In this case  $\mu_0 = 1$  and  $\mu_1 = 15$ . It follows from eq. (24) that there must exist a basis of  $\mathcal{F}_1$  composed of the eigenfunctions of  $\Delta$  in the  $\mathbf{1}$  and  $\mathbf{15}$  irreducible representations of  $SU(4)$  respectively. This is indeed the case. We find that one such basis choice is

$$\phi_{0,1} = \frac{|z_0|^2 + |z_1|^2 + |z_2|^2 + |z_3|^2}{\sum_{j=0}^3 |z_j|^2} = 1, \quad (26)$$

corresponding to the lowest eigenvalue  $\lambda_0 = 0$ , and

$$\begin{aligned} \phi_{1,1} &= z_0 \bar{z}_1 / \sum_{j=0}^3 |z_j|^2 & \phi_{1,2} &= z_1 \bar{z}_0 / \sum_{j=0}^3 |z_j|^2 \\ \phi_{1,3} &= z_0 \bar{z}_2 / \sum_{j=0}^3 |z_j|^2 & \phi_{1,4} &= z_2 \bar{z}_0 / \sum_{j=0}^3 |z_j|^2 \\ \phi_{1,5} &= z_0 \bar{z}_3 / \sum_{j=0}^3 |z_j|^2 & \phi_{1,6} &= z_3 \bar{z}_0 / \sum_{j=0}^3 |z_j|^2 \\ \phi_{1,7} &= z_1 \bar{z}_2 / \sum_{j=0}^3 |z_j|^2 & \phi_{1,8} &= z_2 \bar{z}_1 / \sum_{j=0}^3 |z_j|^2 \\ \phi_{1,9} &= z_1 \bar{z}_3 / \sum_{j=0}^3 |z_j|^2 & \phi_{1,10} &= z_3 \bar{z}_1 / \sum_{j=0}^3 |z_j|^2 \\ \phi_{1,11} &= z_2 \bar{z}_3 / \sum_{j=0}^3 |z_j|^2 & \phi_{1,12} &= z_3 \bar{z}_2 / \sum_{j=0}^3 |z_j|^2 \\ \phi_{1,13} &= (z_1 \bar{z}_1 - z_0 \bar{z}_0) / \sum_{j=0}^3 |z_j|^2 \\ \phi_{1,14} &= (z_2 \bar{z}_2 - z_0 \bar{z}_0) / \sum_{j=0}^3 |z_j|^2 \\ \phi_{1,15} &= (z_3 \bar{z}_3 - z_0 \bar{z}_0) / \sum_{j=0}^3 |z_j|^2, \end{aligned} \quad (27)$$

corresponding to the first non-trivial eigenvalue  $\lambda_1 = \frac{16\pi}{\sqrt[3]{6}}$ . Note that we recover the constant eigenfunction for  $k_\phi = 0$  through the cancellation of the numerator in eq. (26). This pattern, where one recovers all the lower eigenmodes through the factorization of the numerator in each representation by an appropriate power of  $\sum_{j=0}^3 |z_j|^2$ , continues for arbitrary  $k_\phi$ . In other words, there is a sequence of inclusions

$$\{1\} = \mathcal{F}_0 \subset \mathcal{F}_1 \subset \mathcal{F}_2 \subset \dots \subset C^\infty(\mathbb{P}^3, \mathbb{C}). \quad (28)$$

Note that

$$\dim \mathcal{F}_{k_\phi} = \binom{k_\phi + 3}{k_\phi}^2, \quad (29)$$

which, together with eq. (22), explains the multiplicities given in eq. (19).

Although a basis of  $\mathcal{F}_{k_\phi}$  composed of eigenfunctions of  $\Delta$  would be the most natural, there is no need to go through the exercise of decomposing the space into  $SU(4)$ -

irreducible representations. For numerical calculations, it is simpler to use the equivalent basis

$$\begin{aligned} \mathcal{F}_{k_\phi} &= \text{span} \{ f_a \mid a = 0, \dots, \dim \mathcal{F}_{k_\phi} - 1 \} \\ &= \text{span} \left\{ \left( \text{degree } k_\phi \text{ monomial} \right) \overline{\left( \text{degree } k_\phi \text{ monomial} \right)} \Big/ \left( \sum_{j=0}^3 |z_j|^2 \right)^{k_\phi} \right\} \end{aligned} \quad (30)$$

for any finite value of  $k_\phi$ , even though these functions are generically not themselves eigenfunctions of  $\Delta$ . In the limit where  $k_\phi \rightarrow \infty$ , the basis eq. (30) spans the complete space of eigenfunctions.

## 3.2 Numerical Results

Following the algorithm presented at the end of the Section 2, we now numerically solve the eigenvalue problem for the scalar Laplace operator  $\Delta$  on  $\mathbb{P}^3$ . Unlike more phenomenologically interesting Calabi-Yau threefolds, where one must numerically compute the Kähler metric using Donaldson's method [31, 33, 40], on  $\mathbb{P}^3$  the Kähler potential is given by eq. (16) and, hence, the metric and  $\Delta$  are known explicitly. This eliminates the need for the first few steps of our algorithm, greatly simplifying the calculations in this section. Furthermore, the  $SU(4)$  action on the eigenfunctions allows us to identify a complete basis for the space of complex functions in terms of monomials of the form eq. (21). Since we know the exact eigenvalues and eigenfunctions on  $\mathbb{P}^3$ , this is an excellent venue for checking the numerical accuracy of the remaining steps in our algorithm as well as the correctness of our implementation.

Given the metric,  $\Delta$  and the complete basis of functions, the next step in our algorithm is to specify an approximating basis for the linear space of complex functions. This is easily accomplished by restricting to

$$\mathcal{F}_{k_\phi} = \text{span} \left\{ f_a \mid a = 0, \dots, \binom{k_\phi+3}{k_\phi} - 1 \right\}, \quad (31)$$

see eq. (30), for any finite value of  $k_\phi$ . Next, we need to specify the volume measure in the integrals required to evaluate the matrix elements  $\langle f_a | \Delta | f_b \rangle$  and  $\langle f_a | f_b \rangle$ . Each matrix element requires one integral over  $\mathbb{P}^3$ , as in eq. (7). The volume form is completely determined by the metric to be

$$d\text{Vol}_K = \frac{1}{3!} \omega^3, \quad (32)$$

where  $\omega$  is the Kähler (1,1)-form given by the Kähler potential eq. (16). Although  $\mathbb{P}^3$  is simple enough to employ more elaborate techniques of integration, we will use the same numerical integration algorithm as with Calabi-Yau threefolds later on. That is, we approximate the integral by summing over  $n_\phi$  random points,

$$\frac{1}{n_\phi} \sum_{i=1}^{n_\phi} f(p_i) \longrightarrow \int f d\text{Vol}, \quad (33)$$

where  $f$  is an arbitrary function on  $\mathbb{P}^3$ . The integration measure  $d\text{Vol}$  in eq. (33) is determined by the distribution of points. In other words, the random distribution of points must be chosen carefully in order to approximate the integral with our desired volume form  $d\text{Vol}_K$ . However, this can easily be done: simply pick the points in an  $SU(4)$ -uniform distribution. The corresponding integral measure is (up to overall scale) the unique  $SU(4)$ -invariant volume form, the Fubini-Study volume form. The normalization is fixed by our convention that  $\text{Vol}_K(\mathbb{P}^3) = 1$ .

The process of numerically evaluating integrals by summing over a finite number  $n_\phi$  of points has one straightforward consequence. As discussed above, in the analytic solution the  $m$ -th eigenvalue  $\hat{\lambda}_m$  is degenerate with multiplicity  $\mu_m$  given in eq. (19). The reason for the degeneracy is that the  $m$ -th eigenspace carries the  $(m, 0, m)$  highest weight representation of  $SU(4)$ . However, even though the  $n_\phi$  points have an  $SU(4)$ -uniform distribution, the simple fact that they are finite explicitly breaks the  $SU(4)$  symmetry. The consequence of this is that the degeneracy of each eigenvalue is completely broken. It follows that in the numerical calculation, instead of one eigenvalue  $\hat{\lambda}_m$  with multiplicity  $\mu_m$ , one will find  $\mu_m$  non-degenerate eigenvalues  $\lambda_n$ . Only in the limit that  $n_\phi \rightarrow \infty$  will these converge to a single degenerate eigenvalue as

$$\begin{aligned}
\lambda_0 &= \lambda_0, \dots, \lambda_{\mu_0-1} && \rightarrow \hat{\lambda}_0 = 0, \\
\lambda_1, \dots, \lambda_{15} &= \lambda_{\mu_0}, \dots, \lambda_{\mu_0+\mu_1-1} && \rightarrow \hat{\lambda}_1 = \frac{16\pi}{\sqrt[3]{6}}, \\
\lambda_{16}, \dots, \lambda_{99} &= \lambda_{\mu_0+\mu_1}, \dots, \lambda_{\mu_0+\mu_1+\mu_2-1} && \rightarrow \hat{\lambda}_2 = \frac{40\pi}{\sqrt[3]{6}}, \\
&&& \vdots
\end{aligned} \tag{34}$$

We are now ready to numerically compute the finite basis approximation to the Laplace operator  $\langle f_a | \Delta | f_b \rangle$  and the coefficient matrix  $\langle f_a | f_b \rangle$  for any fixed values of  $k_\phi$  and  $n_\phi$ . The coefficients do not form the unit matrix, indicating that the approximating basis eq. (30) of  $\mathcal{F}_{k_\phi}$  is not orthonormal. Even though one could orthonormalize the basis, this would be numerically unsound and it is easier to directly solve the generalized eigenvalue problem eq. (11). We implemented this algorithm in C++. In practice, the most time-consuming part is the evaluation of the numerical integrals for the matrix elements of the Laplace operator. We perform this step in parallel on a 10-node dual Opteron cluster, using MPI [46] for communication. Finally, we use LAPACK [47] to compute the eigenvalues and eigenvectors. Note that the matrix eigenvectors are the coefficients  $\langle f_a | \tilde{\phi} \rangle$  and, hence, the corresponding eigenfunction is

$$\phi = \sum_{a=0}^{\dim \mathcal{F}_{k_\phi} - 1} f_a \langle f_a | \tilde{\phi} \rangle. \tag{35}$$

We present our results in two ways. First fix  $k_\phi$ , thus restricting the total number of non-degenerate eigenvalues  $\lambda_n$  to  $\dim \mathcal{F}_{k_\phi}$ . These eigenvalues are then plotted against the number of points  $n_\phi$  that we use to evaluate an integral. For smaller values of

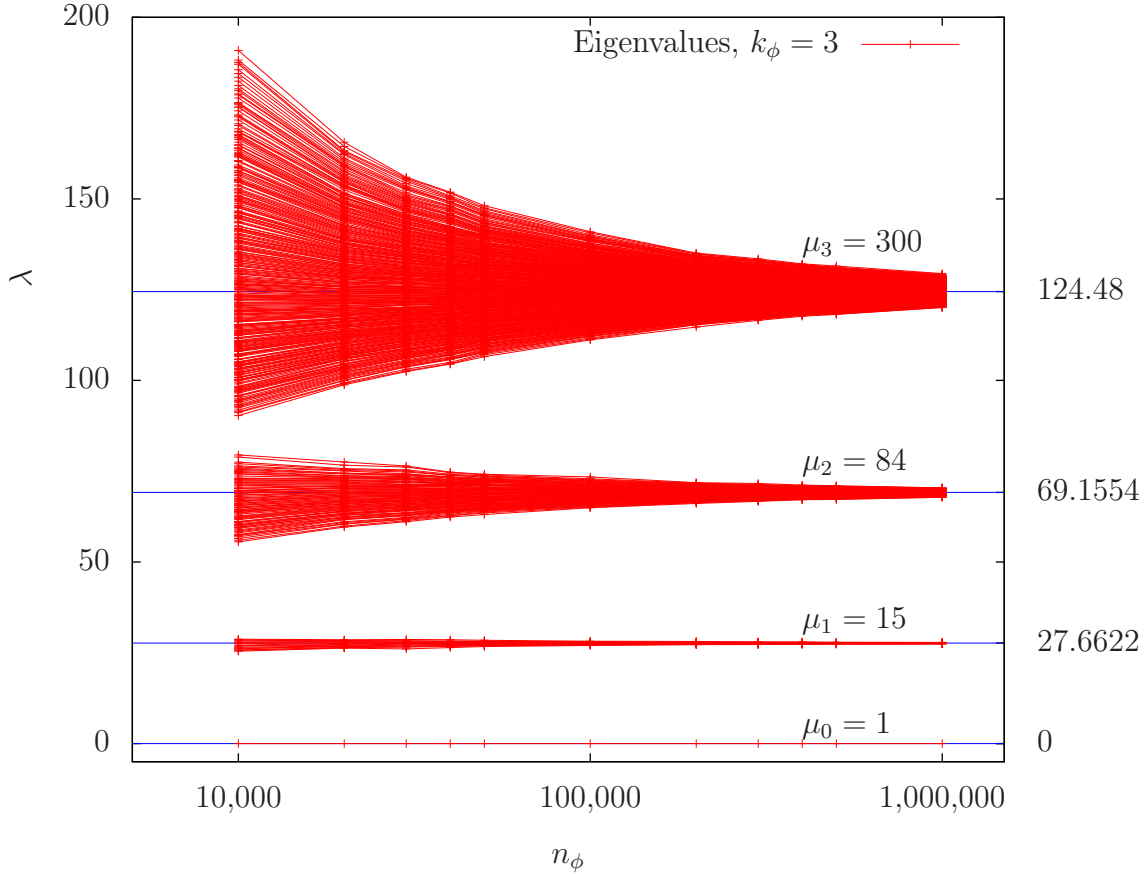


**Figure 1:** Spectrum of the scalar Laplacian on  $\mathbb{P}^3$  with the rescaled Fubini-Study metric. Here we fix the space of functions by choosing degree  $k_\phi = 3$ , and evaluate the Laplace operator at a varying number of points  $n_\phi$ .

$n_\phi$ , the eigenvalues are fairly spread out. However, as  $n_\phi$  is increased the eigenvalues break into distinct groups, each of which rapidly coalesces toward a unique value. One can then compare the limiting value and multiplicity of each group against the exact analytic result. We find perfect agreement. To be concrete, let us present the numerical results for the case  $k_\phi = 3$ . We plot these results in Figure 1. As  $n_\phi$  is increased from 10,000 to 1,000,000, the  $\dim \mathcal{F}_3 = 400$  eigenvalues  $\lambda_n$  cluster into 4 distinct groups with multiplicity 1, 15, 84 and 300. These clusters approach the theoretical values of the first four eigenvalues respectively, as expected. That is, the numerically calculated eigenvalues condense to the analytic results for the eigenvalues and multiplicities listed in Table 1 on page 9. At any  $n_\phi$ , the eigenfunction  $\phi_n$  associated with each  $\lambda_n$  is evaluated as a sum over the basis functions  $\{f_a | a = 0, \dots, 399\}$ . We do not find it enlightening to present the numerical coefficients.

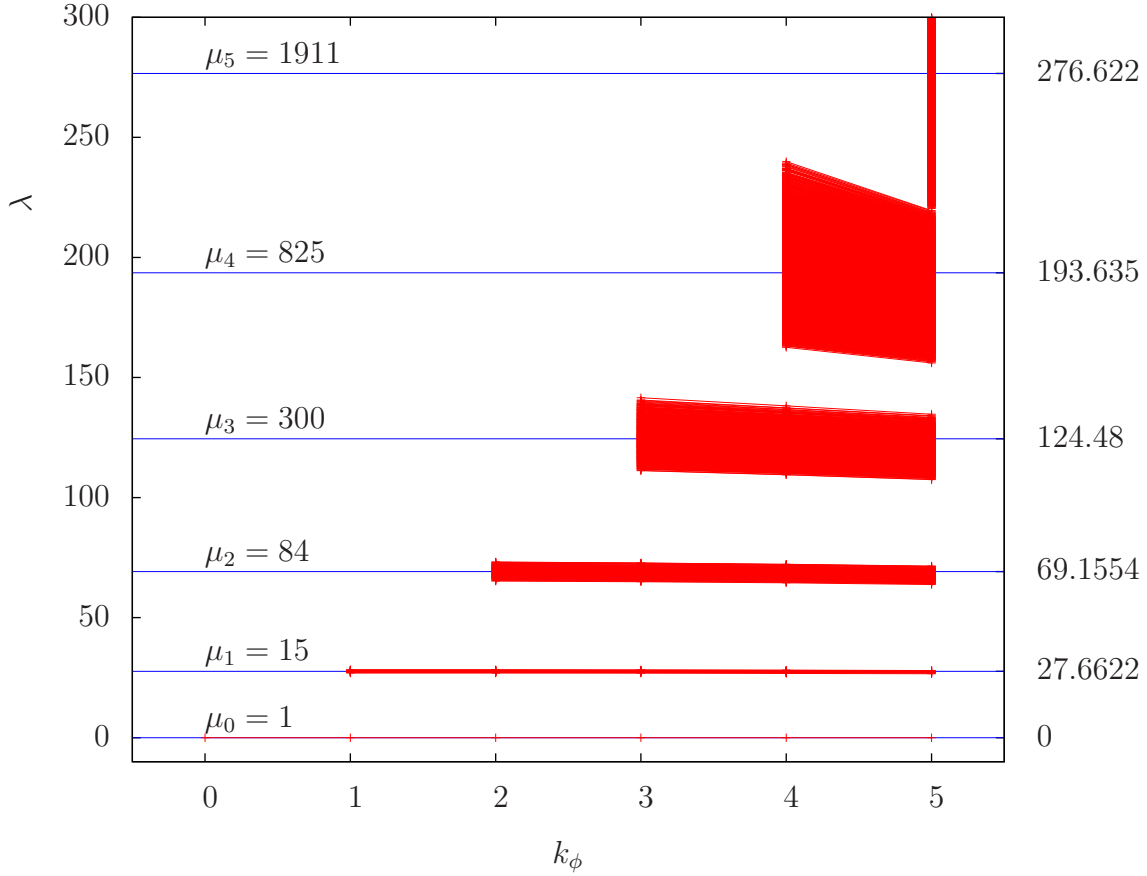


**Figure 2:** Spectrum of the scalar Laplacian on  $\mathbb{P}^3$  with the rescaled Fubini-Study metric. Here we evaluate the spectrum of the Laplace operator as a function of  $k_\phi$ , while keeping the number of points fixed at  $n_\phi = 100,000$ . Note that  $k_\phi$  determines the dimension of the matrix approximation to the Laplace operator.

The second way to present our numerical results is to fix  $n_\phi$  and study the dependence of the eigenvalues on  $k_\phi$ . As was discussed in Subsection 3.1, since the eigenfunctions of the Laplace operator are linear combinations of the elements of our basis, the accuracy of  $\lambda_n$  should not depend on  $k_\phi$ . However, increasing  $k_\phi$  does add higher-frequency functions to the approximating space of functions. More explicitly, going from  $k_\phi$  to  $k_{\phi+1}$  will add an extra  $\mu_{k_{\phi+1}}$  eigenvalues to the numerical spectrum, corresponding to the dimension of the  $(k_{\phi+1}, 0, k_{\phi+1})$  irreducible representation of  $SU(4)$ . This is exactly the behavior that we observe in Figure 2.

### 3.3 Asymptotic Behaviour

It is of interest to compare the asymptotic behaviour of the numerical solution to the theoretical prediction of Weyl's formula, which determines the asymptotic growth of the spectrum of the scalar Laplace operator. Specifically, it asserts that on a Riemannian manifold  $X$  of real dimension  $d$ , the eigenvalues grow as  $\lambda_n \sim n^{\frac{2}{d}}$  for large  $n$ . Here it is important to keep track of multiplicities by including the degenerate eigenvalue multiple times in the sequence  $\{\lambda_n\}$ , as we do in our numerical calculations. The precise statement of Weyl's formula is then that

$$\lim_{n \rightarrow \infty} \frac{\lambda_n^{d/2}}{n} = \frac{(4\pi)^{\frac{d}{2}} \Gamma(\frac{d}{2} + 1)}{\text{Vol}(X)}. \quad (36)$$

Applying this to  $\mathbb{P}^3$ , which has  $d = 6$  and the volume scaled to  $\text{Vol}_K(\mathbb{P}^3) = 1$ , we find that

$$\lim_{n \rightarrow \infty} \frac{\lambda_n^3}{n} = 384\pi^3. \quad (37)$$

In Figure 3 we choose  $k_\phi = 3$  and plot  $\frac{\lambda_n^3}{n}$  as a function of  $n$  for the numerical values of  $\lambda_n$ , as well as for the exact values listed in Table 1. The numerical results are presented for six different values of  $n_\phi$ . For each value of  $n_\phi$ , as well as for the exact result, the  $\frac{\lambda_n^3}{n}$  break into three groups, corresponding to the first three massive levels with multiplicities 15, 84, and 300, respectively. Note that, as  $n_\phi$  gets larger, the numerical results converge to the exact result. That is, each segment approaches a curve of the form  $\frac{\text{const.}}{n}$ . Furthermore, as the number of eigenvalues increase, the end-points of the curves asymptote toward the Weyl limit  $384\pi^3$ .

## 4 Quintic Calabi-Yau Threefolds

Quintics are Calabi-Yau threefolds  $\tilde{Q} \subset \mathbb{P}^4$ . Denote the usual homogeneous coordinates on  $\mathbb{P}^4$  by  $z = [z_0 : z_1 : z_2 : z_3 : z_4]$ . A hypersurface in  $\mathbb{P}^4$  is Calabi-Yau if and only if it is the zero locus of a degree-5 homogeneous polynomial

$$\tilde{Q}(z) = \sum_{n_0+n_1+n_2+n_3+n_4=5} c_{(n_0,n_1,n_2,n_3,n_4)} z_0^{n_0} z_1^{n_1} z_2^{n_2} z_3^{n_3} z_4^{n_4}. \quad (38)$$

By the usual abuse of notation, we denote both the defining polynomial  $\tilde{Q}(z)$  and the corresponding hypersurface  $\{\tilde{Q}(z) = 0\} \subset \mathbb{P}^4$  by  $\tilde{Q}$ . There are  $\binom{5+4-1}{4} = 126$  degree-5 monomials, leading to 126 coefficients  $c_{(n_0,n_1,n_2,n_3,n_4)} \in \mathbb{C}$ . These are not all independent complex structure parameters, since the linear  $GL(5, \mathbb{C})$ -action on the five homogeneous coordinates is simply a choice of coordinates. Hence, the number of complex structure moduli of a generic quintic  $\tilde{Q}$  is  $126 - 25 = 101$ .



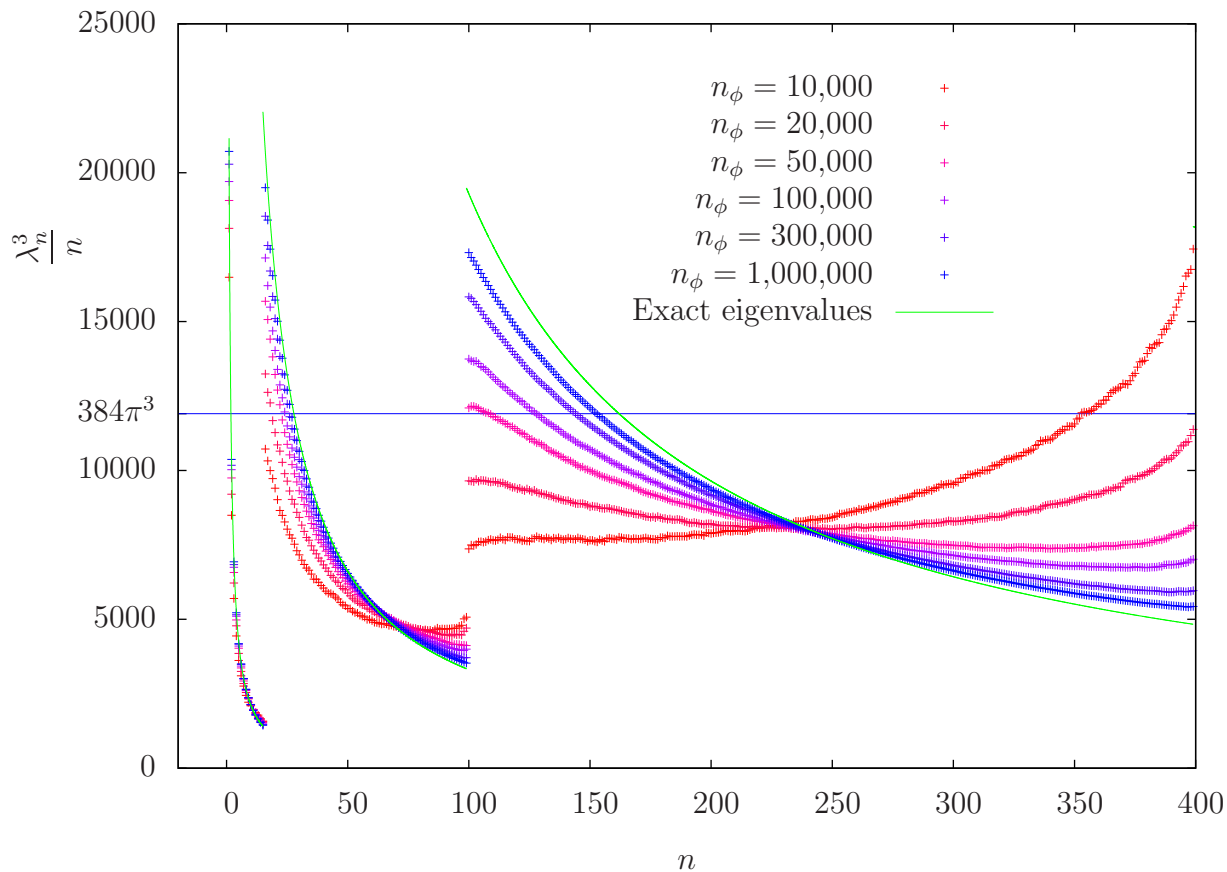


**Figure 3:** Check of Weyl's formula for the spectrum of the scalar Laplacian on  $\mathbb{P}^3$  with the rescaled Fubini-Study metric. We fix the space of functions by taking  $k_\phi = 3$  and evaluate  $\frac{\lambda_n^3}{n}$  as a function of  $n$  at a varying number of points  $n_\phi$ . Note that the data used for the eigenvalues is the same as for  $k_\phi = 3$  in Figure 1.

A natural choice of metric on  $\mathbb{P}^4$  is the Fubini-Study metric  $g_{i\bar{j}} = \partial_i \bar{\partial}_{\bar{j}} K_{\text{FS}}$ , where

$$K_{\text{FS}} = \frac{1}{\pi} \ln \sum_{i=0}^4 z_i \bar{z}_i. \quad (39)$$

This induces a metric on the hypersurface  $\tilde{Q}$ , whose Kähler potential is simply the restriction. Unfortunately, the restriction of the Fubini-Study metric to the quintic is far from Ricci-flat. Recently, however, Donaldson [31] presented an algorithm for numerically approximating Calabi-Yau metrics to any desired accuracy. To do this in the quintic context, one takes a suitable generalization, that is, one containing many more free parameters, of the Fubini-Study metric. The parameters are then numerically adjusted so as to approach the Calabi-Yau metric.

Explicitly, Donaldson's algorithm is the following. Pick a basis for the quotient

$$\mathbb{C}[z_0, \dots, z_4]_k / \langle \tilde{Q}(z) \rangle \quad (40)$$

of the degree- $k$  polynomials on  $\mathbb{P}^4$  modulo the hypersurface equation. Let us denote this basis by  $s_\alpha$ ,  $\alpha = 0, \dots, N(k) - 1$  where

$$N(k) = \begin{cases} \binom{5+k-1}{k} & 0 \leq k < 5 \\ \binom{5+k-1}{k} - \binom{k-1}{k-5} & k \geq 5. \end{cases} \quad (41)$$

For any given quintic polynomial  $\tilde{Q}(z)$  and degree  $k$ , computing an explicit polynomial basis  $\{s_\alpha\}$  is straightforward. Now, make the following ansatz

$$K_{h,k} = \frac{1}{k\pi} \ln \sum_{\alpha, \beta=0}^{N(k)-1} h^{\alpha\bar{\beta}} s_\alpha \bar{s}_\beta \quad (42)$$

for the Kähler potential. The hermitian  $N(k) \times N(k)$ -matrix  $h^{\alpha\bar{\beta}}$  parametrizes the metric on  $\tilde{Q}$  and is chosen to be the unique fixed point of the Donaldson T-operator

$$T(h)_{\alpha\bar{\beta}} = \frac{N(k)}{\text{Vol}_{\text{CY}}(\tilde{Q})} \int_{\tilde{Q}} \frac{s_\alpha \bar{s}_\beta}{\sum_{\gamma, \delta} h^{\gamma\bar{\delta}} s_\gamma \bar{s}_\delta} d\text{Vol}_{\text{CY}}, \quad (43)$$

where

$$d\text{Vol}_{\text{CY}} = \Omega \wedge \bar{\Omega} \quad (44)$$

and  $\Omega$  is the holomorphic volume form. The metric determined by the fixed point of the T-operator is called "balanced". Hence, we obtain for each integer  $k \geq 1$  the balanced metric

$$g_{i\bar{j}}^{(k)} = \frac{1}{k\pi} \partial_i \bar{\partial}_{\bar{j}} \ln \sum_{\alpha, \beta=0}^{N(k)-1} h^{\alpha\bar{\beta}} s_\alpha \bar{s}_\beta. \quad (45)$$

Note that they are formally defined on  $\mathbb{P}^4$  but restrict directly to  $\tilde{Q}$ , by construction. One can show [48] that this sequence

$$g_{i\bar{j}}^{(k)} \xrightarrow{k \rightarrow \infty} g_{i\bar{j}}^{\text{CY}} \quad (46)$$

of balanced metrics converges to the Calabi-Yau metric on  $\tilde{Q}$ .

It is important to have a measure of how closely the balanced metric  $g_{i\bar{j}}^{(k)}$  at a given value of  $k$  approximates the exact Calabi-Yau metric  $g_{i\bar{j}}^{\text{CY}}$ . One way to do this is the following. Let  $g_{i\bar{j}}^{(k)}$  be a balanced metric,  $\omega_k$  the associated  $(1, 1)$ -form and denote by

$$\text{Vol}_K(\tilde{Q}, k) = \int_{\tilde{Q}} \frac{\omega_k^3}{3!}, \quad \text{Vol}_{\text{CY}}(\tilde{Q}) = \int_{\tilde{Q}} \Omega \wedge \bar{\Omega} \quad (47)$$

the volume of  $\tilde{Q}$  evaluated with respect to  $\omega_k$  and the holomorphic volume form  $\Omega$  respectively. Now note that the integral

$$\sigma_k(\tilde{Q}) = \frac{1}{\text{Vol}_{\text{CY}}(\tilde{Q})} \int_{\tilde{Q}} \left| 1 - \frac{\frac{\omega_k^3}{3!} / \text{Vol}_K(\tilde{Q}, k)}{\Omega \wedge \bar{\Omega} / \text{Vol}_{\text{CY}}(\tilde{Q})} \right| d\text{Vol}_{\text{CY}} \quad (48)$$

must vanish as  $\omega_k$  approaches the Calabi-Yau Kähler form. That is

$$\sigma_k \xrightarrow{k \rightarrow \infty} 0. \quad (49)$$

Following [33], we will use  $\sigma_k$  as the error measure for how far balanced metric  $g_{i\bar{j}}^{(k)}$  is from being Calabi-Yau. Finally, to implement our volume normalization we will always scale the balanced metric so that

$$\text{Vol}_K(\tilde{Q}, k) = 1 \quad (50)$$

at each value of  $k$ .

## 4.1 Non-Symmetric Quintic

In this subsection, we will pick random<sup>6</sup> coefficients  $c_{(n_0, n_1, n_2, n_3, n_4)}$  for the 126 different quintic monomials in the 5 homogeneous coordinates. An explicit example, which we use for the analysis in this section, is given by

$$\begin{aligned} \tilde{Q}(z) = & (-0.319235 + 0.709687i)z_0^5 + (-0.327948 + 0.811936i)z_0^4z_1 \\ & + (0.242297 + 0.219818i)z_0^4z_2 + \cdots + (-0.265416 + 0.122292i)z_4^5. \end{aligned} \quad (51)$$

---

<sup>6</sup>To be precise, we pick uniformly distributed random numbers on the unit disk  $\{z \in \mathbb{C} : |z| \leq 1\}$ .

We refer to this as the “random quintic”. Of course, any other random choice of coefficients would lead to similar conclusions. The polynomial eq. (51) completely fixes the complex structure. Furthermore, the single Kähler modulus determines the overall volume, which we set to unity.

Using Donaldson’s algorithm [31, 33, 40] which we outlined above, one can compute an approximation to the Calabi-Yau metric on the quintic defined by eq. (51). The accuracy of this approximation is determined by

- The degree  $k \in \mathbb{Z}_{\geq 0}$  of the homogeneous polynomials used in the ansatz eq. (42) for the Kähler potential. To distinguish this degree from the one in the approximation to the Laplace operator, we denote them from now on by  $k_h$  and  $k_\phi$ , respectively. In this section, we will use

$$k_h = 8. \tag{52}$$

Note that the choice of degree  $k_h$  determines the number of parameters

$$h^{\alpha\bar{\beta}} \in \text{Mat}(N(k_h) \times N(k_h), \mathbb{C}) \tag{53}$$

in the ansatz for the Kähler potential, eq. (42). This is why  $k_h$  is essentially limited by the available memory. We choose  $k_h = 8$  because it gives a good approximation to the Calabi-Yau metric, see below, without using a significant amount of computer memory ( $\approx 7$  MiB).

- The number of points used to numerically integrate within Donaldson’s T-operator [33]. To distinguish this number from the number of points used to evaluate the Laplacian, we denote them by  $n_\phi$  and  $n_h$  respectively. As argued in [40], to obtain a good approximation to the Ricci-flat metric one should choose  $n_h \gg N(k_h)^2$ , where  $N(k_h)$  is the number of degree- $k_h$  homogeneous monomials in the 5 homogeneous coordinates modulo the  $\tilde{Q}(z) = 0$  constraint, see eq. (41). In our computation, we will always take

$$n_h = 10 \cdot N(k_h)^2 + 50,000. \tag{54}$$

This rather arbitrary number is chosen for the following reasons. First, the leading term assures that  $n_h \gg N(k_h)^2$  by an order of magnitude and, second, the addition of 50,000 points guarantees that the integrals are well-approximated even for small values of  $k_h$ . It follows from eq. (41) that for  $k_h = 8$  we will use

$$n_h = 2,166,000 \tag{55}$$

points in evaluating the T-operator.

Using the Donaldson algorithm with  $k_h$  and  $n_h$  given by eqns. (52) and (55) respectively, one can now compute a good approximation to the Calabi-Yau metric in a reasonable amount of time<sup>7</sup>. The expression for the metric itself is given as a sum over monomials on  $\tilde{Q}$  of degree  $k_h = 8$  with numerically generated complex coefficients. It is not enlightening to present it here. However, it is useful to compute the error measure defined in eq. (48) for this metric. We find that

$$\sigma_8 \approx 5 \times 10^{-2}, \quad (56)$$

meaning that, on average, the approximate volume form  $\frac{\omega_8^3}{3!}$  and the exact Calabi-Yau volume form  $\Omega \wedge \bar{\Omega}$  agree to about 5%. Finally, having found an approximation to the Ricci-flat metric, one can insert it into eq. (1) to determine the form of the scalar Laplacian.

We can now compute the spectrum of the scalar Laplace operator as discussed in the previous section. First, one must specify a finite-dimensional approximation to the space of complex-valued functions on  $\tilde{Q}$ . For any finite value of  $k_\phi$ , we choose

$$\mathcal{F}_{k_\phi} = \text{span} \left\{ \frac{s_\alpha \bar{s}_\beta}{(\sum_{i=0}^4 |z_i|^2)^{k_\phi}} \mid \alpha, \beta = 0, \dots, N(k_\phi) - 1 \right\}, \quad (57)$$

where  $\{s_\alpha \mid \alpha = 0, \dots, N(k_\phi) - 1\}$  are a basis for the homogeneous polynomials modulo the hypersurface constraint

$$\text{span}\{s_\alpha\} = \mathbb{C}[z_0, \dots, z_4]_{k_\phi} / \langle \tilde{Q}(z) \rangle. \quad (58)$$

Such a basis was already determined during the Donaldson algorithm for the metric, the only difference being that now the degree is  $k_\phi$  instead of  $k_h$ . The counting function  $N(k_\phi)$  is given by eq. (41). Clearly,

$$\dim \mathcal{F}_{k_\phi} = N(k_\phi)^2. \quad (59)$$

Computing the matrix elements of the Laplace operator requires another numerical integration which is completely independent of the one in the T-operator. We denote the number of points in the matrix element integration by  $n_\phi$ , as we did in the previous section. We first present the resulting eigenvalue spectrum for fixed  $k_\phi = 3$  plotted against an increasing number of points  $n_\phi$ . Our results are shown in Figure 4. From eq. (41) we see that  $N(3) = 35$  and, hence, there are  $35^2 = 1,225$  non-degenerate eigenvalues  $\lambda_0, \dots, \lambda_{1,224}$ . Note that for smaller values of  $n_\phi$  the eigenvalues are fairly spread out, and that they remain so as  $n_\phi$  is increased. This reflects the fact that for any Calabi-Yau manifold there is no continuous isometry, as there was for the  $\mathbb{P}^3$ . Furthermore, for the random quintic eq. (51) there is no finite isometry

---

<sup>7</sup>That is, within a few hours of “wall” time.

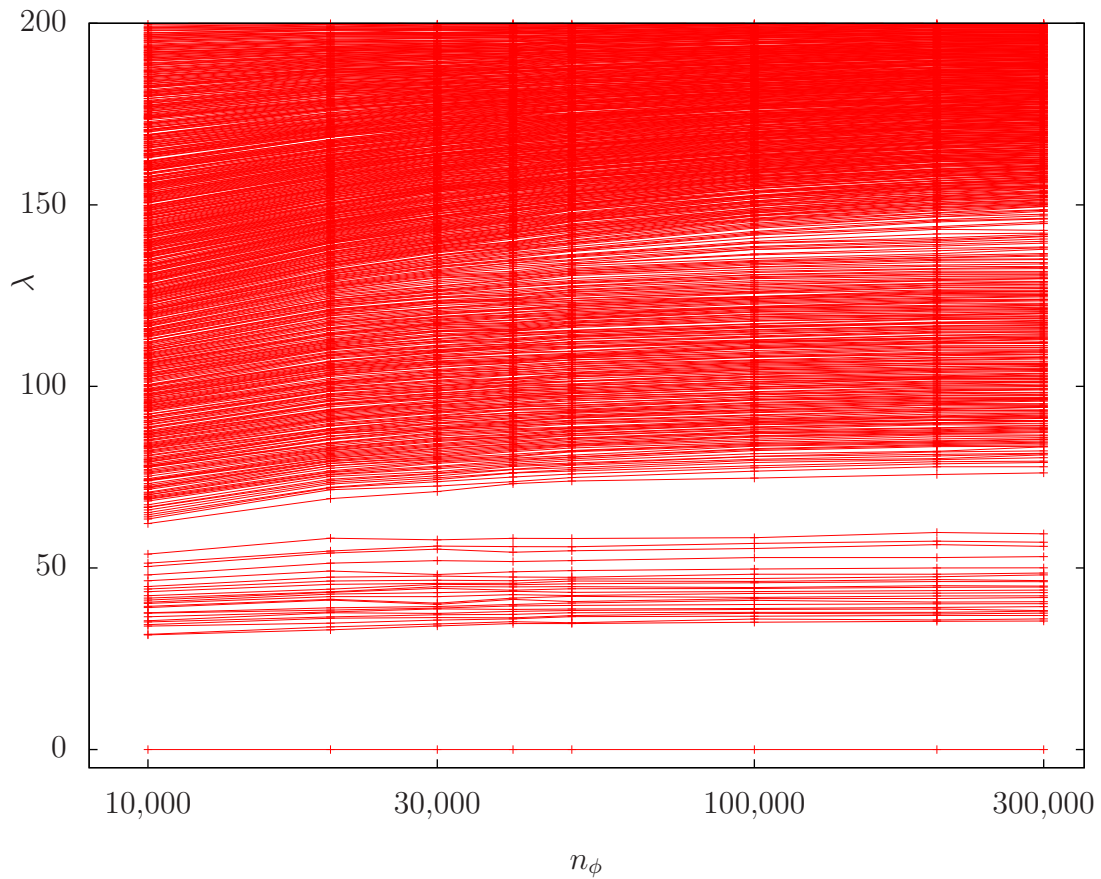


**Figure 4:** Eigenvalues of the scalar Laplace operator on the same “random quintic” defined in eq. (51). The metric is computed at degree  $k_h = 8$ , using  $n_h = 2,166,000$  points. The Laplace operator is evaluated at degree  $k_\phi = 3$  on a varying number  $n_\phi$  of points.

group either. Therefore, one expects each eigenvalue to be non-degenerate, and our numerical results are clearly consistent with this. At any  $n_\phi$ , the eigenfunctions  $\phi_n$  are a linear combination of the 1,225 basis functions. We do not find it enlightening to list the numerical coefficients explicitly.

Note that the accuracy of the numerical integration for the matrix elements<sup>8</sup> is not as crucial as in the T-operator, since we are primarily interested in the low lying eigenvalues corresponding to slowly-varying eigenfunctions. This is nicely illustrated by Figure 4, where the eigenvalues rather quickly approach a constant value as we increase  $n_\phi$ , even though  $n_\phi \ll n_h$ . For this reason,  $n_\phi = 200,000$  gives a sufficiently good approximation and we will use this value for the remainder of this subsection.

A second way to present our numerical results is to fix  $n_\phi$  and study the dependence of the eigenvalues on  $k_\phi$ . This is presented in Figure 5. We first note that the number of eigenvalues indeed grows as  $N(k_\phi)^2$ , as it must. Second, as one expects, the smaller eigenvalues do not change much as one increases  $k_\phi$ . The higher eigenvalues, however, depend strongly on the truncation of the space of functions, since their eigenfunctions vary quickly.

Finally, we plot  $\lambda_n^3/n$  as a function of  $n$  in Figure 6. We see that this ratio does approach the theoretical value of  $384\pi^3$  as  $k_\phi$  and  $n$  increase. This confirms that the volume normalization in eq. (50) is being correctly implemented and that our numerical results are consistent with Weyl's formula eq. (36).

## 4.2 Fermat Quintic

We repeat the analysis of the previous section for the Fermat quintic defined by

$$\tilde{Q}_F(z) = z_0^5 + z_1^5 + z_2^5 + z_3^5 + z_4^5. \quad (60)$$

As before, the single Kähler modulus is chosen so that the volume of the Fermat quintic is unity. Now, however, we are at a different point in the complex structure moduli space, eq. (60) instead of the random quintic eq. (51). Hence, we will perform the numerical integrations now using points lying on a different hypersurface inside  $\mathbb{P}^4$ . Except for using different points, we compute the Calabi-Yau metric on  $\tilde{Q}_F$  using Donaldson's algorithm exactly as in the previous subsection. In particular

- The degree  $k_h \in \mathbb{Z}_{\geq 0}$  of the homogeneous polynomials used in the ansatz eq. (42) for the Kähler potential is chosen to be

$$k_h = 8. \quad (61)$$

This is the same degree as we used for the random quintic.

---

<sup>8</sup>Recall that  $n_h \rightarrow \infty$  is the continuum limit for the numerical integration in the T-operator, and  $n_\phi \rightarrow \infty$  is the continuum limit for the numerical integration determining the matrix elements of the Laplace operator.

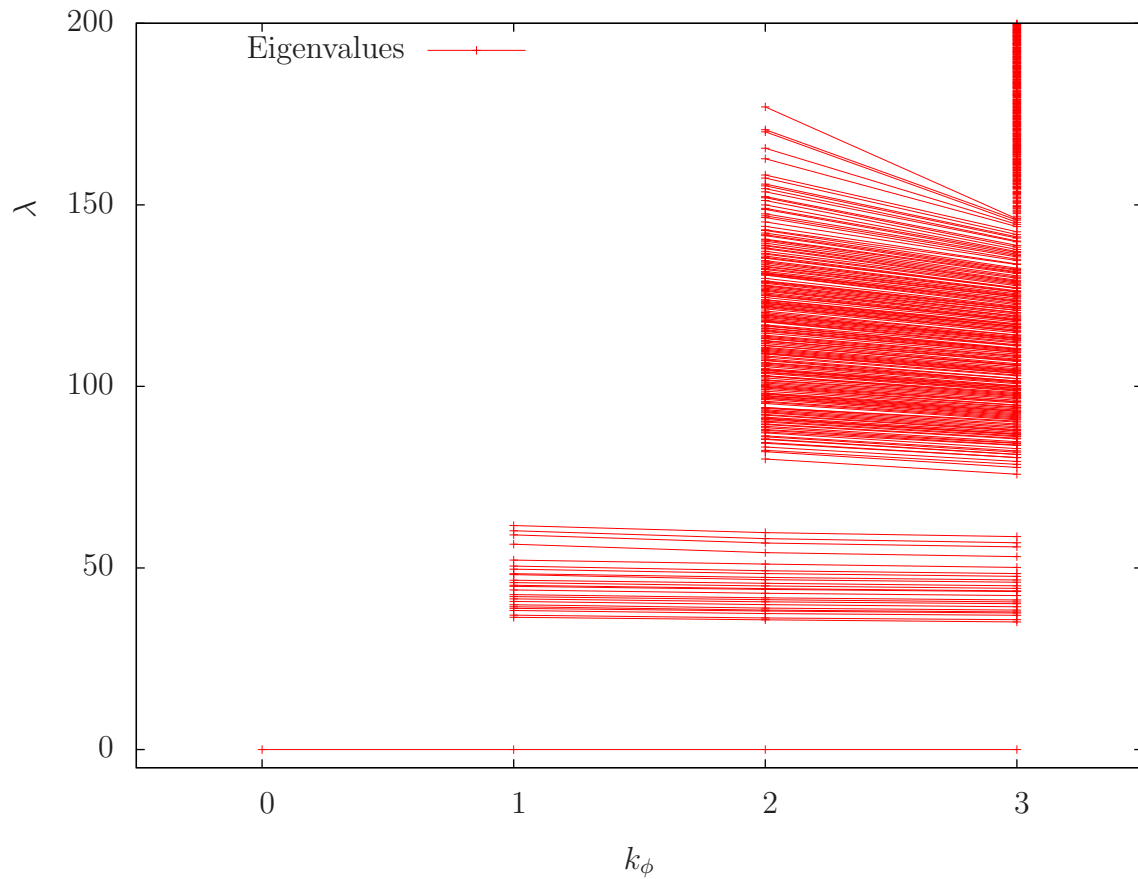


**Figure 5:** Eigenvalues of the scalar Laplace operator on a random quintic plotted against  $k_\phi$ . The metric is computed at degree  $k_h = 8$ , using  $n_h = 2,166,000$  points. The Laplace operator is then evaluated at  $n_\phi = 200,000$  points.



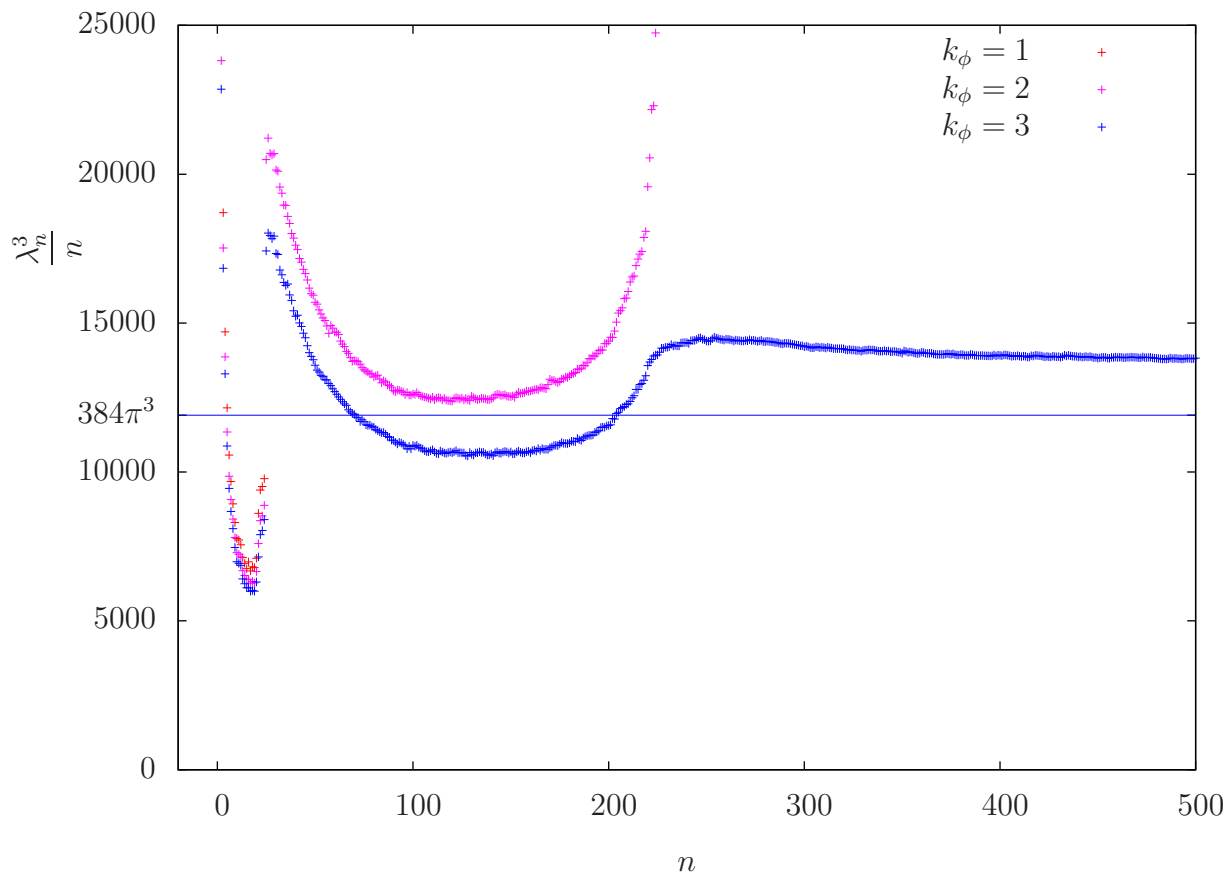


**Figure 6:** Check of Weyl's formula for the spectrum of the scalar Laplace operator on a random quintic. The metric is computed at degree  $k_h = 8$ , using  $n_h = 2,166,000$  points. The Laplace operator is evaluated at  $n_\phi = 200,000$  points and degrees  $k_\phi = 1, 2, 3$ . Note that the data for the eigenvalues is the same as in Figure 5. According to Weyl's formula, the exact eigenvalues have to satisfy  $\lim_{n \rightarrow \infty} \lambda_n^3/n = 384\pi^3$ .

- We take the number of points used to numerically integrate Donaldson's T-operator to be

$$n_h = 10 \cdot N(8)^2 + 50,000 = 2,166,000 \quad (62)$$

This satisfies the condition that  $n_h \gg N(k_h)^2$ , ensuring that the numerical integration is sufficiently accurate.

Using  $k_h$  and  $n_h$  given by eqns. (61) and (62) respectively, one can compute an approximation to the Calabi-Yau metric using Donaldson's algorithm. The numerical expression for the metric is tedious and will not be presented here. The error measure eq. (48) for this  $k_h = 8$  balanced metric is

$$\sigma_8 \approx 5 \times 10^{-2}. \quad (63)$$

Hence, the approximate volume form  $\frac{\omega_8^3}{3!}$  and the exact Calabi-Yau volume form  $\Omega \wedge \bar{\Omega}$  agree to about 5%. The metric determines the scalar Laplacian, eq. (1).

To determine the matrix elements of the Laplace operator, one has to select an approximating basis for the linear space of complex functions on  $\tilde{Q}_F$ , eq. (60). For any finite  $k_\phi$ , we again choose the function space  $\mathcal{F}_{k_\phi}$  as in eqns. (57) and (58). This basis was already determined during the Donaldson algorithm for the metric. Computing the matrix elements of the Laplace operator requires another numerical integration which is completely independent of the one in the T-operator. As we did previously, we denote the number of points in the matrix element integration by  $n_\phi$ .

We first present the resulting eigenvalue spectrum for fixed  $k_\phi = 3$  plotted against an increasing number of points  $n_\phi$ . Our results are shown in Figure 7. Note from eq. (59) that the total number of eigenvalues is given by  $\dim \mathcal{F}_3 = N(3)^2 = 1,225$ . One immediately notices a striking difference compared to the analogous graph for the random quintic, Figure 4. Here, the eigenvalues converge towards degenerate levels. For smaller values of  $n_\phi$ , the eigenvalues are fairly spread out. However, as  $n_\phi$  is increased the eigenvalues begin to condense into degenerate levels. Clearly, this must be due to symmetries of the Fermat quintic. As mentioned above, no Calabi-Yau manifold has a continuous isometry. However, unlike the random quintic, the Fermat quintic eq. (60) does possess a finite isometry group, which we will specify below in detail. Therefore, the exact eigenvalues of  $\Delta$  on  $\tilde{Q}_F$  should be degenerate with multiplicities given by the irreducible representations of this finite group. As we will see in Subsection 4.3, the numerically computed degeneracies of the eigenvalues exactly match the irreducible representations of a this finite isometry group. Again, we do not find it enlightening to present the numerical results for the eigenfunctions. Moreover, as discussed previously, the accuracy of the matrix element integration for low-lying eigenvalues need not be as great as for the T-operator. As is evident from Figure 7, a value of  $n_\phi = 500,000$  is already highly accurate and we will use this value in the remainder of this subsection.

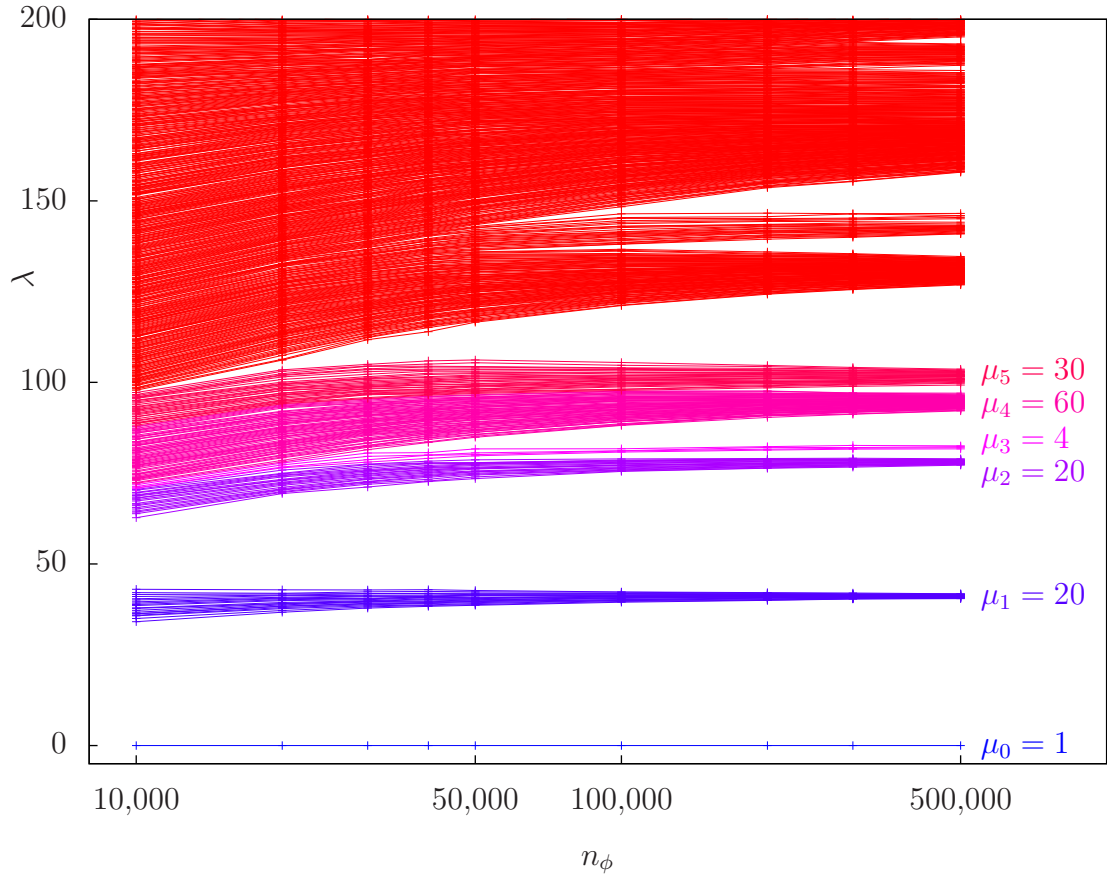


**Figure 7:** Eigenvalues of the scalar Laplace operator on the Fermat quintic. The metric is computed at degree  $k_h = 8$ , using  $n_h = 2,166,000$  points. The Laplace operator is evaluated at degree  $k_\phi = 3$  using a varying number  $n_\phi$  of points.

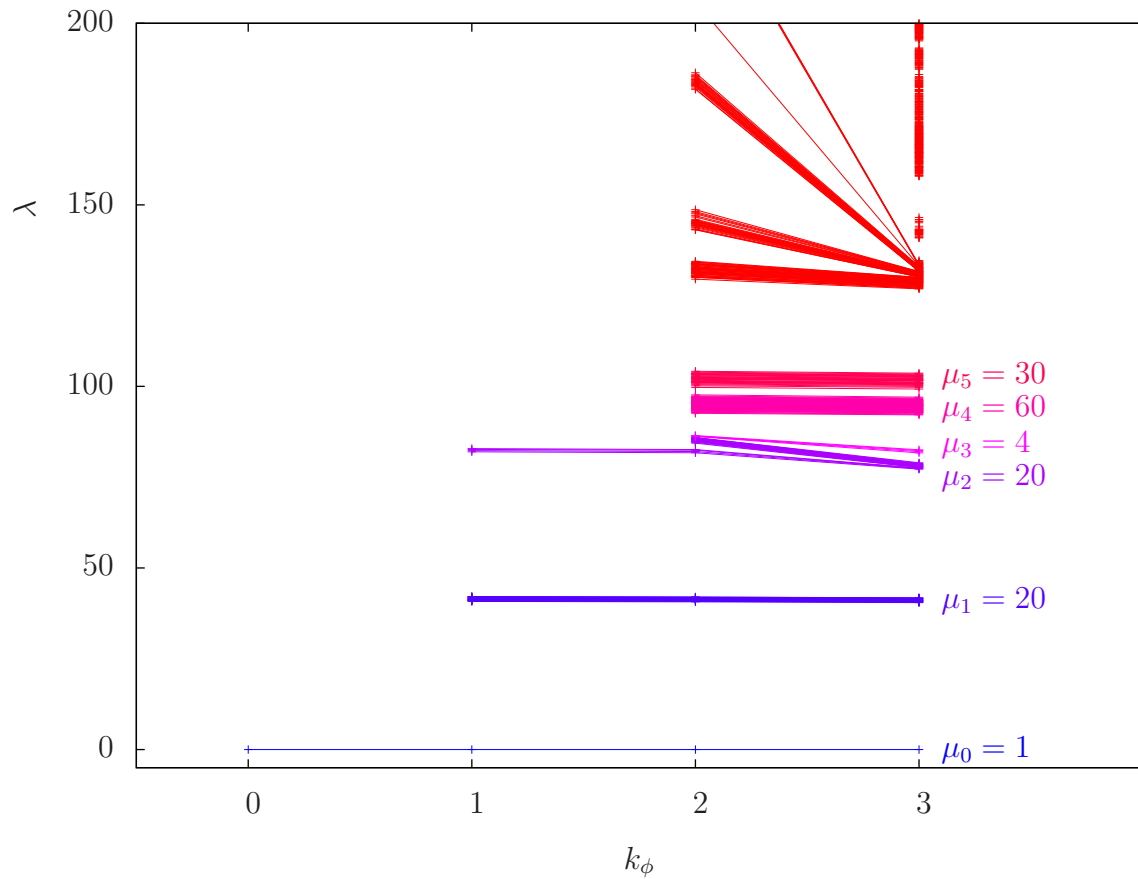


**Figure 8:** Eigenvalues of the scalar Laplace operator on the Fermat quintic. The metric is computed at degree  $k_h = 8$ , using  $n_h = 2,166,000$  points. The Laplace operator is evaluated at  $n_\phi = 500,000$  points with varying degrees  $k_\phi$ .

A second way to present our numerical results is to fix  $n_\phi$  as in the previous paragraph and study the dependence of the eigenvalues on  $k_\phi$ . This is presented in Figure 8. We first note that the number of eigenvalues grows as  $N(k_\phi)^2$ , as it must. Second, as one expects, the smaller eigenvalues do not change much as one increases  $k_\phi$ , whereas the higher eigenvalues depend strongly on the truncation of the space of functions. This is also to be expected, since their eigenfunctions vary quickly.

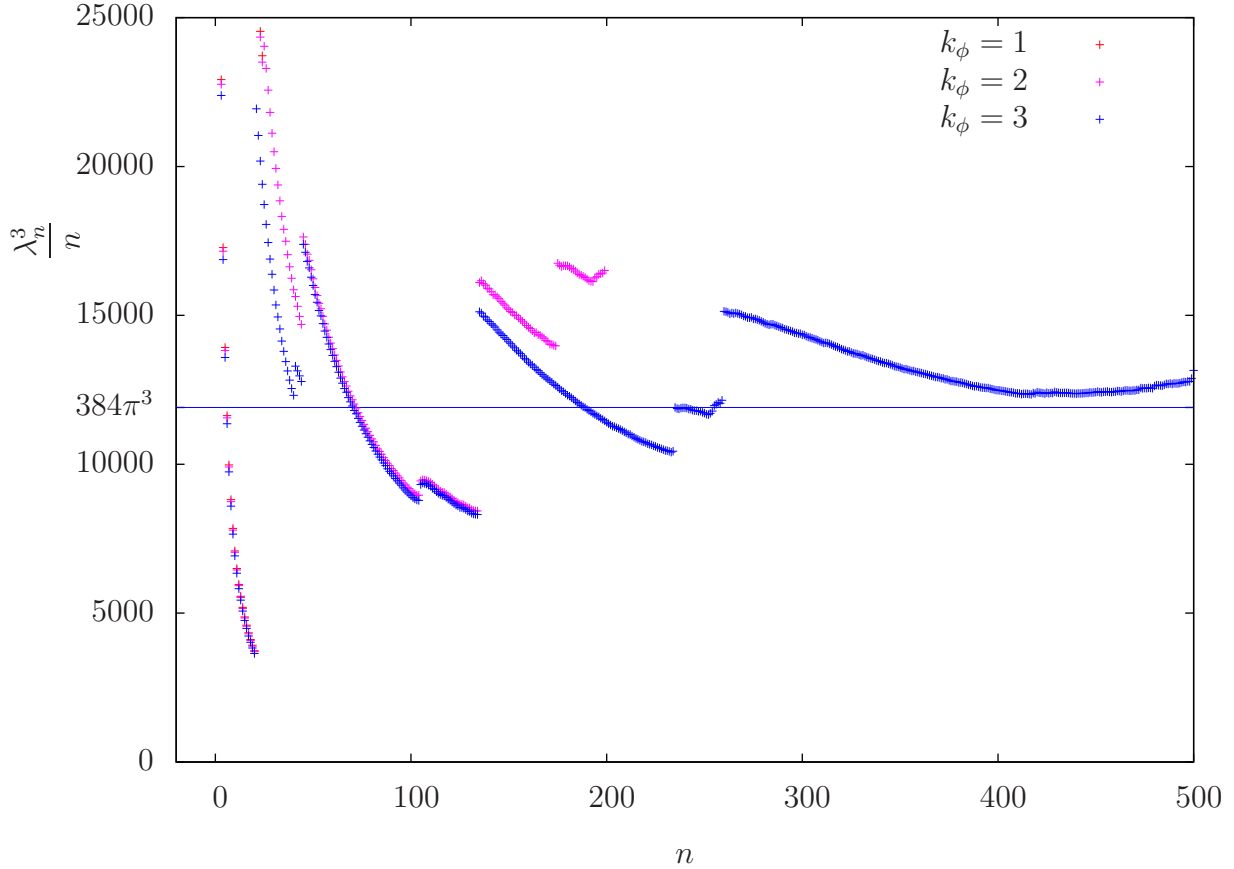


**Figure 9:** Check of Weyl’s formula for the spectrum of the scalar Laplace operator on the Fermat quintic. The metric is computed at degree  $k_h = 8$ , using  $n_h = 2,166,000$  points. The Laplace operator is evaluated at  $n_\phi = 500,000$  points and degrees  $k_\phi = 1, 2, 3$ . Note that the data for the eigenvalues is the same as in Figure 8. According to Weyl’s formula, the exact eigenvalues have to satisfy  $\lim_{n \rightarrow \infty} \lambda_n^3/n = 384\pi^3$ .

Third, let us plot  $\lambda_n^3/n$  as a function of  $n$  in Figure 9. This ratio approaches the theoretical value of  $384\pi^3$  as  $k_\phi$  and  $n$  increase. This confirms that the volume normalization in eq. (50) is being correctly implemented and that our numerical results are consistent with Weyl’s formula eq. (36).

### 4.3 Symmetry Considerations

Recall from Figure 7 that the eigenvalues of the scalar Laplace operator condense to a smaller number of degenerate levels as  $n_\phi \rightarrow \infty$ , that is, in the limit where the numerical integration becomes exact. The same phenomenon is clearly visible at different values of  $k_\phi$ , see Figure 8. Of course the eigenvalues are never exactly degenerate due to numerical errors, but counting the nearby eigenvalues allows one to determine the multiplicities. Averaging over the eigenvalues in each cluster yields an approximation to the associated degenerate eigenvalue. Using the data from Figure 8, we list the low-lying degenerate eigenvalues and their multiplicities<sup>9</sup> in Table 2. As

$m$	0	1	2	3	4	5
$\hat{\lambda}_m$	$1.18 \times 10^{-14}$	$41.1 \pm 0.4$	$78.1 \pm 0.5$	$82.1 \pm 0.3$	$94.5 \pm 1$	$102 \pm 1$
$\mu_m$	1	20	20	4	60	30

**Table 2:** The degenerate eigenvalues  $\hat{\lambda}_m$  and their multiplicities  $\mu_m$  on the Fermat quintic, as computed from the numerical values calculated with  $k_h = 8$ ,  $n_h = 2,166,000$ ,  $k_\phi = 3$ ,  $n_\phi = 500,000$ . The errors are the standard deviation within the cluster of  $\mu_n$  numerical eigenvalues.

discussed previously, multiplicities in the spectrum of the Laplace-Beltrami operator results must follow from some symmetry. In Section 3, we saw that the  $SU(4)$  symmetry of  $\mathbb{P}^3$  leads to degenerate eigenspaces of the scalar Laplacian. However, a proper Calabi-Yau threefold never has continuous isometries, unlike projective space. Nevertheless, a suitable non-Abelian<sup>10</sup> *finite* group action is possible and, in fact, explains the observed multiplicities, as we now show.

First, note that for each distinct eigenvalue the corresponding space of eigenfunctions must form a representation<sup>11</sup> of the symmetry group. Clearly, the degeneracies of the eigenvalues observed in Figure 7 and Figure 8 must arise from an isometry of  $\tilde{Q}_F$ . In fact, the Fermat quintic does have a large non-Abelian finite symmetry group. To see this, note that the zero set of eq. (60) is invariant under

- Multiplying a homogeneous coordinate by a fifth root of unity. However, not all  $(\mathbb{Z}_5)^5$  phases act effectively because the projective coordinates are identified

<sup>9</sup>Interestingly, the correct multiplicity  $\mu_1 = 20$  was derived by a completely different argument in [49].

<sup>10</sup>An Abelian symmetry group would only have one-dimensional representations and, hence, need not lead to degenerate eigenvalues. Note that any finite group has a finite number of irreducible representations and, therefore, one expects only a finite number of possible multiplicities for the eigenvalues of the Laplace operator. This is in contrast to the aforementioned  $\mathbb{P}^3$  case, where the multiplicities grow without bound.

<sup>11</sup>An actual linear representation, *not* just a representation up to phases (projective representation).

$d$	1	2	4	5	6	8	10	12	20	30	40	60	80	120
# of irreps in dim $d$	4	4	4	4	2	4	4	2	8	8	12	18	4	2

**Table 3:** Number of irreducible representations of  $\overline{\text{Aut}}(\tilde{Q}_F) = \mathbb{Z}_2 \times \text{Aut}(\tilde{Q}_F)$  in each complex dimension.

under the rescaling

$$[z_0 : z_1 : z_2 : z_3 : z_4] = [\lambda z_0 : \lambda z_1 : \lambda z_2 : \lambda z_3 : \lambda z_4]. \quad (64)$$

Only  $(\mathbb{Z}_5)^5/\mathbb{Z}_5 \simeq (\mathbb{Z}_5)^4$  acts effectively.

- Any permutation of the 5 homogeneous coordinates. The symmetric group  $S_5$  acts effectively.
- Complex conjugation  $\mathbb{Z}_2$ .

The first two groups act by analytic maps, and together generate the semidirect product

$$\text{Aut}(\tilde{Q}_F) = S_5 \times (\mathbb{Z}_5)^4 \quad (65)$$

of order 75,000. Our notation and the relevant group theory is discussed in Appendix B. The full discrete symmetry group, including the complex conjugation  $\mathbb{Z}_2$ , is

$$\overline{\text{Aut}}(\tilde{Q}_F) = \mathbb{Z}_2 \times \text{Aut}(\tilde{Q}_F) = (S_5 \times \mathbb{Z}_2) \times (\mathbb{Z}_5)^4 \quad (66)$$

and of order 150,000. Note that even though the  $\mathbb{Z}_2$  acts as complex conjugation on the base space, the whole  $\overline{\text{Aut}}(\tilde{Q}_F)$  acts linearly on the the basis of complex functions on  $\tilde{Q}_F$  and, hence, on the eigenfunctions. There are 80 distinct irreducible representations occurring in 14 different dimensions, ranging from 1 to 120. We list them in Table 3.

We conclude by noting that the multiplicities listed in Table 2 also occur in Table 3. That is, the eigenspaces of the degenerate eigenvalues of the scalar Laplacian on  $\tilde{Q}_F$ , computed using our numerical algorithm, indeed fall into irreducible representations of the finite symmetry group  $(S_5 \times \mathbb{Z}_2) \times (\mathbb{Z}_5)^4$ , as they must. This gives us further confidence that our numerical computation of the Laplacian spectrum is reliable.

## 4.4 Donaldson's Method

Donaldson [31] conjectured a method to compute the eigenvalues of the scalar Laplace operator that is completely independent of our approach. His calculation of the spectrum of the scalar Laplacian is very much tied into his algorithm for computing

balanced (Calabi-Yau) metrics. In our algorithm, on the other hand side, any metric could be used and no particular simplifications arise just because the metric happens to be balanced or Calabi-Yau. Because they are so different, it is quite interesting to compare both methods. We will now review his proposal, and then compare it with our previous computation of the eigenvalues on the Fermat quintic as well as the random quintic.

In this alternative approach to calculating the spectrum of the Laplace-Beltrami operator, one first has to run through Donaldson's algorithm for the metric. In particular, one had to choose a degree  $k$ , fix a basis  $\{s_\alpha | \alpha = 0, \dots, N(k) - 1\}$ , and obtain the balanced metric  $h^{\alpha\bar{\beta}}$  as the fixed point of Donaldson's T-operator. Let us write

$$(s_\alpha, s_\beta) = \frac{s_\alpha \bar{s}_\beta}{\sum_{\gamma\bar{\delta}} h^{\gamma\bar{\delta}} s_\gamma \bar{s}_\delta} \quad (67)$$

for the integrand of the T-operator eq. (43). Donaldson's alternative calculation of the eigenvalues then hinges on the evaluation of the integral

$$Q_{\alpha\bar{\beta}, \bar{\gamma}\delta} = N(k) \int_X (s_\alpha, s_\beta) \overline{(s_\gamma, s_\delta)} d\text{Vol}_{\text{CY}}, \quad (68)$$

where we again normalize  $\text{Vol}(X) = 1$ . One can think of  $Q$  as a linear operator on the space of functions<sup>12</sup>

$$\mathcal{F}_k^{\text{D}} = \text{span} \left\{ (s_\alpha, s_\beta) \mid 0 \leq \alpha, \bar{\beta} \leq N(k) - 1 \right\}, \quad (69)$$

acting via

$$Q : \mathcal{F}_k^{\text{D}} \rightarrow \mathcal{F}_k^{\text{D}}, (s_\alpha, s_\beta) \mapsto \sum Q_{\alpha\bar{\beta}, \bar{\gamma}\delta} h^{\bar{\gamma}\sigma} h^{\bar{\tau}\delta} (s_\sigma, s_\tau). \quad (70)$$

In [31], Donaldson conjectures that

$$\lim_{k \rightarrow \infty} Q = e^{-\frac{\Delta}{4\pi \sqrt[3]{N(k)}}} \quad (71)$$

as operators on

$$\lim_{k \rightarrow \infty} \mathcal{F}_k^{\text{D}} = C^\infty(X, \mathbb{C}). \quad (72)$$

For explicitness, let us look in more detail at the individual steps as they apply to any quintic  $X = \tilde{Q} \subset \mathbb{P}^4$ :

1. First, pick a degree  $k$  and a basis  $\{s_0, \dots, s_{N(k)-1}\}$  of degree- $k$  homogeneous polynomials modulo the hypersurface equation  $\tilde{Q} = 0$ .

---

<sup>12</sup>Note the similarity with the approximate space of functions  $\mathcal{F}_{k,\phi}$  used previously, eq. (57). When computing the matrix elements of the Laplace operator directly, the precise form of the denominator is not overly important as long as it has the correct homogeneous degree, and we always chose  $(\sum |z_j|^2)^{k_\phi}$  for simplicity.



2. Compute the Calabi-Yau metric via Donaldson's algorithm. It is determined by the  $N(k) \times N(k)$  hermitian matrix  $h^{\alpha\bar{\beta}}$ .
3. Compute the  $N(k)^4$  scalar integrals in eq. (68). The numerical integration can be performed just as in Donaldson's T-operator, see Section 4.
4. Compute the  $N(k)^2 \times N(k)^2$  matrix

$$Q_{N(k)\alpha+\bar{\beta}}^{N(k)\gamma+\bar{\delta}} = \sum_{\bar{\sigma}, \tau=0}^{N(k_h)-1} Q_{\alpha\bar{\beta}, \bar{\sigma}\tau} h^{\gamma\bar{\sigma}} h^{\tau\bar{\delta}} \quad (73)$$

and find its eigenvalues  $\Lambda_n$ . Note that  $Q_i^j$  is not hermitian<sup>13</sup> and one should use the Schur factorization<sup>14</sup> to compute eigenvalues.

5. Discard all  $\Lambda_n \leq 0$ , these correspond to high eigenvalues of the Laplacian that are not approximated well at the chosen degree  $k$ . The eigenvalues of the scalar Laplace operator are

$$\lambda_n = -4\pi \sqrt[3]{N(k)} \ln \Lambda_n. \quad (74)$$

We note that, in this approach to the spectrum of the Laplace-Beltrami operator, there is only one degree  $k$  that controls the accuracy of the eigenvalues of the scalar Laplacian and at the same time the accuracy of the Calabi-Yau metric. In fact, computing the integral eq. (68) at degree  $k$  is about as expensive as computing Donaldson's T-operator at degree  $2k$ . In other words, a general limitation of this approach is that one has to work with a relatively low precision metric.

In Figure 10 we compare the two approaches for computing the spectrum of the Laplace-Beltrami operator on the Fermat quintic. We compute the eigenvalues using Donaldson's method at degrees  $k = 1, 2, 3$  and evaluate the necessary integral eq. (68) using  $n = 10N(k)^2 + 100,000$  points. For comparison, we also plot the eigenvalues obtained by directly computing the matrix elements of the Laplacian which we always compute at degree  $k_\phi = 3$  using  $n_\phi = 500,000$  points. To estimate the effect of the metric on the eigenvalues, we run our algorithm first with the metric obtained at degree  $k_h = 3$  and<sup>15</sup>  $n_h = 62250$  (bad approximation to the Calabi-Yau metric, red diagonal crosses) as well as with  $k_h = 8$  and  $n_h = 2,166,000$  (good approximation to the Calabi-Yau metric, blue upright crosses). We find that the eigenvalues do not strongly depend on the details of the metric. Generally, Donaldson's method and the direct computation yield very similar results. There is a slight disagreement for the second and third massive level, where the matrix element calculation points toward  $\mu_2 = 20, \mu_3 = 4$  while Donaldson's method suggests the opposite order  $\mu_3 = 4, \mu_4 = 20$ . We suspect this is to be a numerical error due to the finite degrees and it would be interesting to go to higher degree in  $k, k_\phi$ , and  $k_h$ .

<sup>13</sup> $Q_i^j$  is, however, conjugate to a hermitian matrix and hence has real eigenvalues.

<sup>14</sup>Instead of the dqds algorithm we use for computing eigenvalues of hermitian matrices.

<sup>15</sup>The number of points  $n_h$  is always obtained from the heuristic eq. (54).

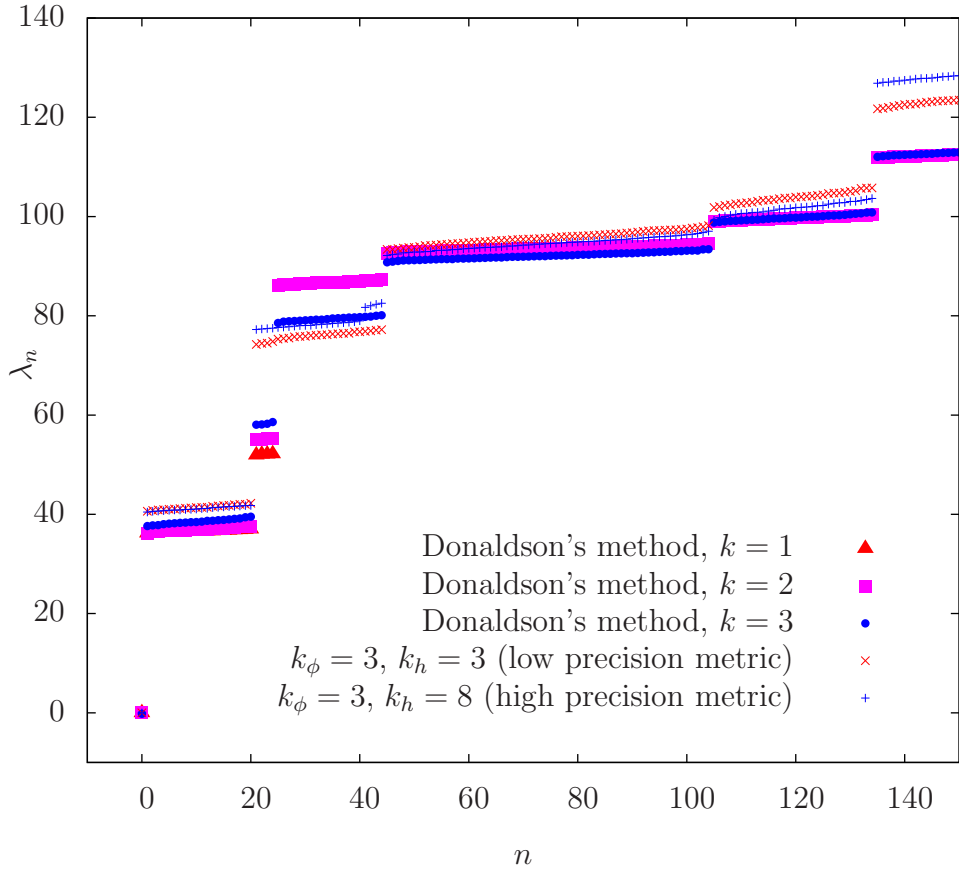


**Figure 10:** Donaldson's method of computing the spectrum (polygon symbols) of the scalar Laplace operator on the Fermat quintic compared to our direct computation (crosses). Note that the blue symbols are the highest-accuracy values, respectively. See Subsection 4.4 for further discussion.

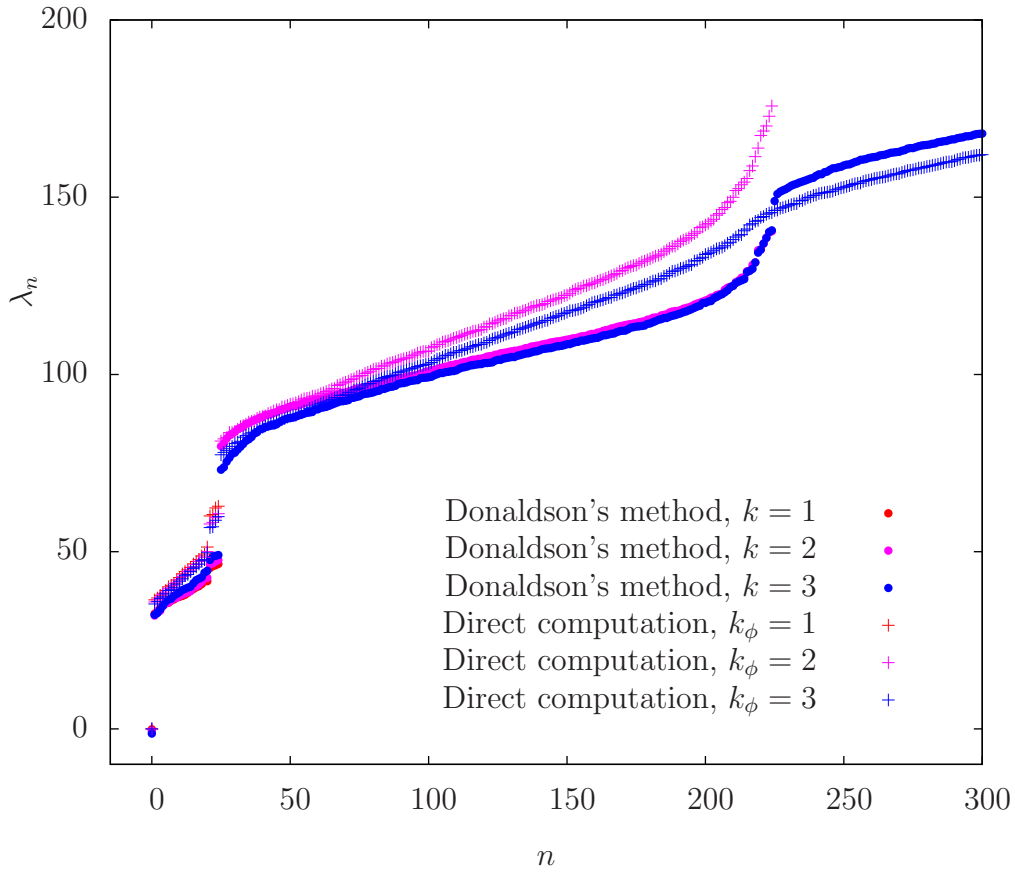


**Figure 11:** Donaldson's method of computing the spectrum (polygon symbols) of the scalar Laplace operator on the random quintic compared to our direct computation (crosses). Note that the blue symbols are the highest-accuracy values, respectively. In Donaldson's method the numerical integration was performed with  $n = 10N(k) + 100,000$  points. In the direct computation, the metric was approximated at degree  $k_h = 8$  using  $n_h = 2,166,000$  points and the Laplace operator was evaluated at  $n_\phi = 500,000$  points.

Finally, in Figure 11 we repeat this comparison for the quintic eq. (51) with random coefficients. In this case, there are no discrete symmetries and one expects all massive levels to be non-degenerate. We again find good agreement between the two approaches towards solving the Laplace equation.

## 5 $\mathbb{Z}_5 \times \mathbb{Z}_5$ Quotients of Quintics

Thus far, we have restricted our examples to quintic Calabi-Yau threefolds  $\tilde{Q} \subset \mathbb{P}^4$ . These manifolds are simply connected by construction. However, for a wide range of applications in heterotic string theory we are particularly interested in non-simply connected manifolds where one can reduce the number of quark/lepton generations as well as turn on discrete Wilson lines. Therefore, in this section we will consider the free  $\mathbb{Z}_5 \times \mathbb{Z}_5$  quotient of quintic threefolds, see [40] for more details.

### 5.1 $\mathbb{Z}_5 \times \mathbb{Z}_5$ Symmetric Quintics and their Metrics

Explicitly, the group action on the homogeneous coordinates  $[z_0 : \dots : z_4] \in \mathbb{P}^4$  is

$$\begin{aligned} g_1 : [z_0 : z_1 : z_2 : z_3 : z_4] &\longrightarrow [z_0 : e^{\frac{2\pi i}{5}} z_1 : e^{2\frac{2\pi i}{5}} z_2 : e^{3\frac{2\pi i}{5}} z_3 : e^{4\frac{2\pi i}{5}} z_4], \\ g_2 : [z_0 : z_1 : z_2 : z_3 : z_4] &\longrightarrow [z_1 : z_2 : z_3 : z_4 : z_0]. \end{aligned} \quad (75)$$

As we discussed in Section 4, a generic quintic is a zero locus of a degree-5 polynomial containing 126 complex coefficients. However, only a small subset of these quintics is invariant under the  $\mathbb{Z}_5 \times \mathbb{Z}_5$  action above. As we will show below, the dimension of the space of invariant homogeneous degree-5 polynomials is 6. Taking into account that one can always multiply the defining equation by a constant, there are 5 independent parameters  $\phi_1, \dots, \phi_5 \in \mathbb{C}$ . Thus, the  $\mathbb{Z}_5 \times \mathbb{Z}_5$  symmetric quintics form a five parameter family which can be written as

$$\begin{aligned} \tilde{Q}(z) = & (z_0^5 + z_1^5 + z_2^5 + z_3^5 + z_4^5) \\ & + \phi_1(z_0 z_1 z_2 z_3 z_4) \\ & + \phi_2(z_0^3 z_1 z_4 + z_0 z_1^3 z_2 + z_0 z_3 z_4^3 + z_1 z_2^3 z_3 + z_2 z_3^3 z_4) \\ & + \phi_3(z_0^2 z_1 z_2^2 + z_1^2 z_2 z_3^2 + z_2^2 z_3 z_4^2 + z_3^2 z_4 z_0^2 + z_4^2 z_0 z_1^2) \\ & + \phi_4(z_0^2 z_1^2 z_3 + z_1^2 z_2^2 z_4 + z_2^2 z_3^2 z_0 + z_3^2 z_4^2 z_1 + z_4^2 z_0^2 z_2) \\ & + \phi_5(z_0^3 z_2 z_3 + z_1^3 z_3 z_4 + z_2^3 z_4 z_0 + z_3^3 z_0 z_1 + z_4^3 z_1 z_2), \end{aligned} \quad (76)$$

where  $\phi_1, \dots, \phi_5 \in \mathbb{C}$  are local coordinates on the complex structure moduli space. From now on,  $\tilde{Q} \subset \mathbb{P}^4$  will always refer to a quintic of this form.

For generic coefficients<sup>16</sup>  $\phi_i$ , the hypersurface  $\tilde{Q}$  is a smooth Calabi-Yau threefold. Moreover, although the group action eq. (75) necessarily has fixed points in  $\mathbb{P}^4$ , these fixed points do not intersect a generic hypersurface  $\tilde{Q}$ . Thus the quotient

$$Q = \tilde{Q} / (\mathbb{Z}_5 \times \mathbb{Z}_5) \quad (77)$$

is again a smooth Calabi-Yau threefold. As a general principle, we will compute quantities on the quotient  $Q$  by computing the corresponding invariant quantities on the covering space  $\tilde{Q}$ . For example, the complex structure moduli space of  $Q$  is the moduli space of  $\mathbb{Z}_5 \times \mathbb{Z}_5$ -invariant complex structures on  $\tilde{Q}$ . Hence, its dimension is

$$h^{2,1}(Q) = \dim H^{2,1}(Q) = \dim H^{2,1}(\tilde{Q})^{\mathbb{Z}_5 \times \mathbb{Z}_5} = 5, \quad (78)$$

corresponding to the 5 independent parameters  $\phi_1, \dots, \phi_5$  in a  $\mathbb{Z}_5 \times \mathbb{Z}_5$ -invariant quintic  $\tilde{Q}(z)$ .

In the same spirit, we will compute the Calabi-Yau metric on  $Q$  by performing the analogous computation on the covering space  $\tilde{Q}$ . To begin, one must choose a degree  $k_h$  and determine a basis  $s_\alpha$  for the corresponding  $\mathbb{Z}_5 \times \mathbb{Z}_5$ -invariant homogeneous degree- $k_h$  polynomials

$$\text{span}\{s_\alpha\} = \mathbb{C}[z_0, \dots, z_4]_{k_h}^{\mathbb{Z}_5 \times \mathbb{Z}_5} / \langle \tilde{Q}(z) \rangle \quad (79)$$

on  $\tilde{Q}$ . Note, however, that for any homogeneous degree- $k_h$  polynomial  $p_{k_h}(z)$

$$g_1 g_2 g_1^{-1} g_2^{-1} (p_{k_h}(z)) = e^{2\pi i \frac{k_h}{5}} p_{k_h}(z) \quad (80)$$

and, hence, the two  $\mathbb{Z}_5$  generators in eq. (75) do not always commute. It follows that for a space of homogeneous polynomials to carry a linear representation of  $\mathbb{Z}_5 \times \mathbb{Z}_5$ , let alone have an invariant subspace, their degree  $k_h$  must be divisible by 5; that is,

$$k_h \in 5\mathbb{Z}. \quad (81)$$

This can be understood in various ways, and we refer to [40] for more details. Henceforth, we will assume that eq. (81) is satisfied.

The first step in determining the basis of sections  $\{s_\alpha\}$  on  $\tilde{Q}$  is to find a basis for the invariant polynomials  $\mathbb{C}[z_0, \dots, z_4]_{k_h}^{\mathbb{Z}_5 \times \mathbb{Z}_5}$  on  $\mathbb{P}^4$ . Such a basis is given by the Hironaka decomposition

$$\mathbb{C}[z_0, z_1, z_2, z_3, z_4]_{k_h}^{\mathbb{Z}_5 \times \mathbb{Z}_5} = \bigoplus_{i=1}^{100} \eta_i \mathbb{C}[\theta_1, \theta_2, \theta_3, \theta_4, \theta_5]_{k_h - \deg(\eta_i)}. \quad (82)$$

---

<sup>16</sup>For example, any sufficiently small neighbourhood of  $(\phi_1, \dots, \phi_5) = (0, \dots, 0) \in \mathbb{C}^5$ . Note that setting all  $\phi_i = 0$  yields the Fermat quintic  $\tilde{Q}_F$ , see eq. (60).

Here, the  $\theta_j = \theta_j(z)$  and  $\eta_i = \eta_i(z)$  are themselves homogeneous polynomials of various degrees<sup>17</sup>. The  $\theta_1, \dots, \theta_5$  are called “primary invariants” and the  $\eta_1, \dots, \eta_{100}$  are called “secondary invariants”. The primary and secondary invariants are not unique, but one minimal choice is [40]

$$\begin{aligned}
\theta_1 &= z_0^5 + z_1^5 + z_2^5 + z_3^5 + z_4^5 \\
\theta_2 &= z_0 z_1 z_2 z_3 z_4 \\
\theta_3 &= z_0^3 z_1 z_4 + z_1^3 z_2 z_0 + z_2^3 z_3 z_1 + z_3^3 z_4 z_2 + z_4^3 z_0 z_3 \\
\theta_4 &= z_0^{10} + z_1^{10} + z_2^{10} + z_3^{10} + z_4^{10} \\
\theta_5 &= z_0^8 z_2 z_3 + z_1^8 z_3 z_4 + z_2^8 z_4 z_0 + z_3^8 z_0 z_1 + z_4^8 z_1 z_2
\end{aligned} \tag{83}$$

and

$$\begin{aligned}
\eta_1 &= 1, \\
\eta_2 &= z_0^2 z_1 z_2^2 + z_1^2 z_2 z_3^2 + z_2^2 z_3 z_4^2 + z_3^2 z_4 z_0^2 + z_4^2 z_0 z_1^2, \\
\eta_3 &= z_0^2 z_1^2 z_3 + z_1^2 z_2^2 z_4 + z_2^2 z_3^2 z_0 + z_3^2 z_4^2 z_1 + z_4^2 z_0^2 z_2, \\
\eta_4 &= z_0^3 z_2 z_3 + z_1^3 z_3 z_4 + z_2^3 z_4 z_0 + z_3^3 z_0 z_1 + z_4^3 z_1 z_2, \\
\eta_5 &= z_0^5 z_2^5 + z_1^5 z_3^5 + z_2^5 z_4^5 + z_3^5 z_0^5 + z_4^5 z_1^5, \\
&\vdots \\
\eta_{100} &= z_0^{30} + z_1^{30} + z_2^{30} + z_3^{30} + z_4^{30}.
\end{aligned} \tag{84}$$

For example, the 6-dimensional space of invariant degree-5 homogeneous polynomials on  $\mathbb{P}^4$  is

$$\begin{aligned}
\mathbb{C}[z_0, z_1, z_2, z_3, z_4]_{5}^{\mathbb{Z}_5 \times \mathbb{Z}_5} &= \bigoplus_{i=1}^{100} \eta_i \mathbb{C}[\theta_1, \theta_2, \theta_3, \theta_4, \theta_5]_{5-\deg(\eta_i)} \\
&= \eta_1 \theta_1 \mathbb{C} \oplus \eta_1 \theta_2 \mathbb{C} \oplus \eta_1 \theta_3 \mathbb{C} \oplus \eta_2 \mathbb{C} \oplus \eta_3 \mathbb{C} \oplus \eta_4 \mathbb{C},
\end{aligned} \tag{85}$$

thus proving eq. (76).

Using the Hironaka decomposition, we can now determine the basis  $s_\alpha$  in eq. (79) by modding out the equation  $\tilde{Q}(z) = 0$  which defines the covering space. This was discussed in [40]. The result is that one can simply eliminate the first primary invariant using

$$\theta_1 = -\phi_1 \theta_2 - \phi_2 \theta_3 - \phi_3 \eta_2 - \phi_4 \eta_3 - \phi_5 \eta_4, \tag{86}$$

yielding

$$\text{span}\{s_\alpha\} = \bigoplus_{i=1}^{100} \eta_i \mathbb{C}[\theta_2, \theta_3, \theta_4, \theta_5]_{k_h - \deg(\eta_i)} \tag{87}$$

---

<sup>17</sup>The degrees of the  $\theta_j, \eta_i$  are multiples of 5, of course.

where  $\alpha = 0, \dots, N^{\mathbb{Z}_5 \times \mathbb{Z}_5}(k_h) - 1$ . The number  $N^{\mathbb{Z}_5 \times \mathbb{Z}_5}(k_h)$  of  $\mathbb{Z}_5 \times \mathbb{Z}_5$ -invariant homogeneous degree- $k_h$  polynomials modulo  $\tilde{Q} = 0$  was tabulated in [40]. In particular, the first three values are

$$N^{\mathbb{Z}_5 \times \mathbb{Z}_5}(0) = 1, \quad N^{\mathbb{Z}_5 \times \mathbb{Z}_5}(5) = 5, \quad N^{\mathbb{Z}_5 \times \mathbb{Z}_5}(10) = 35, \quad (88)$$

which we will use below.

We now have everything in place to compute the metric on  $Q$ . First, one specifies the five complex structure parameters  $\phi_i$  which define the  $\mathbb{Z}_5 \times \mathbb{Z}_5$ -symmetric covering space  $\tilde{Q}$ . Then, all one has to do is to replace the homogeneous polynomials in the procedure outlined in Section 4 by  $\mathbb{Z}_5 \times \mathbb{Z}_5$ -invariant homogeneous polynomials. Donaldson's algorithm then calculates the Calabi-Yau metric on the  $\mathbb{Z}_5 \times \mathbb{Z}_5$ -symmetric quintic  $\tilde{Q}$  and, hence, the metric on the quotient  $Q = \tilde{Q}/(\mathbb{Z}_5 \times \mathbb{Z}_5)$ . In fact, we use a refinement of this method which is even more efficient, that is, achieves higher numerical accuracy in less computing time. As it is not relevant to the spectrum of the Laplace operator, we relegate the details to Appendix C. Henceforth, we will always use the following parameters in the computation of the metric.

- The degree of the invariant homogeneous polynomials for the Kähler potential is taken to be

$$k_h = 10. \quad (89)$$

- The number of points used to evaluate the T-operator is

$$n_h = 10 \times \left( \# \text{ of independent entries in } h^{\alpha\bar{\beta}} \right) + 100,000 = 406,250. \quad (90)$$

Note that  $h^{\alpha\bar{\beta}}$ , the matrix of free parameters in Donaldson's ansatz for the metric, is block diagonal in Appendix C. Therefore, the total number of independent entries is in fact 30,625 and not simply  $N^{\mathbb{Z}_5 \times \mathbb{Z}_5}(10)^2 = 1,225$ .

As always, it is unenlightening to present the numerical result for the approximation to the Calabi-Yau metric. It is useful, however, to consider the error measure  $\sigma_{10}$ . As an important example, let us choose as our Calabi-Yau manifold the  $\mathbb{Z}_5 \times \mathbb{Z}_5$  quotient of the Fermat quintic  $\tilde{Q}_F$ . The computation of the metric takes about half an hour of wall time, with the resulting error measure of  $\sigma_{10} = 2.8 \times 10^{-2}$ .

## 5.2 The Laplacian on the Quotient

Having computed the Calabi-Yau metric on the quotient  $Q = \tilde{Q}/(\mathbb{Z}_5 \times \mathbb{Z}_5)$ , we now turn to the calculation of the spectrum of the Laplace-Beltrami operator  $\Delta$ . To begin, one must specify a finite-dimensional approximation to the space of complex valued functions on  $Q$ . Note, however, that the scalar functions on  $Q$  are precisely the invariant functions on the covering space  $\tilde{Q}$ . More formally, an invariant function on

$\tilde{Q}$  is of the form  $q^*f = f \circ q$ , where  $f$  is a function on the quotient  $Q$  and  $q : \tilde{Q} \rightarrow Q$  is the quotient map. Hence, we will specify a finite-dimensional approximation to the space of complex-valued  $\mathbb{Z}_5 \times \mathbb{Z}_5$ -invariant functions on  $\tilde{Q}$ . For any finite value of  $k_\phi$ , we choose

$$\mathcal{F}_{k_\phi}^{\mathbb{Z}_5 \times \mathbb{Z}_5} = \text{span} \left\{ \frac{s_\alpha \bar{s}_\beta}{\left( \sum_{i=0}^4 |z_i|^2 \right)^{k_\phi}} \mid \alpha, \beta = 0, \dots, N^{\mathbb{Z}_5 \times \mathbb{Z}_5}(k_\phi) - 1 \right\}, \quad (91)$$

where  $\{s_\alpha\}$  is a basis for the invariant homogeneous polynomials modulo the hyper-surface constraint

$$\text{span}\{s_\alpha\} = \mathbb{C} [z_0, \dots, z_4]_{k_\phi}^{\mathbb{Z}_5 \times \mathbb{Z}_5} / \langle \tilde{Q}(z) \rangle. \quad (92)$$

We already had to determine such a basis while applying Donaldson's algorithm for the metric, the only difference now is that the degree is  $k_\phi$  instead of  $k_h$ . The counting function  $N^{\mathbb{Z}_5 \times \mathbb{Z}_5}(k_\phi)$  is the same, and some of its values were given in eq. (88). Clearly,

$$\dim \mathcal{F}_{k_\phi}^{\mathbb{Z}_5 \times \mathbb{Z}_5} = \left( N^{\mathbb{Z}_5 \times \mathbb{Z}_5}(k_\phi) \right)^2. \quad (93)$$

Having specified  $\mathcal{F}_{k_\phi}^{\mathbb{Z}_5 \times \mathbb{Z}_5}$ , we can now calculate any matrix element on  $Q$  simply by replacing the approximating space of functions on  $Q$  by the invariant functions on  $\tilde{Q}$  and integrating over  $\tilde{Q}$ . For example, the matrix elements of the Laplacian on  $Q$  are

$$\Delta_{ab} = \langle f_a | \Delta | f_b \rangle = \int_Q \bar{f}_a \Delta f_b \, d\text{Vol}(Q) = \frac{1}{|\mathbb{Z}_5 \times \mathbb{Z}_5|} \int_{\tilde{Q}} (q^* \bar{f}_a) \Delta (q^* f_b) \, d\text{Vol}(\tilde{Q}). \quad (94)$$

Computing the matrix elements requires another numerical integration that is completely independent of the one in the T-operator. As previously, we denote the number of points in the matrix element integration by  $n_\phi$ .

Having evaluated the matrix elements, one can now numerically solve the matrix eigenvalue equation eq. (11) for the eigenvalues and eigenfunctions of the Laplacian. Note that the factors of  $\frac{1}{|\mathbb{Z}_5 \times \mathbb{Z}_5|}$  cancel out of this equation, leaving identical eigenvalues and eigenfunctions on  $\tilde{Q}$  and  $Q$ , respectively. Since the functions in  $\mathcal{F}_{k_\phi}^{\mathbb{Z}_5 \times \mathbb{Z}_5}$  live on the covering space, we are actually solving

$$\Delta_{\tilde{Q}} \phi_n = \lambda_n^{\mathbb{Z}_5 \times \mathbb{Z}_5} \phi_n, \quad \phi_n \in C^\infty(\tilde{Q}, \mathbb{C})^{\mathbb{Z}_5 \times \mathbb{Z}_5} \quad (95)$$

on  $\tilde{Q}$ . Note that, as always, the volume measure of the integrals is chosen so that  $\text{Vol}(\tilde{Q}) = 1$ . For the reasons stated above, the invariant eigenfunctions on  $\tilde{Q}$  can be identified with the eigenfunctions of the Laplacian on  $Q$  at the same eigenvalue, but with  $\text{Vol}(Q) = \frac{1}{|\mathbb{Z}_5 \times \mathbb{Z}_5|} = \frac{1}{25}$ . However, since we want to adhere to our convention of normalizing  $\text{Vol}(Q) = 1$ , we have to rescale the volume and hence the eigenvalues  $\lambda_n^{\mathbb{Z}_5 \times \mathbb{Z}_5}$ . Using eqns. (3) and (4), the eigenvalues  $\lambda_n$  on  $Q$  are

$$\lambda_n = \frac{\lambda_n^{\mathbb{Z}_5 \times \mathbb{Z}_5}}{\sqrt[3]{25}}. \quad (96)$$



Using this method, one can compute the spectrum of the Laplace-Beltrami operator on the quotient of any  $\mathbb{Z}_5 \times \mathbb{Z}_5$  symmetric quintic.

### 5.3 Quotient of the Fermat Quintic

As an explicit example, let us consider the quotient of the Fermat quintic,

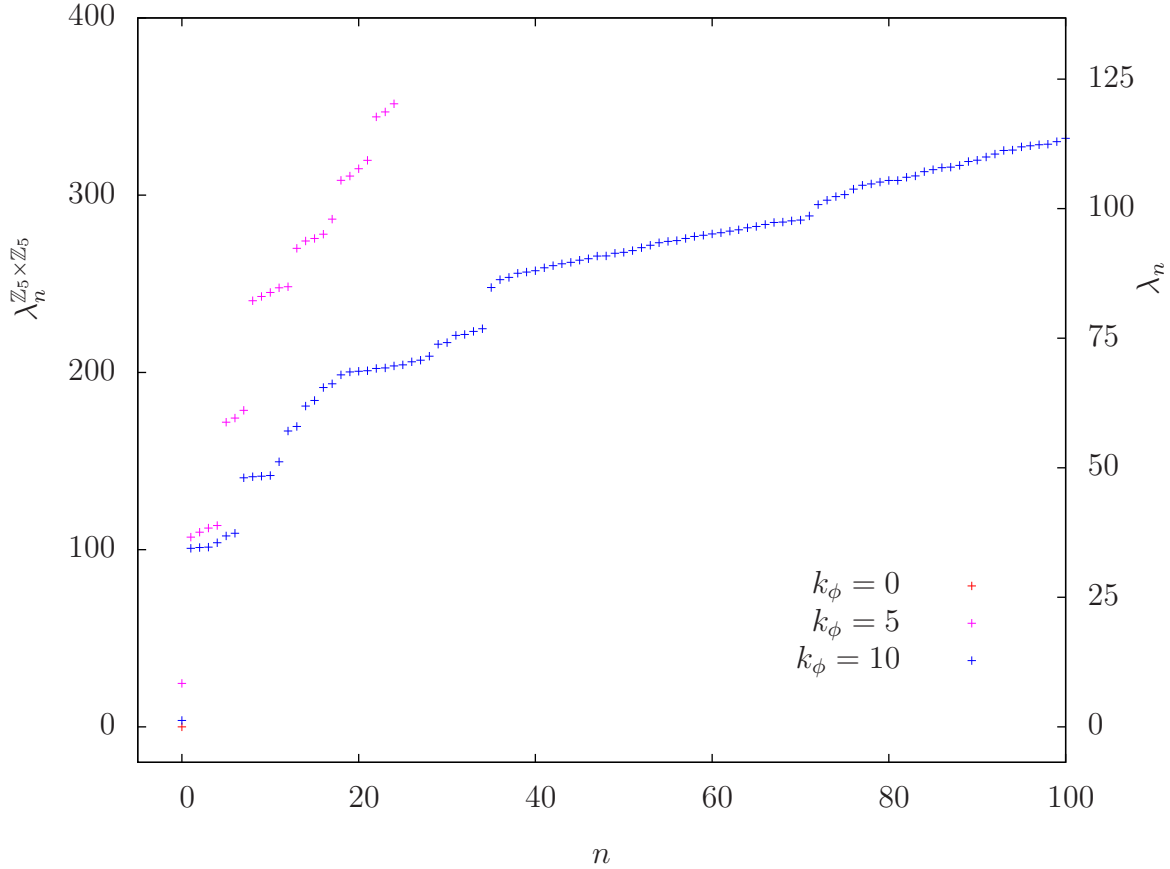


**Figure 12:** Eigenvalues  $\lambda_n^{\mathbb{Z}_5 \times \mathbb{Z}_5}$  of the scalar Laplace operator on the Fermat quintic  $\tilde{Q}_F$  acting on  $\mathbb{Z}_5 \times \mathbb{Z}_5$ -invariant eigenfunctions. Up to an overall factor due to our volume normalization, these are the same as the eigenvalues  $\lambda_n$  of the scalar Laplace operator on the quotient  $Q_F = \tilde{Q}_F / (\mathbb{Z}_5 \times \mathbb{Z}_5)$ . The metric is computed at degree  $k_h = 10$  and  $n_h = 406,250$  points. The Laplace operator is evaluated using  $n_\phi = 100,000$  points.

$$Q_F = \tilde{Q}_F / (\mathbb{Z}_5 \times \mathbb{Z}_5). \quad (97)$$

$n$	$\lambda_n^{\mathbb{Z}_5 \times \mathbb{Z}_5}$	$\lambda_n = \frac{\lambda_n^{\mathbb{Z}_5 \times \mathbb{Z}_5}}{\sqrt[3]{25}}$	$\hat{\lambda}$	$\mu$
0	3.586	1.226	$\hat{\lambda}_0 = 1.23$	$\mu_0 = 1$
1	100.7	34.45	$\hat{\lambda}_1 = 34.8 \pm 0.5$	$\mu_1 = 4$
2	101.2	34.61		
3	101.4	34.68		
4	103.9	35.53		
5	107.8	36.86	$\hat{\lambda}_2 = 37.1 \pm 0.4$	$\mu_2 = 2$
6	109.2	37.36		
7	140.50	48.05	$\hat{\lambda}_3 = 48.3 \pm 0.2$	$\mu_3 = 4$
8	141.16	48.28		
9	141.47	48.38		
10	141.78	48.49		
11	149.57	51.15	$\hat{\lambda}_4 = 51.2$	$\mu_4 = 1$
12	166.91	57.08	$\hat{\lambda}_5 = 57.5 \pm 0.6$	$\mu_5 = 2$
13	169.48	57.96		
14	181.00	61.90	$\hat{\lambda}_6 = 62.4 \pm 0.8$	$\mu_6 = 2$
15	184.15	62.98		
16	191.49	65.48	$\vdots$	$\vdots$
17	193.55	66.19		
18	198.65	67.94		
$\vdots$	$\vdots$	$\vdots$		

**Table 4:** Low-lying eigenvalues of the scalar Laplace operator on  $Q_F$ , the  $\mathbb{Z}_5 \times \mathbb{Z}_5$ -quotient of the Fermat quintic, computed with  $k_h = k_\phi = 10$ ,  $n_h = 406,250$ ,  $n_\phi = 100,000$ . The first two columns are the numerical results. The third column specifies  $\hat{\lambda}$ , the average over the eigenvalues that are converging to a single degenerate level. The final column counts the multiplicities of each such level.

We numerically computed the spectrum of the scalar Laplace operator for each of the three values  $k_\phi = 0, 5, 10$  using eq. (88). The resulting eigenvalues are shown in Figure 12. Note that we present both the eigenvalues  $\lambda_n^{\mathbb{Z}_5 \times \mathbb{Z}_5}$  on  $\tilde{Q}$  as well as the normalized eigenvalues  $\lambda_n$  on  $Q$  defined by eq. (96).

We list the numerical values of the first few eigenvalues in Table 4 and make the following two observations. First, the lowest eigenvalue  $\lambda_0$  is no longer zero up to machine precision, as it was in Table 2. This is so because the constant function is not part of the approximate space of functions at  $k_\phi = 10$  and, therefore, the lowest eigenvalue  $\lambda_0$  only approaches zero as  $k_\phi$  increases. The actual numerical value  $\lambda_0 \approx 1.2$  gives us an estimate of the error introduced by truncating the space of functions. Second, the low-lying eigenvalues clearly form degenerate levels. As usual, the numerical error caused by the truncation of the space of functions increases as we go to higher eigenvalues. However, the first 16 eigenvalues are sufficiently well separated that we can conjecture the underlying multiplicities  $\mu$ . We list these degeneracies together with the best approximation to the true eigenvalue  $\hat{\lambda}$  in Table 4. Clearly, the degeneracies in the spectrum strongly hint at an underlying symmetry. We will discuss the associated isometry group in the following subsection.

## 5.4 Group Theory and the Quotient Eigenmodes

The free  $\mathbb{Z}_5 \times \mathbb{Z}_5$  action eq. (75) is a subgroup of the symmetries of the Fermat quintic,

$$\mathbb{Z}_5 \times \mathbb{Z}_5 \subset \overline{\text{Aut}}(\tilde{Q}_F), \quad (98)$$

given in eq. (66). Naively, one now would like to form the quotient to obtain the remaining symmetries on  $Q_F = \tilde{Q}_F / (\mathbb{Z}_5 \times \mathbb{Z}_5)$ . However, the  $\mathbb{Z}_5 \times \mathbb{Z}_5$  subgroup is not normal, that is, not closed under conjugation. The only possibility is to form the normal closure<sup>18</sup>

$$\langle \mathbb{Z}_5 \times \mathbb{Z}_5 \rangle^{\overline{\text{Aut}}(\tilde{Q}_F)} = \left\{ h^{-1}gh \mid g \in \mathbb{Z}_5 \times \mathbb{Z}_5, h \in \overline{\text{Aut}}(\tilde{Q}_F) \right\}. \quad (99)$$

The quotient by the normal closure is well-defined, and we obtain

$$\overline{\text{Aut}}(Q_F) = \overline{\text{Aut}}(\tilde{Q}_F) / \langle \mathbb{Z}_5 \times \mathbb{Z}_5 \rangle^{\overline{\text{Aut}}(\tilde{Q}_F)} = D_{20}, \quad (100)$$

the dihedral group with 20 elements. However, just looking at the representation theory of  $\overline{\text{Aut}}(Q_F)$  is insufficient to understand the multiplicities of the eigenvalues of the Laplacian. Instead, one must use all of  $\overline{\text{Aut}}(\tilde{Q}_F)$ , even those elements (called “pseudo-symmetries” in [41]) that do not correspond to symmetries of the quotient  $Q_F$ . On a practical level, we also note that  $D_{20}$  has only 1- and 2-dimensional irreducible representations and could never explain the multiplicity  $\mu_1(Q_F) = 4$ , for example, listed in Table 4.

---

<sup>18</sup>Also called the conjugate closure.

$d$	1	2	4	5	6	8	10	12	20	30	40	60	80	120
$n_d$	4	4	4	4	2	4	4	2	8	8	12	18	4	2
$\dim_d^{\mathbb{Z}_5 \times \mathbb{Z}_5}$	1	2	0	1	2	0	2	4	0	2	0	4	0	4

**Table 5:** Number  $n_d$  of distinct irreducible representations of  $\overline{\text{Aut}}(\tilde{Q}_F)$  in complex dimension  $d$ . We also list the dimension  $\dim_d^{\mathbb{Z}_5 \times \mathbb{Z}_5}$  of the  $\mathbb{Z}_5 \times \mathbb{Z}_5$ -invariant subspace for each representation, see eq. (103). Note that it turns out to only depend on the dimension  $d$  of the representation.

$\tilde{Q}_F$	$\longrightarrow$	$Q_F$
$\mu_0(\tilde{Q}_F) = 1$	$\longrightarrow$	$\mu_0(Q_F) = 1$
$\mu_1(\tilde{Q}_F) = 20$	$\longrightarrow$	0
$\mu_2(\tilde{Q}_F) = 20$	$\longrightarrow$	0
$\mu_3(\tilde{Q}_F) = 4$	$\longrightarrow$	0
$\mu_4(\tilde{Q}_F) = 60$	$\longrightarrow$	$\mu_1(Q_F) = 4$
$\mu_5(\tilde{Q}_F) = 30$	$\longrightarrow$	$\mu_2(Q_F) = 2$

**Table 6:** Projection of the multiplicity of eigenvalues on the Fermat quintic  $\tilde{Q}_F$  to the  $\mathbb{Z}_5 \times \mathbb{Z}_5$ -quotient  $Q_F$ .

As we discussed in Subsection 4.3, the symmetry group of the Fermat quintic has 80 distinct irreducible representations occurring in 14 different dimensions. Let us label them by  $\rho_{d,i}$ , where  $d$  is the complex dimension and  $i = 1, \dots, n_d$  distinguishes the  $n_d$  different representations in dimension  $d$ . Under the  $\mathbb{Z}_5 \times \mathbb{Z}_5$  quotient

$$\tilde{Q}_F \longrightarrow Q_F = \tilde{Q}_F / (\mathbb{Z}_5 \times \mathbb{Z}_5) \quad (101)$$

all non-invariant eigenfunctions of the Laplacian are projected out and each invariant eigenfunction descends to an eigenfunction on  $Q_F$ . Hence, the degeneracies of the eigenvalues are counted by the dimension

$$\dim(\rho_{d,i}^{\mathbb{Z}_5 \times \mathbb{Z}_5}) \quad (102)$$

of the  $\mathbb{Z}_5 \times \mathbb{Z}_5$ -invariant subspace. It turns out that, for the chosen  $\mathbb{Z}_5 \times \mathbb{Z}_5 \subset \overline{\text{Aut}}(\tilde{Q}_F)$ , this dimension depends only on  $d$ , and not on the index  $i$ . We denote the common value by

$$\dim_d^{\mathbb{Z}_5 \times \mathbb{Z}_5} = \dim(\rho_{d,1}^{\mathbb{Z}_5 \times \mathbb{Z}_5}) = \dots = \dim(\rho_{d,n_d}^{\mathbb{Z}_5 \times \mathbb{Z}_5}) \quad (103)$$

and tabulate it in Table 5.

Using this and the multiplicities of the eigenvalues on the Fermat quintic  $\tilde{Q}_F$  given in Table 2, we can now perform the  $\mathbb{Z}_5 \times \mathbb{Z}_5$ -quotient and obtain the degeneracies of

the scalar Laplacian on the  $Q_F$ . The results are listed in Table 6. We find complete agreement with the spectrum found by directly computing the eigenvalues on  $Q_F$  given in Table 4. Naturally, this comparison is limited by the number of eigenvalues we were able to compute on  $\tilde{Q}_F$ . The agreement of the lower lying levels, however, gives us confidence that the values of  $\hat{\lambda}_m$  and  $\mu_m$  for  $m = 3, 4, 5, 6, \dots$  given in Table 4 are also a good approximation to the exact results on the quotient.

## 5.5 Varying the Complex Structure

To numerically compute any metric-dependent quantity on a Calabi-Yau manifold, one has to fix the complex structure and Kähler moduli to specific values. This was done, for example, in Subsection 5.3, where the moduli were chosen so that the covering space was the Fermat quintic with unit volume. In this section, we will extend our results to the one-parameter family of  $\mathbb{Z}_5 \times \mathbb{Z}_5$  symmetric quintics  $\tilde{Q}_\psi$  defined by the vanishing of the polynomial

$$\tilde{Q}_\psi = \sum z_i^5 - 5\psi \prod z_i. \quad (104)$$

The Kahler modulus will always be fixed so that the volume of  $\tilde{Q}_\psi$  is unity. The complex structure parameter  $\psi$  can, in principle, take on any complex value. However, for simplicity, we will only consider  $\psi \in \mathbb{R}$  in this subsection. Note that each  $\tilde{Q}_\psi$  is indeed a quintic with the free  $\mathbb{Z}_5 \times \mathbb{Z}_5$  symmetry in eq. (76). Hence, the quotient

$$Q_\psi = \tilde{Q}_\psi / (\mathbb{Z}_5 \times \mathbb{Z}_5) \quad (105)$$

is a smooth Calabi-Yau threefold.

We have computed the spectrum of the scalar Laplace operator on this one-parameter family of quotients for various values of  $\psi$ . The resulting  $\psi$ -dependent spectrum can be found in Figure 13. Note that this one-parameter family of  $\mathbb{Z}_5 \times \mathbb{Z}_5$ -symmetric quintics passes through two special points,

$\psi = 0$ : Without the  $\prod z_i$  term,  $\tilde{Q}_{\psi=0} = \tilde{Q}_F$  is exactly the Fermat quintic. We will investigate the symmetry enhancement at this point in the next subsection.

$\psi = 1$ : This is the so-called conifold point, where the quintic is singular. On the covering space  $\tilde{Q}_{\psi=1} \subset \mathbb{P}^4$ , the singularity is at

$$z_C = [1 : 1 : 1 : 1 : 1] \quad (106)$$

and its images under the  $\mathbb{Z}_5 \times \mathbb{Z}_5$  symmetry group. At these points the hypersurface equation fails to be transversal,

$$\frac{\partial \tilde{Q}_{\psi=1}}{\partial z_0}(z_C) = \dots = \frac{\partial \tilde{Q}_{\psi=1}}{\partial z_4}(z_C) = \tilde{Q}_{\psi=1}(z_C) = 0, \quad (107)$$

causing the singularity.

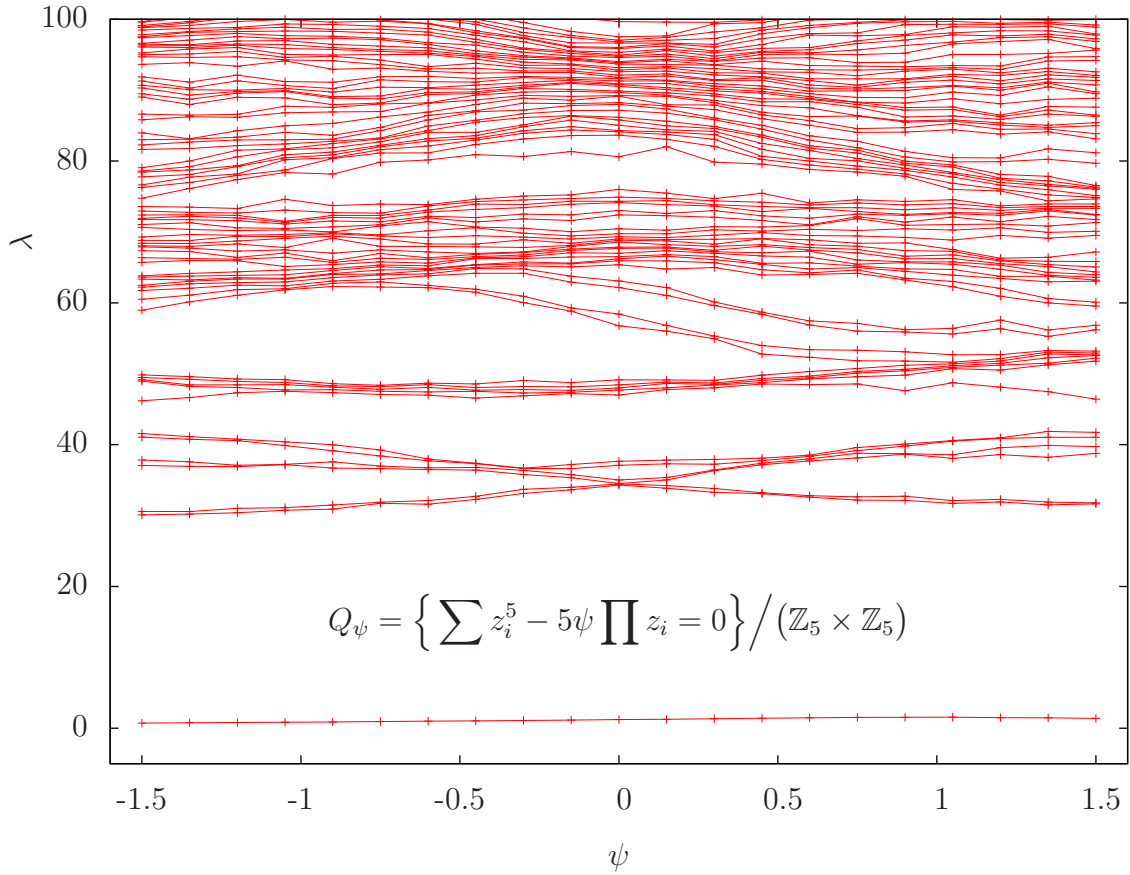


**Figure 13:** Spectrum of the scalar Laplace operator on the real 1-parameter family  $Q_\psi$  of quintic quotients. The metric is computed at degree  $k_h = 10$  with  $n_h = 406,250$ . The Laplace operator is evaluated at  $k_\phi = 10$  and  $n_\phi = 50,000$  points.

Perhaps surprisingly, the spectrum of the scalar Laplace operator shows no trace of the conifold singularity at  $\psi = 1$ . However, the reason for this is straightforward. The low-lying modes are slowly-varying functions and, in particular, are almost constant near any point-like singularity. For example, the first massive eigenvalue is essentially determined by the diameter of the manifold, see Subsection 7.2, and does not depend on local details of the metric.

## 5.6 Branching Rules

Let us return to spectrum of the Laplace-Beltrami operator in Figure 13 and focus on the neighbourhood of  $\psi = 0$ . Clearly,  $Q_{\psi=0} = Q_F$  is the quotient of the Fermat quintic, while  $Q_{\psi \neq 0}$  is a deformation of the Fermat quotient that breaks part of its discrete isometry group. In particular, note that for small non-zero values of  $\psi$

- The first massive level  $\mu_1(Q_F) = 4$  splits into two pairs of eigenvalues.
- The second massive level  $\mu_2(Q_F) = 2$  remains two-fold degenerate.

In this subsection, we will attempt to understand this from the group-theoretical perspective.

As discussed in Subsection 5.4, the multiplicities of the eigenvalues on the quotient  $Q_\psi = \tilde{Q}_\psi / (\mathbb{Z}_5 \times \mathbb{Z}_5)$  are really determined by the representation theory of the symmetry group of the covering space. We have to distinguish two cases.

$\psi = 0$ : This is the case of the Fermat quintic, whose symmetries we already discussed in Subsection 4.3,

$$\overline{\text{Aut}}(\tilde{Q}_{\psi=0}) = \overline{\text{Aut}}(\tilde{Q}_F) = (S_5 \times \mathbb{Z}_2) \times (\mathbb{Z}_5)^4. \quad (108)$$

The irreducible representations of  $\overline{\text{Aut}}(\tilde{Q}_F)$  were presented in Table 5.

$\psi \neq 0$ : In this case, the invariance of the  $\prod z_i$  monomial gives one further constraint on the  $(\mathbb{Z}_5)^4$  phase rotations. In other words, turning on  $\psi$  breaks the phase rotation symmetry to  $(\mathbb{Z}_5)^3$ . The remaining symmetry group is<sup>19</sup>

$$\overline{\text{Aut}}(\tilde{Q}_{\psi \neq 0}) = (S_5 \times \mathbb{Z}_2) \times (\mathbb{Z}_5)^3. \quad (109)$$

The irreducible representations of  $\overline{\text{Aut}}(\tilde{Q}_{\psi \neq 0})$  are given in Table 7. Note that, by construction, this group is a proper subgroup of the full symmetry group, both of which containing the free  $\mathbb{Z}_5 \times \mathbb{Z}_5$  action. That is,

$$\overline{\text{Aut}}(\tilde{Q}_{\psi=0}) \supset \overline{\text{Aut}}(\tilde{Q}_{\psi \neq 0}) \supset \mathbb{Z}_5 \times \mathbb{Z}_5. \quad (110)$$

$d$	1	4	5	6	20	24	30	40	48	60
$n_d$	4	4	4	2	8	2	8	4	2	2
$\dim_d^{\mathbb{Z}_5 \times \mathbb{Z}_5}$	1	0	1	2	0	4	2	0	0	4

**Table 7:** Number  $n_d$  of distinct irreducible representations of  $\overline{\text{Aut}}(\tilde{Q}_{\psi \neq 0})$  in complex dimension  $d$ . We also list the dimension  $\dim_d^{\mathbb{Z}_5 \times \mathbb{Z}_5}$  of the  $\mathbb{Z}_5 \times \mathbb{Z}_5$ -invariant subspace for each representation. Note that it turns out to only depend on the dimension  $d$  of the representation.

$\overline{\text{Aut}}(\tilde{Q}_F)$	$\supset$	$\overline{\text{Aut}}(\tilde{Q}_{\psi \neq 0})$	$\overline{\text{Aut}}(\tilde{Q}_F)$	$\supset$	$\overline{\text{Aut}}(\tilde{Q}_{\psi \neq 0})$
<u>1</u>	$\longrightarrow$	<u>1</u>	<u>20</u>	$\longrightarrow$	<u>20</u>
<u>2</u>	$\longrightarrow$	<u>1</u> $\oplus$ <u>1</u>	<u>30</u>	$\longrightarrow$	<u>30</u>
<u>4</u>	$\longrightarrow$	<u>4</u>	<u>40</u> <sub>1</sub>	$\longrightarrow$	<u>40</u>
<u>5</u>	$\longrightarrow$	<u>5</u>	<u>40</u> <sub>2</sub>	$\longrightarrow$	<u>20</u> $\oplus$ <u>20</u>
<u>6</u>	$\longrightarrow$	<u>6</u>	<u>60</u> <sub>1</sub>	$\longrightarrow$	<u>60</u>
<u>8</u>	$\longrightarrow$	<u>4</u> $\oplus$ <u>4</u>	<u>60</u> <sub>2</sub>	$\longrightarrow$	<u>30</u> $\oplus$ <u>30</u>
<u>10</u>	$\longrightarrow$	<u>5</u> $\oplus$ <u>5</u>	<u>80</u>	$\longrightarrow$	<u>40</u> $\oplus$ <u>40</u>
<u>12</u>	$\longrightarrow$	<u>6</u> $\oplus$ <u>6</u>	<u>120</u>	$\longrightarrow$	<u>48</u> $\oplus$ <u>48</u> $\oplus$ <u>24</u>

**Table 8:** Branching rules for the decomposition of the irreducible representations of  $\overline{\text{Aut}}(\tilde{Q}_F)$  into the irreducible representations of its subgroup  $\overline{\text{Aut}}(\tilde{Q}_{\psi \neq 0})$ . Note that there are always numerous distinct representations in each dimension, see Table 5 and 7. In particular, in dimension 60 there are 10 irreps of  $\overline{\text{Aut}}(\tilde{Q}_F)$ , which we denote by 60<sub>1</sub>, that remain irreducible under  $\overline{\text{Aut}}(\tilde{Q}_{\psi \neq 0})$  and 8 irreps, denoted by 60<sub>2</sub>, that branch into two distinct 30-dimensional irreducible representations.



As one turns on the  $\psi$ -deformation, the eigenvalues must split according to the group-theoretical branching rules. We list these in Table 8.

Finally, we are really interested in the eigenvalues on the quotient  $Q_\psi$ , which means that one must restrict to the  $\mathbb{Z}_5 \times \mathbb{Z}_5$ -invariants of each representation. For the Fermat quintic, we listed the number and the dimension,  $\dim_d^{\mathbb{Z}_5 \times \mathbb{Z}_5}$ , of these invariants in Table 5. We list the analogous information for the  $\mathbb{Z}_5 \times \mathbb{Z}_5$ -invariants within the irreducible representations of  $\overline{\text{Aut}}(\tilde{Q}_{\psi \neq 0})$  in Table 7. This allows us to compute the splitting of the eigenvalues on the quotient  $Q_\psi$ . However, just knowing the multiplicities turns out to be not quite enough since same-dimensional but different irreducible representations can branch in different ways. In particular, the first massive level on  $Q_{\psi=0}$  comes from a 60-dimensional representation of  $\tilde{Q}_{\psi=0}$ , which can branch in two ways according to Table 8. However, since we have seen in Figure 13 that the eigenvalues do branch, this 60-dimensional representation must be of the type **60**<sub>2</sub>.

To summarize, these group theoretical considerations are completely compatible with the observed branching of the eigenvalues under the complex structure deformation by  $\psi$ . The low-lying eigenvalues of the scalar Laplacian on  $Q_\psi$  split as

$\mathbb{Z}_5 \times \mathbb{Z}_5$ invariants	$\subset$	$\overline{\text{Aut}}(\tilde{Q}_{\psi=0})$ irreps	$\overline{\text{Aut}}(\tilde{Q}_{\psi \neq 0})$ irreps	$\supset$	$\mathbb{Z}_5 \times \mathbb{Z}_5$ invariants	
$\mu_0(Q_{\psi=0}) = 1$	$\subset$	<b>1</b>	$\longrightarrow$ <b>1</b>	$\supset$	$\mu_0(Q_{\psi \neq 0}) = 1$	(111)
$\mu_1(Q_{\psi=0}) = 4$	$\subset$	<b>60</b> <sub>2</sub>	$\begin{array}{c} \nearrow \text{30} \\ \oplus \\ \searrow \text{30} \end{array}$	$\supset$	$\mu_2(Q_{\psi \neq 0}) = 2$	
$\mu_2(Q_{\psi=0}) = 2$	$\subset$	<b>30</b>	$\longrightarrow$ <b>30</b>	$\supset$	$\mu_1(Q_{\psi \neq 0}) = 2$	
$\mu_3(Q_{\psi=0}) = 2$	$\subset$	<b>30</b>	$\longrightarrow$ <b>30</b>	$\supset$	$\mu_3(Q_{\psi \neq 0}) = 2$ .	

## 5.7 Another Family

Finally, let us consider another family of complex structure moduli. First, we deform the Fermat quintic to a generic  $\mathbb{Z}_5 \times \mathbb{Z}_5$  invariant polynomial; that is, switch on all coefficients in eq. (76). Then restrict to the real one-parameter family of covering spaces defined by

$$\begin{aligned}
\tilde{Q}_\varphi = & \sum z_i^5 + \varphi \prod z_i^5 + i\varphi(z_0^3 z_1 z_4 + \text{cyc}) \\
& + (1 - i)\varphi(z_0^2 z_1 z_2^2 + \text{cyc}) - (1 - 2i)\varphi(z_0^2 z_1^2 z_3 + \text{cyc}) \\
& - (2 - i)\varphi(z_0^3 z_2 z_3 + \text{cyc})
\end{aligned} \tag{112}$$

and form the quotient spaces

$$Q_\varphi = \tilde{Q}_\varphi / (\mathbb{Z}_5 \times \mathbb{Z}_5). \tag{113}$$

---

<sup>19</sup>Since we chose  $\psi$  to be real, the complex conjugation  $\mathbb{Z}_2$  remains unbroken.

For generic values of  $\varphi$ , this breaks all symmetries of the Fermat quintic except for the free  $\mathbb{Z}_5 \times \mathbb{Z}_5$  that we are dividing out. Consequently, we expect no degeneracies in the spectrum of the Laplace-Beltrami operator. In Figure 14, we plot the spectrum of

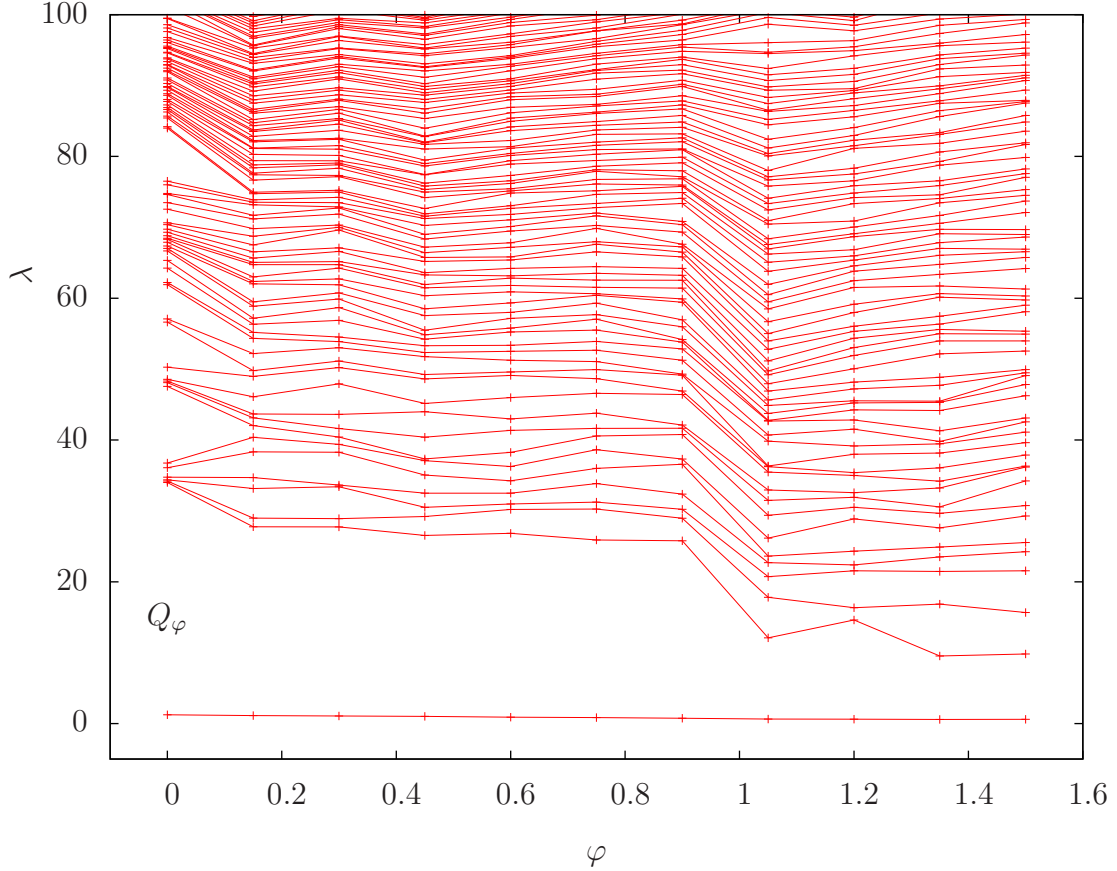


**Figure 14:** *Spectrum of the scalar Laplace operator on the real 1-parameter family  $Q_\varphi$  of quintic quotients. The metric is computed at degree  $k_h = 10$ ,  $n_h = 406,250$  and the Laplace operator evaluated at  $k_\phi = 10$  and  $n_\phi = 50,000$  points.*

$\Delta$  and, indeed, observe that the degeneracies of the eigenvalues on the Fermat quintic  $Q_{\varphi=0}$  are broken as  $\varphi$  is turned on.

## 6 A Heterotic Standard Model Manifold

In this last section, we will compute the spectrum of the Laplace-Beltrami operator on the torus-fibered Calabi-Yau threefold  $X$  with  $\pi_1(X) = \mathbb{Z}_3 \times \mathbb{Z}_3$  that was used in [50] to construct a heterotic standard model. The threefold  $X$  is most easily described in

terms of its universal cover  $\tilde{X}$ , which is the complete intersection

$$\tilde{X} = \left\{ \tilde{P}(x, t, y) = 0 = \tilde{R}(x, t, y) \right\} \subset \mathbb{P}_{[x_0:x_1:x_2]}^2 \times \mathbb{P}_{[t_0:t_1]}^1 \times \mathbb{P}_{[y_0:y_1:y_2]}^2 \quad (114)$$

defined by the degree-(3, 1, 0) and (0, 1, 3) polynomials

$$\begin{aligned} \tilde{P}(x, t, y) &= t_0 \left( x_0^3 + x_1^3 + x_2^3 + \lambda_1 x_0 x_1 x_2 \right) + t_1 \lambda_3 \left( x_0^2 x_2 + x_1^2 x_0 + x_2^2 x_1 \right) \\ \tilde{R}(x, t, y) &= t_1 \left( y_0^3 + y_1^3 + y_2^3 + \lambda_2 y_0 y_1 y_2 \right) + t_0 \left( y_0^2 y_1 + y_1^2 y_2 + y_2^2 y_0 \right). \end{aligned} \quad (115)$$

Note that  $\lambda_1, \lambda_2, \lambda_3 \in \mathbb{C}$  end up parametrizing the complex structure of  $X$ . For generic  $\lambda_i$ , the two maps

$$\gamma_1 : \begin{cases} [x_0 : x_1 : x_2] \mapsto [x_0 : \omega x_1 : \omega^2 x_2] \\ [t_0 : t_1] \mapsto [t_0 : \omega t_1] \\ [y_0 : y_1 : y_2] \mapsto [y_0 : \omega y_1 : \omega^2 y_2] \end{cases} \quad (116a)$$

and

$$\gamma_2 : \begin{cases} [x_0 : x_1 : x_2] \mapsto [x_1 : x_2 : x_0] \\ [t_0 : t_1] \mapsto [t_0 : t_1] \\ [y_0 : y_1 : y_2] \mapsto [y_1 : y_2 : y_0] \end{cases} \quad (116b)$$

generate a free  $\mathbb{Z}_3 \times \mathbb{Z}_3$  group action on  $\tilde{X}$ . Hence, the quotient

$$X = \tilde{X} / (\mathbb{Z}_3 \times \mathbb{Z}_3) \quad (117)$$

is a smooth Calabi-Yau threefold. In addition to the  $h^{2,1}(X) = 3$  complex structure moduli of  $X$ , there are also  $h^{1,1}(X) = 3$  Kähler moduli. The Kähler class on the algebraic variety  $X$  is determined by a line bundle  $\mathcal{L}$  whose first Chern class is represented by the Kähler class,

$$c_1(\mathcal{L}) = [\omega_X] \in H^{1,1}(X, \mathbb{Z}) = H^{1,1}(X, \mathbb{C}) \cap H^2(X, \mathbb{Z}). \quad (118)$$

Pulling back to the covering space with the quotient map  $q$ , the Kähler class is equivalently encoded by an equivariant<sup>20</sup> line bundle

$$q^*(\mathcal{L}) = \mathcal{O}_{\tilde{X}}(a_1, b, a_2), \quad (119)$$

which is determined by some  $a_1, b, a_2 \in \mathbb{Z}_{>0}$ . Note that, by definition, the sections of  $\mathcal{O}_{\tilde{X}}(a_1, b, a_2)$  are the homogeneous polynomials in  $x, t$ , and  $y$  of multidegree  $(a_1, b, a_2)$ .

We now want to compute the Calabi-Yau metric on the quotient  $X$  using Donaldson's algorithm. However, as discussed in detail in the previous section, we will

---

<sup>20</sup>As was shown in [42, 40], equivariance requires  $a_1 + a_2 \equiv 0 \pmod{3}$ . We will always use the equivariant action specified by eqns. (116a) and (116b).

formulate everything in terms of  $\mathbb{Z}_3 \times \mathbb{Z}_3$ -invariant data on the covering space  $\tilde{X}$ . First, one has to pick a multidegree

$$k_h = (a_1, b, a_2) \in (\mathbb{Z}_{>0})^3, \quad a_1 + a_2 \equiv 0 \pmod{3} \quad (120)$$

determining the Kähler class of the metric. Then one has to find a basis

$$\begin{aligned} \text{span} \{s_\alpha | \alpha = 0, \dots, N(k_h) - 1\} = \\ = \mathbb{C}[x_0, x_1, x_2, t_0, t_1, y_0, y_1, y_2]_{k_h}^{\mathbb{Z}_3 \times \mathbb{Z}_3} / \langle \tilde{R}(x, t, y), \tilde{P}(x, t, y) \rangle \end{aligned} \quad (121)$$

for the invariant sections of  $\mathcal{O}_{\tilde{X}}(a_1, b, a_2)$  modulo the complete intersection equations, as described in detail in [40]. This is all the data needed to apply Donaldson's algorithm and compute the approximate Calabi-Yau metric. Note that, since we always normalize the volume to unity, the exact Calabi-Yau metric only depends on the ray  $\mathbb{Q}k_h$  but not on the "radial" distance  $\gcd(a_1, b, a_2)$ . However, the number of sections  $N(k_h)$  and, therefore, the number of parameters in the matrix  $h^{\alpha\beta}$ , does depend on  $k_h$  explicitly. Going from  $k_h$  to  $2k_h, 3k_h, \dots$  increases the number of parameters and subsequently improves the accuracy of the Calabi-Yau metric computed through Donaldson's algorithm.

## 6.1 The Spectrum of the Laplacian on $X$

Having determined the metric, we now turn towards the spectrum of the Laplace-Beltrami operator. We do this again by computing the matrix elements of the Laplacian on the covering in an approximate basis of  $\mathbb{Z}_3 \times \mathbb{Z}_3$ -invariant functions, completely analogous to Subsection 5.1. To specify the truncated space of invariant functions on  $\tilde{X}$ , fix a multidegree  $k_\phi$  proportional to  $k_h$ ; that is,

$$k_\phi = (k_{\phi_1}, k_{\phi_2}, k_{\phi_3}) \in \mathbb{Q}k_h \cap (\mathbb{Z}_{\geq 0})^3. \quad (122)$$

Then pick a basis  $\{s_\alpha | \alpha = 0, \dots, N(k_\phi) - 1\}$  of degree- $k_\phi$  homogeneous,  $\mathbb{Z}_3 \times \mathbb{Z}_3$ -invariant polynomials. These define a finite-dimensional space of invariant functions on  $\tilde{X}$  as

$$\mathcal{F}_{k_\phi}^{\mathbb{Z}_3 \times \mathbb{Z}_3} = \left\{ \frac{s_\alpha \bar{s}_\beta}{(\sum |x_i|^2)^{k_{\phi_1}} (\sum |t_i|^2)^{k_{\phi_2}} (\sum |y_i|^2)^{k_{\phi_3}}} \mid \alpha, \beta = 0, \dots, N(k_\phi) - 1 \right\}. \quad (123)$$

By computing the matrix elements of the Laplacian and solving the (generalized) matrix eigenvalue problem, we obtain the eigenvalues  $\lambda_n^{\mathbb{Z}_3 \times \mathbb{Z}_3}$  of the Laplacian on the covering space  $\tilde{X}$  acting on  $\mathbb{Z}_3 \times \mathbb{Z}_3$ -invariant functions. These are identical to the eigenvalues of the Laplacian on  $X$ , but with volume

$$\text{Vol}(X) = \frac{1}{|\mathbb{Z}_3 \times \mathbb{Z}_3|} \text{Vol}(\tilde{X}). \quad (124)$$

In the computation on  $\tilde{X}$  we normalized the volume to unity. Hence, after rescaling the volume of  $X$  back to one, the eigenvalues of the scalar Laplacian on  $X$  are

$$\lambda_n = \frac{\lambda_n^{\mathbb{Z}_3 \times \mathbb{Z}_3}}{\sqrt[3]{9}}. \quad (125)$$

In Figure 15, we compute the spectrum of the Laplace-Beltrami operator on  $X$  at two different points in the Kähler moduli space but with the same complex structure. Recall that we always normalize the volume, corresponding to the “radial” distance in the Kähler moduli space, to unity. The non-trivial Kähler moduli are the “angular” directions in the Kähler cone, and we consider the two different rays  $\mathbb{Q} \cdot (2, 1, 1)$  and  $\mathbb{Q} \cdot (2, 2, 1)$ . As expected, the actual eigenvalues do depend on the Kähler moduli, as is evident from Figure 15.

Furthermore, note that there appear to be no multiplicities in the spectrum. At first sight, this might be a surprise to the cognoscente, as there *is* a residual symmetry. By construction [42], the covering space  $\tilde{X}$  comes with a  $(\mathbb{Z}_3)^4$  group action of which only a  $\mathbb{Z}_3 \times \mathbb{Z}_3$  subgroup acts freely and can be divided out to obtain  $X$ . The remaining generators are

$$\gamma_3 : \begin{cases} [x_0 : x_1 : x_2] \mapsto [x_1 : x_2 : x_0] \\ [t_0 : t_1] \mapsto [t_0 : t_1] \\ [y_0 : y_1 : y_2] \mapsto [y_0 : y_1 : y_2] \end{cases} \quad (126a)$$

and

$$\gamma_4 : \begin{cases} [x_0 : x_1 : x_2] \mapsto [x_0 : x_1 : x_2] \\ [t_0 : t_1] \mapsto [t_0 : t_1] \\ [y_0 : y_1 : y_2] \mapsto [y_1 : y_2 : y_0] \end{cases} \quad (126b)$$

in addition to  $\gamma_1$  and  $\gamma_2$ , see eqns. (116a) and (116b). Moreover, we used the point  $\lambda_1 = 0 = \lambda_2$ ,  $\lambda_3 = 1$  where the polynomials eq. (115) are also invariant under complex conjugation. Hence, the symmetry group on the covering space is

$$\overline{\text{Aut}}(\tilde{X}) = \mathbb{Z}_2 \times (\mathbb{Z}_3)^4 = D_6 \times (\mathbb{Z}_3)^3. \quad (127)$$

To understand the latter identity, note the  $\mathbb{Z}_2$  action in the semidirect product:

- Complex conjugation commutes with  $\gamma_2$ ,  $\gamma_3$ , and  $\gamma_4$ .
- Complex conjugation does not commute with  $\gamma_1$ , but satisfies

$$\gamma_1 \left( [\bar{x}_0 : \bar{x}_1 : \bar{x}_2], [\bar{t}_0 : \bar{t}_1], [\bar{y}_0, \bar{y}_1, \bar{y}_2] \right) = \overline{\gamma_1^2 \left( [x_0 : x_1 : x_2], [t_0 : t_1], [y_0, y_1, y_2] \right)}. \quad (128)$$

Hence,  $\gamma_1$  together with complex conjugation generate  $D_6$ , the dihedral group with 6 elements.

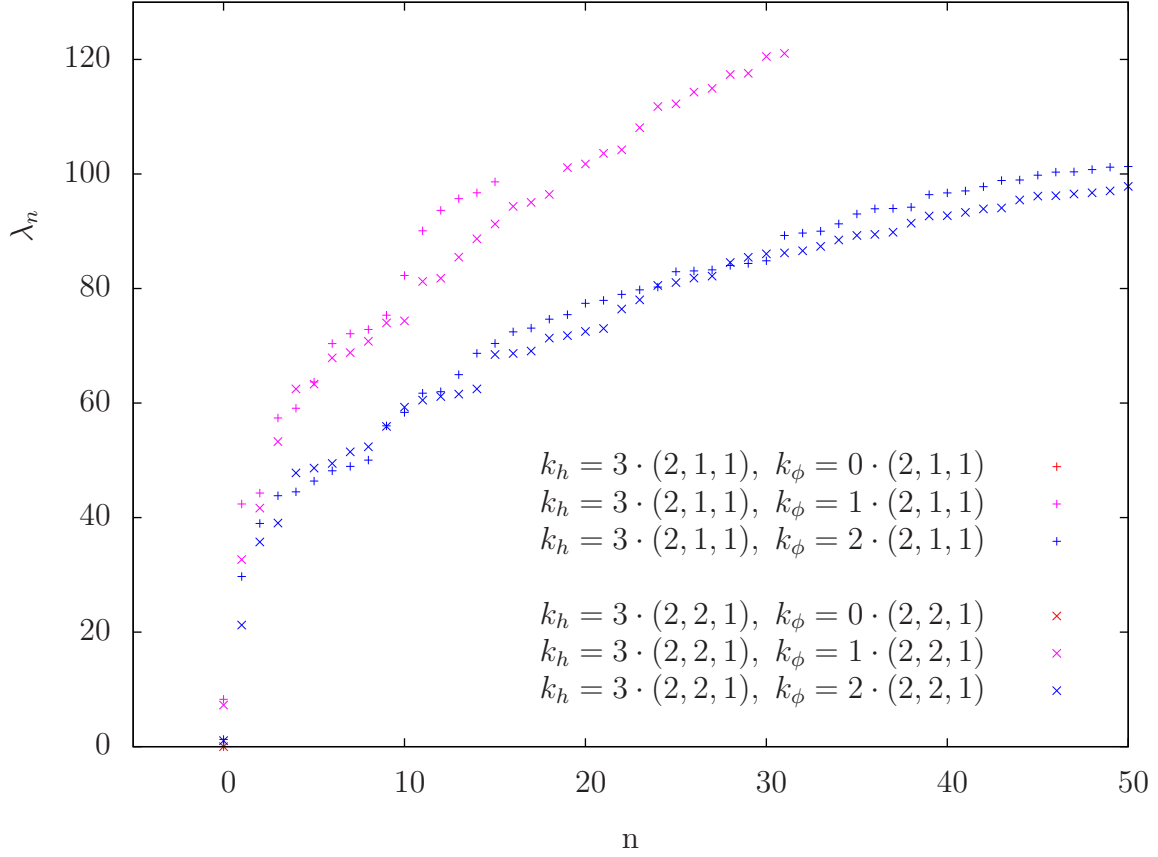


**Figure 15:** Eigenvalues of the scalar Laplace operator on the  $\mathbb{Z}_3 \times \mathbb{Z}_3$ -threefold  $X$  with complex structure  $\lambda_1 = 0 = \lambda_2$ ,  $\lambda_3 = 1$  and at two distinct points in the Kähler moduli space. The metric is computed at degree  $k_h = (6, 3, 3)$  and  $n_h = 170,560$  points as well as degree  $k_h = (6, 6, 3)$  and  $n_h = 290,440$  points, corresponding to the two different Kähler moduli. The matrix elements of the scalar Laplacian are always evaluated on  $n_\phi = 500,000$  points. The blue pluses and crosses, corresponding in each case to  $k_\phi$  with the largest radial distance, are the highest precision eigenvalues for the two metrics.

$\overline{\text{Aut}}(\tilde{X})$ -Rep.	$\rho_1, \dots, \rho_{36}$	$\rho_{37}, \dots, \rho_{54}$	$\rho_{55}, \dots, \rho_{81}$
$\dim(\rho)$	1	1	2
$\dim(\rho^{\mathbb{Z}_3 \times \mathbb{Z}_3})$	0	1	0

**Table 9:** Number  $n_d$  of distinct irreducible representations of  $\overline{\text{Aut}}(\tilde{X})$  in complex dimension  $d$ . We also list the dimension  $\dim_d^{\mathbb{Z}_3 \times \mathbb{Z}_3}$  of the  $\mathbb{Z}_3 \times \mathbb{Z}_3$ -invariant subspace for each representation.

The group  $\overline{\text{Aut}}(\tilde{X})$  is of order  $162 = 6 \times 3^3$  and has one- and two-dimensional representations due to the  $D_6$  factor. As discussed previously, the surviving eigenfunctions on the quotient  $X$  are the  $\mathbb{Z}_3 \times \mathbb{Z}_3$ -invariant eigenfunctions on the covering space  $\tilde{X}$ . Hence, we have to determine the subspace invariant under the freely acting  $\mathbb{Z}_3 \times \mathbb{Z}_3$  inside of  $\overline{\text{Aut}}(\tilde{X})$ . We list all this data in Table 9. We find that all the multiplicities on  $\tilde{X}$  are, indeed, one.

## 7 The Sound of Space-Time

### 7.1 Kaluza-Klein Modes of the Graviton

Consider a 10-dimensional spacetime of the form  $\mathbb{R}^{3,1} \times Y$ , where  $Y$  is some real, compact 6-dimensional Calabi-Yau manifold. Since  $Y$  is compact, there is a scale associated with it. Let us agree on a unit of length  $L$  such that  $\text{Vol}(Y) = 1 \cdot L^6$ . The gravitational interactions in this world are complicated, but have two easy limiting cases. First, if the separation  $r$  of two probe masses  $M_1$  and  $M_2$  is large, then the gravitational potential between them is given by Newton's law

$$V(r \gg L) = -G_4 \frac{M_1 M_2}{r}. \quad (129)$$

In the other extreme, when  $r$  is very small, the potential becomes the Green-Schwarz-Witten law

$$V(r \ll L) = -G_{10} \frac{M_1 M_2}{r^7}. \quad (130)$$

By dimensional analysis

$$G_4 \sim \frac{G_{10}}{L^6}, \quad (131)$$

with a constant of proportionality independent of  $Y$  to be determined below. In-between these two extremal limits for the separation  $r$ , the gravitational potential is a complicated interpolation between eq. (129) and eq. (130).

There are two alternative ways of describing fields on  $\mathbb{R}^{3,1} \times Y$ . One can either directly use 10-dimensional field theory, or work with an infinite tower of massive Kaluza-Klein fields depending on  $\mathbb{R}^{3,1}$  only. Both methods are equivalent, but for the purposes of this paper we only consider the Kaluza-Klein compactification [51, 52, 53]. In this approach, the single 10-dimensional massless graviton  $g_{AB}^{(10D)}$ ,  $A, B = 0, \dots, 9$  is decomposed into 4-dimensional gravitons, vectors, and scalars. For simplicity, let us only consider 4-dimensional gravity, that is, 4-d fields with symmetrized indices  $a, b = 0, \dots, 3$ . Then

$$g_{ab}^{(10D)}(x_0, \dots, x_3, y_1, \dots, y_6) = \sum_{n=0}^{\infty} \phi_n(y_1, \dots, y_6) \cdot g_{ab}^{(4D),n}(x_0, \dots, x_3), \quad (132)$$

where the  $(y_1, \dots, y_6) \in Y$ -dependence of the 10-dimensional metric is now encoded in a basis of functions  $\phi_n \in \mathbb{C}^\infty(Y, \mathbb{R})$ . The most useful such basis consists of the solutions to the equations of motion on  $Y$ , that is, the eigenfunctions of the scalar Laplace operator

$$\Delta_Y \phi_n(y_1, \dots, y_6) = \lambda_n \phi_n(y_1, \dots, y_6), \quad \lambda_n \leq \lambda_{n+1}. \quad (133)$$

The corresponding 4-dimensional Lagrangian contains the infinite tower of fields  $g_{ab}^{(4D),n}$  of mass

$$m_n = \sqrt{\lambda_n}, \quad n = 0, \dots, \infty. \quad (134)$$

As discussed previously, there is a unique zero mode  $\lambda_0 = 0$  leading to a single massless graviton in 4 dimensions. The gravitational potential is then the sum of the potential due to the massless graviton plus the Yukawa-interaction of the massive modes,

$$V(r) = -G_4 \frac{M_1 M_2}{r} \sum_{n=0}^{\infty} e^{-m_n r} = -G_4 \frac{M_1 M_2}{r} \left( 1 + \sum_{n=1}^{\infty} e^{-m_n r} \right). \quad (135)$$

At distance scales  $r \gg \frac{1}{m_1}$ , only the massless graviton propagates. This expected behaviour is clearly visible in the  $r \gg \frac{1}{m_1}$  limit of eq. (135), and one immediately recovers eq. (129). At distance scales  $r \ll \frac{1}{m_1}$ , on the other hand, the massless graviton as well as the infinite tower of massive spin-2 fields propagate. The corresponding asymptotic behaviour of the gravitational potential is less obvious. However, note that the asymptotic growth

$$\lim_{n \rightarrow \infty} \frac{\lambda_n^3}{n} = 384\pi^3 L^{-6} \quad \Leftrightarrow \quad m_n \xrightarrow{n \rightarrow \infty} 2\sqrt[6]{6}\sqrt{\pi} n^{1/6} L^{-1} \quad (136)$$

of the Kaluza-Klein masses is known from Weyl's formula, see Subsection 3.3. Hence, the  $r \ll \frac{1}{m_1}$  limit of eq. (135) is

$$\begin{aligned} V(r) &= -G_4 \frac{M_1 M_2}{r} \sum_{n=0}^{\infty} e^{-m_n r} \\ &\longrightarrow \sim -G_4 \frac{M_1 M_2}{r} \int_{n=0}^{\infty} e^{-2\sqrt[6]{6}\sqrt{\pi} n^{1/6} r/L} dn = -\underbrace{\frac{15G_4 L^6}{8\pi^3}}_{=G_{10}} \frac{M_1 M_2}{r^7}. \end{aligned} \quad (137)$$

Again, this matches the expected behaviour eq. (130).

The purpose of this section is to fill the gap between the extremal limits and determine the gravitational potential at distances  $r \simeq L$ . This explicitly depends on the details of the internal Calabi-Yau threefold  $Y$ , and there is no way around solving eq. (133). The eigenvalues  $\lambda_n$  and corresponding eigenfunctions  $\phi_n$  depend on the Calabi-Yau metric and can only be computed numerically. We have presented



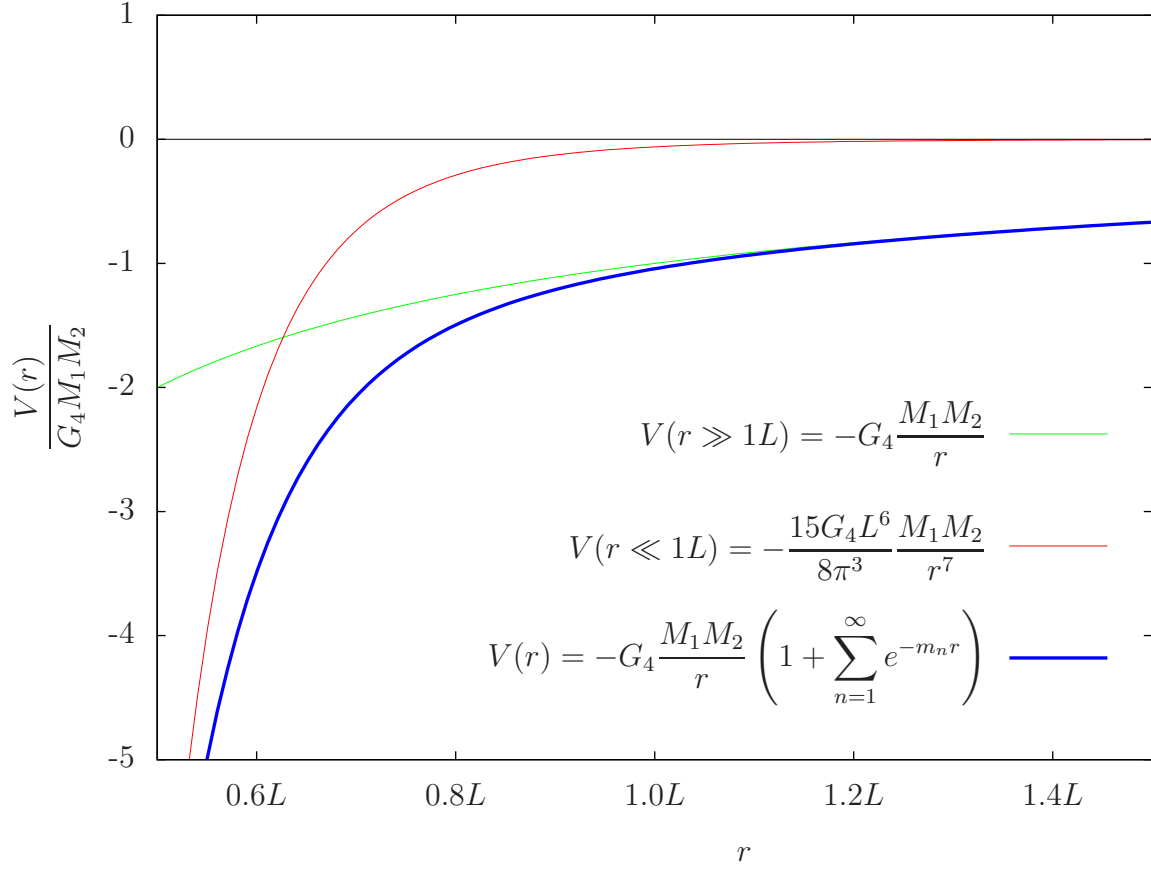


**Figure 16:** The gravitational potential  $V(r)$  computed from eq. (135) on  $\mathbb{R}^{3,1} \times \tilde{Q}_F$ , where  $\tilde{Q}_F$  is the Fermat quintic with unit volume,  $\text{Vol}(\tilde{Q}_F) = 1 \cdot L^6$ . The Kaluza-Klein masses  $m_n = \sqrt{\lambda_n}$  are computed using the numerical results for  $\lambda_n$  given in Subsection 4.2.

a detailed algorithm for calculating the spectrum of  $\Delta$  in this paper, and given the results for a number of different Calabi-Yau threefolds. As an example, let us compute the gravitational potential  $V(r)$  derived from the numerical eigenvalues of the scalar Laplace operator on the Fermat quintic discussed in Subsection 4.2. The result is plotted in Figure 16.

## 7.2 Spectral Gap

As is evident from Figure 16, deviations from the pure  $\frac{1}{r}$  (green line) and  $\frac{1}{r^7}$  (red line) potentials occur for  $r$  in the region where these gravitational potentials have a similar magnitude. In fact, these curves intersect at

$$G_4 \frac{M_1 M_2}{r_0} = \frac{15 G_4 L^6}{8 \pi^3} \frac{M_1 M_2}{r_0^7} \Leftrightarrow r_0 = \sqrt[6]{\frac{15}{8 \pi^3}} L \approx 0.627 L. \quad (138)$$

Note that this point of intersection is independent of the Calabi-Yau manifold and its geometry. As will become clear below, for Calabi-Yau threefolds which are relatively “round”, such as the Fermat quintic,  $r_0$  is a good estimate for the point of substantial deviation from the  $\frac{1}{r}$  potential. However, for geometries that are stretched or develop a throat in at least one direction, this deviation point is best determined by another scale, in principle independent of the volume of the internal space. This other scale is the mass  $m_1$  of the lightest Kaluza-Klein mode<sup>21</sup>, see eq. (135). For such manifolds, the spectral gap<sup>22</sup>  $\lambda_1$  and, hence, the mass  $m_1$  becomes smaller. Eventually, the manifold may be sufficiently elongated that  $\frac{1}{m_1} \gg r_0$ . In this case  $\frac{1}{m_1}$  becomes the best estimate of the point of deviation from the  $\frac{1}{r}$  potential.

Of course, both the volume and  $\lambda_1 = m_1^2$  are determined by the geometry of the internal Calabi-Yau manifold. However, what geometric property really determines

---

<sup>21</sup>The leading order correction to the gravitational potential is often [54, 49] parametrized by the lowest Kaluza-Klein mass  $m_1$  and its multiplicity  $\mu_1$  as

$$V(r) \approx -G_4 \frac{M_1 M_2}{r} (1 + \mu_1 e^{-m_1 r}). \quad (139)$$

While this works well for symmetric spaces like spheres and tori with their large multiplicities and widely-separated eigenvalues, there are two issues when dealing with more general manifolds:

- The multiplicity is caused by symmetries, and tiny non-symmetric deformations can (and will) make the eigenvalues non-degenerate (see Section 5).
- The separation between the zero mode and the first massive mode is, in general, much larger than the separation between the first and second mode. For example, on the non-symmetric “random quintic” Calabi-Yau threefold in Subsection 4.1,

$$m_0 = 0, \quad m_1 \approx 5.95, \quad m_2 \approx 6.00. \quad (140)$$

<sup>22</sup>The first massive eigenvalue of the scalar Laplacian,  $\lambda_1$ , is also called the spectral gap since it is the gap between the unique zero mode  $\lambda_0 = 0$  and the first massive mode.

the spectral gap  $\lambda_1$ ? In fact, this is determined by the “diameter” of the manifold. Recall that the diameter  $D$  is defined to be the largest separation of any two points, as measured by the shortest geodesic between them. Then, on an arbitrary real  $d$ -dimensional manifold with non-negative scalar curvature<sup>23</sup>, the spectral gap is essentially determined by the diameter via [55, 56, 57]

$$\frac{\pi^2}{D^2} \leq \lambda_1 \leq \frac{2d(d+4)}{D^2} \quad \Leftrightarrow \quad \frac{\pi}{D} \leq m_1 \leq \frac{\sqrt{2d(d+4)}}{D}. \quad (141)$$

Clearly, in a compactification where all internal directions are essentially of equal size, the diameter is of the order of  $1 \cdot L$ . However, as soon as there is even one elongated internal direction or one long throat/spike develops, the diameter can be very large. Hence, the spectral gap becomes very small and deviations from  $\frac{1}{r}$  gravity appear for relatively large values of  $r \sim \frac{1}{m_1}$ .

The definition of the diameter  $D$  is very impractical if one wants to explicitly calculate it, since this would require global knowledge about the shortest geodesics. However, to get a rough estimate of  $D$ , one can reverse the inequalities eq. (141) and then use the numerically computed value for  $\lambda_1$ . For example, on the Fermat quintic our numerical computation in Subsection 4.3 yielded  $\lambda_1 \approx 41.1$ . Therefore, the diameter must be in the range

$$0.490 \approx \frac{\pi}{\sqrt{\lambda_1}} \leq D \leq \frac{\sqrt{2 \cdot 6(6+4)}}{\sqrt{\lambda_1}} \approx 1.71. \quad (142)$$

Thus, computing the value of  $\lambda_1$  numerically on a Calabi-Yau threefold for specific values of its moduli gives us direct information about the “shape” of the manifold; information that would be hard to obtain by direct calculation of the diameter  $D$ . For example, it follows from eq. (142) that the Fermat quintic is relatively “round”.

## Acknowledgments

We are grateful to Evelyn Thomson for letting us use her 10 node dual-core Opteron cluster. This research was supported in part at Rutgers by the U. S. Department of Energy grant DE-FG02-96ER40959, and by the Department of Physics and the Math/Physics Research Group at the University of Pennsylvania under cooperative research agreement DE-FG02-95ER40893 with the U. S. Department of Energy, and an NSF Focused Research Grant DMS0139799 for “The Geometry of Superstrings”.

## A Spectrum of the Laplacian on Projective Space

In this Appendix, we compute the lowest eigenvalue of the Laplace operator on  $\mathbb{P}^3$  using the rescaled Fubini-Study Kähler potential eq. (16). To do this, go to the

---

<sup>23</sup>In particular, a Calabi-Yau  $\frac{d}{2}$ -fold.

coordinate patch where  $z_0 = 1$  and use  $z_1, z_2, z_3$  as local coordinates. We find that

$$g^{\bar{i}j} = \sqrt[3]{6}\pi(1 + |z_1|^2 + |z_2|^2 + |z_3|^2) \begin{pmatrix} 1 + |z_1|^2 & z_2\bar{z}_1 & z_3\bar{z}_1 \\ z_1\bar{z}_2 & 1 + |z_2|^2 & z_3\bar{z}_2 \\ z_1\bar{z}_3 & z_2\bar{z}_3 & 1 + |z_3|^2 \end{pmatrix}, \quad (143)$$

$$\det(g_{i\bar{j}}) = \frac{6}{(1 + |z_1|^2 + |z_2|^2 + |z_3|^2)^4 \pi^3}$$

and, hence,

$$\Delta = 2 \frac{1}{\det(g)} \left( \bar{\partial}_i g^{\bar{i}j} \det(g) \partial_i + \partial_j g^{\bar{i}j} \det(g) \bar{\partial}_j \right). \quad (144)$$

One can now compute the eigenvalue corresponding to the eigenfunction  $\phi_{1,1}$  in eq. (27). We find that

$$\begin{aligned} \Delta \phi_{1,1} &= 2 \frac{1}{\det(g)} \left( \bar{\partial}_i g^{\bar{i}j} \det(g) \partial_i + \partial_j g^{\bar{i}j} \det(g) \bar{\partial}_j \right) \frac{\bar{z}_1}{1 + |z_1|^2 + |z_2|^2 + |z_3|^2} \\ &= \left( \frac{16\pi}{\sqrt[3]{6}} \right) \frac{\bar{z}_1}{1 + |z_1|^2 + |z_2|^2 + |z_3|^2}. \end{aligned} \quad (145)$$

Hence,  $\phi_{1,1}$  is indeed an eigenfunction of  $\Delta$  with eigenvalue

$$\lambda_1 = \frac{16\pi}{\sqrt[3]{6}} = \frac{4\pi}{\sqrt[3]{6}} \cdot 1 \cdot (1 + 3). \quad (146)$$

Hence, the numerical coefficient in eq. (18) is indeed the correct one for our volume normalization  $\text{Vol}_K(\mathbb{P}^3) = 1$ .

## B Semidirect Products

Let  $G$  and  $N$  be two groups, and let

$$\psi : G \rightarrow \text{Aut}(N) \quad (147)$$

be a map from  $G$  to the automorphisms of  $N$ . The semi-direct product

$$G \rtimes_{\psi} N = \left\{ (n, g) \mid n \in N, g \in G \right\} \quad (148)$$

is defined to be the group consisting of pairs  $(n, g)$  with the group action

$$(n_1, g_1) \cdot (n_2, g_2) = (n_1 \cdot \psi(g_1)(n_2), g_1 \cdot g_2). \quad (149)$$

Usually, one just writes  $G \rtimes N$  with the map  $\psi$  implied but not explicitly named. Note that  $G$  is a subgroup and  $N$  is a normal subgroup of the semidirect product.

For example, consider the semidirect product with  $G = S_5$  and  $N = (\mathbb{Z}_5)^4$  used in Subsection 4.3. These two groups are acting on five homogeneous via permutations<sup>24</sup> and phase rotations

$$\left( (n_1, n_2, n_3, n_4), [z_0, z_1, z_2, z_3, z_4] \right) \mapsto \left[ z_0, z_1 e^{\frac{2\pi i n_1}{5}}, z_2 e^{\frac{2\pi i n_2}{5}}, z_3 e^{\frac{2\pi i n_3}{5}}, z_4 e^{\frac{2\pi i n_4}{5}} \right], \quad (150)$$

respectively. The two group actions do not commute, and, therefore, the total symmetry group is not simply the product  $S_5 \times (\mathbb{Z}_5)^4$ . The “non-commutativity” between  $S_5$  and  $(\mathbb{Z}_5)^4$  is encoded in a map

$$\psi : S_5 \rightarrow \text{Aut} \left( (\mathbb{Z}_5)^4 \right), \quad \sigma \mapsto \left( \vec{n} \mapsto \sigma^{-1} \circ \vec{n} \circ \sigma \right). \quad (151)$$

To be completely explicit, note that the permutation group  $S_5$  is generated by the cyclic permutation  $c$  and a transposition  $t$ , acting as

$$\begin{aligned} t : [z_0, z_1, z_2, z_3, z_4] &\mapsto [z_0, z_1, z_2, z_4, z_3], \\ c : [z_0, z_1, z_2, z_3, z_4] &\mapsto [z_1, z_2, z_3, z_4, z_0]. \end{aligned} \quad (152)$$

The generators  $\langle c, t \rangle = S_5$  act, via  $\psi$ , on  $(\mathbb{Z}_5)^4$  as

$$\begin{aligned} \psi(t) : (\mathbb{Z}_5)^4 &\rightarrow (\mathbb{Z}_5)^4, & (n_1, n_2, n_3, n_4) &\mapsto (n_1, n_2, n_4, n_3) \\ \psi(c) : (\mathbb{Z}_5)^4 &\rightarrow (\mathbb{Z}_5)^4, & (n_1, n_2, n_3, n_4) &\mapsto (-n_4, n_1 - n_4, n_2 - n_4, n_3 - n_4) \end{aligned} \quad (153)$$

It is straightforward, if tedious, to show that  $\psi$  is a group homomorphism and that the total symmetry group generated by  $S_5$  and  $(\mathbb{Z}_5)^4$  is, in fact, the semidirect product

$$S_5 \psi \ltimes (\mathbb{Z}_5)^4. \quad (154)$$

By the usual abuse of notation, we always drop the subscript  $\psi$  in the main part of this paper.

## C Notes on Donaldson’s Algorithm on Quotients

For explicitness, let us consider the same setup as in Subsection 5.1, that is,  $\tilde{Q} \subset \mathbb{P}^4$  is a  $\mathbb{Z}_5 \times \mathbb{Z}_5$  symmetric quintic and we want to compute the metric on the quotient  $Q = \tilde{Q}/(\mathbb{Z}_5 \times \mathbb{Z}_5)$ . To fix notation, let us denote the two generators for the character ring of the group by

$$\begin{aligned} \chi_1(g_1) &= e^{2\pi i/5}, & \chi_1(g_2) &= 1, \\ \chi_2(g_1) &= 1, & \chi_2(g_2) &= e^{2\pi i/5}. \end{aligned} \quad (155)$$

We consider homogeneous polynomials in degrees  $k_h \in 5\mathbb{Z}$ , so there is a linear  $\mathbb{Z}_5 \times \mathbb{Z}_5$  group action. In eq. (82) we determined the invariant polynomials. Now, let us

---

<sup>24</sup> $S_5$  is, by definition, the group of permutations of five objects.

slightly generalize this result and determine “covariant polynomials” transforming as some character  $\chi$  of the group,

$$p \circ g(z) = \chi(g)p(z) \quad g \in \mathbb{Z}_5 \times \mathbb{Z}_5. \quad (156)$$

These again form a linear space of  $\chi$ -covariant polynomials, which we denote as

$$\mathbb{C}[z_0, z_1, z_2, z_3, z_4]_{k_h}^\chi = \left\{ p(z) \mid p \circ g(z) = \chi(g)p(z) \right\}. \quad (157)$$

Note that the covariant polynomials do not form a ring, but rather a module over the invariant ring. Nevertheless, by a slight generalization of the Hironaka decomposition, we can express the covariants as a direct sum

$$\mathbb{C}[z_0, z_1, z_2, z_3, z_4]_{k_h}^\chi = \bigoplus_{i=1}^{100} \eta_i^\chi \mathbb{C}[\theta_1, \theta_2, \theta_3, \theta_4, \theta_5]_{k_h - \deg(\eta_i^\chi)}, \quad (158)$$

where the  $\theta_1, \dots, \theta_5 \in \mathbb{C}[z_0, z_1, z_2, z_3, z_4]^{\mathbb{Z}_5 \times \mathbb{Z}_5}$  can be taken to be the primary invariants of the original Hironaka decomposition eq. (82) and the “secondary covariants”  $\eta_1^\chi, \dots, \eta_{100}^\chi$  are certain  $\chi$ -covariant polynomials that need to be computed [58]. For example, we find

$$\begin{aligned} \eta_1^{\chi_1} &= z_0^4 z_1 + z_1^4 z_2 + z_2^4 z_3 + z_3^4 z_4 + z_4^4 z_0, \\ \eta_2^{\chi_1} &= z_0 z_1^3 z_3 + z_1 z_2^3 z_4 + z_2 z_3^3 z_0 + z_3 z_4^3 z_1 + z_4 z_0^3 z_2, \dots \end{aligned} \quad (159)$$

and

$$\begin{aligned} \eta_1^{\chi_2} &= z_0^5 + e^{\frac{2\pi i}{5}} z_1^5 + e^{\frac{2 \cdot 2\pi i}{5}} z_2^5 + e^{\frac{3 \cdot 2\pi i}{5}} z_3^5 + e^{\frac{4 \cdot 2\pi i}{5}} z_4^5, \\ \eta_2^{\chi_2} &= z_0 z_1^3 z_2 + e^{\frac{2\pi i}{5}} z_1 z_2^3 z_3 + e^{\frac{2 \cdot 2\pi i}{5}} z_2 z_3^3 z_4 + e^{\frac{3 \cdot 2\pi i}{5}} z_3 z_4^3 z_0 + e^{\frac{4 \cdot 2\pi i}{5}} z_4 z_0^3 z_1, \dots \end{aligned} \quad (160)$$

Note that we always take the defining quintic polynomial  $\tilde{Q}(z)$  to be completely<sup>25</sup> invariant, see eq. (76). Restricting everything to the hypersurface  $\tilde{Q}(z) = 0$ , we get homogeneous polynomials on the Calabi-Yau threefold. We pick bases  $\{s_\alpha^\chi\}$  for the  $\chi$ -covariant polynomials, that is,

$$\begin{aligned} \chi = 1 : \quad & \text{span} \{s_\alpha^1\} = \mathbb{C}[z_0, z_1, z_2, z_3, z_4]_{k_h}^{\mathbb{Z}_5 \times \mathbb{Z}_5} / \langle \tilde{Q}(z) \rangle, \\ \chi \neq 1 : \quad & \text{span} \{s_\alpha^\chi\} = \left( \mathbb{C}[z_0, z_1, z_2, z_3, z_4]_{k_h} / \langle \tilde{Q}(z) \rangle \right)^\chi \\ & = \mathbb{C}[z_0, z_1, z_2, z_3, z_4]_{k_h}^\chi. \end{aligned} \quad (161)$$

---

<sup>25</sup>If  $\tilde{Q}(z)$  were a  $\chi$ -covariant polynomial, it would still define a  $\mathbb{Z}_5 \times \mathbb{Z}_5$  invariant Calabi-Yau hypersurface. Everything in this paper would generalize straightforwardly, so we ignore this possibility to simplify notation.

We now turn towards computing the metric on the quotient  $Q$  or, equivalently, computing the  $\mathbb{Z}_5 \times \mathbb{Z}_5$ -invariant metric on the covering space  $\tilde{Q}$  by a variant of Donaldson’s algorithm. For this, we pick the ansatz

$$K(z, \bar{z}) = \frac{1}{\pi} \sum_{\chi=\chi_1^0 \chi_2^0}^{\chi_1^4 \chi_2^4} \sum_{\alpha\bar{\beta}} h^{\chi\alpha\bar{\beta}} s_\alpha^\chi \bar{s}_\beta^{\bar{\chi}} \quad (162)$$

for the Calabi-Yau metric. One can think of  $h$  as a block-diagonal matrix with blocks labelled by the characters  $\chi$ . The  $T$ -operator is likewise block-diagonal, and therefore one obtains a balanced metric as the fixed point of the iteration

$$h_n^{\chi\alpha\bar{\beta}} \longrightarrow h_{n+1}^{\chi\alpha\bar{\beta}} = T(h_n^{\chi\alpha\bar{\beta}})^{-1}. \quad (163)$$

Note that this fixed point is the same<sup>26</sup> as what one would obtain from Donaldson’s algorithm on the covering space  $\tilde{Q}$  (without using any symmetry). Only now the basis of sections is such that the impact of the  $\mathbb{Z}_5 \times \mathbb{Z}_5$  symmetry is clearly visible:  $h$  is block-diagonal with blocks labelled by the characters  $\chi$ .

As usual, the balanced metrics are better and better approximations to the Calabi-Yau metric as one increases the degree  $k_h$ . We find that this method of computing the Calabi-Yau metric on the quotient  $Q$  is the most effective.

## Bibliography

- [1] P. Candelas, G. T. Horowitz, A. Strominger, and E. Witten, “Vacuum Configurations for Superstrings,” *Nucl. Phys.* **B258** (1985) 46–74.
- [2] A. Lukas, B. A. Ovrut, and D. Waldram, “On the four-dimensional effective action of strongly coupled heterotic string theory,” *Nucl. Phys.* **B532** (1998) 43–82, [hep-th/9710208](#).
- [3] R. Donagi, A. Lukas, B. A. Ovrut, and D. Waldram, “Non-perturbative vacua and particle physics in M-theory,” *JHEP* **05** (1999) 018, [hep-th/9811168](#).
- [4] A. Lukas, B. A. Ovrut, and D. Waldram, “Non-standard embedding and five-branes in heterotic M- theory,” *Phys. Rev.* **D59** (1999) 106005, [hep-th/9808101](#).
- [5] A. Lukas, B. A. Ovrut, K. S. Stelle, and D. Waldram, “The universe as a domain wall,” *Phys. Rev.* **D59** (1999) 086001, [hep-th/9803235](#).

---

<sup>26</sup>And different from the fixed point where one restricts to only the invariant sections. The latter is just the  $\chi = 1$  block.

- [6] A. Lukas, B. A. Ovrut, and D. Waldram, “The ten-dimensional effective action of strongly coupled heterotic string theory,” *Nucl. Phys.* **B540** (1999) 230–246, [hep-th/9801087](#).
- [7] R. Donagi, A. Lukas, B. A. Ovrut, and D. Waldram, “Holomorphic vector bundles and non-perturbative vacua in M- theory,” *JHEP* **06** (1999) 034, [hep-th/9901009](#).
- [8] R. Donagi, B. A. Ovrut, and D. Waldram, “Moduli spaces of fivebranes on elliptic Calabi-Yau threefolds,” *JHEP* **11** (1999) 030, [hep-th/9904054](#).
- [9] R. Donagi, B. A. Ovrut, T. Pantev, and D. Waldram, “Standard models from heterotic M-theory,” *Adv. Theor. Math. Phys.* **5** (2002) 93–137, [hep-th/9912208](#).
- [10] R. Donagi, B. A. Ovrut, T. Pantev, and D. Waldram, “Standard-model bundles,” *Adv. Theor. Math. Phys.* **5** (2002) 563–615, [math/0008010](#).
- [11] E. I. Buchbinder, R. Donagi, and B. A. Ovrut, “Vector bundle moduli superpotentials in heterotic superstrings and M-theory,” *JHEP* **07** (2002) 066, [hep-th/0206203](#).
- [12] R. Donagi, B. A. Ovrut, T. Pantev, and D. Waldram, “Standard-model bundles on non-simply connected Calabi-Yau threefolds,” *JHEP* **08** (2001) 053, [hep-th/0008008](#).
- [13] R. Donagi, B. A. Ovrut, T. Pantev, and D. Waldram, “Spectral involutions on rational elliptic surfaces,” *Adv. Theor. Math. Phys.* **5** (2002) 499–561, [math/0008011](#).
- [14] B. A. Ovrut, T. Pantev, and R. Reinbacher, “Invariant homology on standard model manifolds,” *JHEP* **01** (2004) 059, [hep-th/0303020](#).
- [15] R. Donagi, Y.-H. He, B. A. Ovrut, and R. Reinbacher, “The particle spectrum of heterotic compactifications,” *JHEP* **12** (2004) 054, [hep-th/0405014](#).
- [16] R. Donagi, Y.-H. He, B. A. Ovrut, and R. Reinbacher, “Moduli dependent spectra of heterotic compactifications,” *Phys. Lett.* **B598** (2004) 279–284, [hep-th/0403291](#).
- [17] R. Donagi, Y.-H. He, B. A. Ovrut, and R. Reinbacher, “The spectra of heterotic standard model vacua,” *JHEP* **06** (2005) 070, [hep-th/0411156](#).
- [18] R. Donagi, Y.-H. He, B. A. Ovrut, and R. Reinbacher, “Higgs doublets, split multiplets and heterotic  $SU(3)_C \times SU(2)_L \times U(1)_Y$  spectra,” *Phys. Lett.* **B618** (2005) 259–264, [hep-th/0409291](#).



- [19] V. Braun, Y.-H. He, B. A. Ovrut, and T. Pantev, “Heterotic standard model moduli,” *JHEP* **01** (2006) 025, [hep-th/0509051](#).
- [20] V. Bouchard and R. Donagi, “An SU(5) heterotic standard model,” *Phys. Lett.* **B633** (2006) 783–791, [hep-th/0512149](#).
- [21] V. Braun, Y.-H. He, B. A. Ovrut, and T. Pantev, “A standard model from the E(8) x E(8) heterotic superstring,” *JHEP* **06** (2005) 039, [hep-th/0502155](#).
- [22] V. Braun, Y.-H. He, B. A. Ovrut, and T. Pantev, “The exact MSSM spectrum from string theory,” *JHEP* **05** (2006) 043, [hep-th/0512177](#).
- [23] V. Braun, Y.-H. He, B. A. Ovrut, and T. Pantev, “A heterotic standard model,” *Phys. Lett.* **B618** (2005) 252–258, [hep-th/0501070](#).
- [24] P. Candelas and S. Kalara, “Yukawa couplings for a three generation superstring compactification,” *Nucl. Phys.* **B298** (1988) 357.
- [25] V. Braun, Y.-H. He, and B. A. Ovrut, “Yukawa couplings in heterotic standard models,” *JHEP* **04** (2006) 019, [hep-th/0601204](#).
- [26] V. Braun, Y.-H. He, B. A. Ovrut, and T. Pantev, “Moduli dependent mu-terms in a heterotic standard model,” *JHEP* **03** (2006) 006, [hep-th/0510142](#).
- [27] V. Bouchard, M. Cvetič, and R. Donagi, “Tri-linear couplings in an heterotic minimal supersymmetric standard model,” [hep-th/0602096](#).
- [28] P. Candelas, X. C. De La Ossa, P. S. Green, and L. Parkes, “A pair of Calabi-Yau manifolds as an exactly soluble superconformal theory,” *Nucl. Phys.* **B359** (1991) 21–74.
- [29] B. R. Greene, D. R. Morrison, and M. R. Plesser, “Mirror manifolds in higher dimension,” *Commun. Math. Phys.* **173** (1995) 559–598, [hep-th/9402119](#).
- [30] R. Donagi, R. Reinbacher, and S.-T. Yau, “Yukawa couplings on quintic threefolds,” [hep-th/0605203](#).
- [31] S. K. Donaldson, “Some numerical results in complex differential geometry,” [math.DG/0512625](#).
- [32] M. R. Douglas, R. L. Karp, S. Lukic, and R. Reinbacher, “Numerical solution to the hermitian Yang-Mills equation on the Fermat quintic,” [hep-th/0606261](#).
- [33] M. R. Douglas, R. L. Karp, S. Lukic, and R. Reinbacher, “Numerical Calabi-Yau metrics,” [hep-th/0612075](#).

- [34] S. K. Donaldson, “Scalar curvature and projective embeddings. II,” *Q. J. Math.* **56** (2005), no. 3, 345–356.
- [35] G. Tian, “On a set of polarized Kähler metrics on algebraic manifolds,” *J. Differential Geom.* **32** (1990), no. 1, 99–130.
- [36] M. Headrick and T. Wiseman, “Numerical Ricci-flat metrics on K3,” *Class. Quant. Grav.* **22** (2005) 4931–4960, [hep-th/0506129](#).
- [37] C. Doran, M. Headrick, C. P. Herzog, J. Kantor, and T. Wiseman, “Numerical Kaehler-Einstein metric on the third del Pezzo,” [hep-th/0703057](#).
- [38] X. Wang, “Canonical metrics on stable vector bundles,” *Comm. Anal. Geom.* **13** (2005), no. 2, 253–285.
- [39] B. Sturmfels, *Algorithms in invariant theory*. Texts and Monographs in Symbolic Computation. Springer-Verlag, Vienna, 1993.
- [40] V. Braun, T. Brelidze, M. R. Douglas, and B. A. Ovrut, “Calabi-Yau Metrics for Quotients and Complete Intersections,” [arXiv:0712.3563 \[hep-th\]](#).
- [41] M. B. Green, J. H. Schwarz, and E. Witten, “Superstring Theory. Vol. 2: Loop Amplitudes, Anomalies and Phenomenology,”. Cambridge, Uk: Univ. Pr. (1987) 596 P. (Cambridge Monographs On Mathematical Physics).
- [42] V. Braun, B. A. Ovrut, T. Pantev, and R. Reinbacher, “Elliptic Calabi-Yau threefolds with  $Z(3) \times Z(3)$  Wilson lines,” *JHEP* **12** (2004) 062, [hep-th/0410055](#).
- [43] P. Candelas, X. de la Ossa, Y.-H. He, and B. Szendroi, “Triadophilia: A Special Corner in the Landscape,” [arXiv:0706.3134 \[hep-th\]](#).
- [44] C. Iuliu-Lazaroiu, D. McNamee, and C. Saemann, “Generalized Berezin quantization, Bergman metrics and fuzzy Laplacians,” [0804.4555](#).
- [45] A. Ikeda and Y. Taniguchi, “Spectra and eigenforms of the Laplacian on  $S^n$  and  $P^n(\mathbf{C})$ ,” *Osaka J. Math.* **15** (1978), no. 3, 515–546.
- [46] E. Gabriel, G. E. Fagg, G. Bosilca, T. Angskun, J. J. Dongarra, J. M. Squyres, V. Sahay, P. Kambadur, B. Barrett, A. Lumsdaine, R. H. Castain, D. J. Daniel, R. L. Graham, and T. S. Woodall, “Open MPI: Goals, Concept, and Design of a Next Generation MPI Implementation,” in *Proceedings, 11th European PVM/MPI Users’ Group Meeting*, pp. 97–104. Budapest, Hungary, September, 2004.

- [47] E. Anderson, Z. Bai, C. Bischof, S. Blackford, J. Demmel, J. Dongarra, J. Du Croz, A. Greenbaum, S. Hammarling, A. McKenney, and D. Sorensen, *LAPACK Users' Guide*. Society for Industrial and Applied Mathematics, Philadelphia, PA, third ed., 1999.
- [48] S. K. Donaldson, “Scalar curvature and projective embeddings. I,” *J. Differential Geom.* **59** (2001), no. 3, 479–522.
- [49] A. Kehagias and K. Sfetsos, “Deviations from the  $1/r^2$  Newton law due to extra dimensions,” *Phys. Lett.* **B472** (2000) 39–44, [hep-ph/9905417](#).
- [50] B. A. Ovrut, “A heterotic standard model,” *AIP Conf. Proc.* **805** (2006) 236–239.
- [51] T. Kaluza, “On the Problem of Unity in Physics,” *Sitzungsber. Preuss. Akad. Wiss. Berlin (Math. Phys. )* **1921** (1921) 966–972.
- [52] O. Klein, “Quantum theory and five-dimensional theory of relativity,” *Z. Phys.* **37** (1926) 895–906.
- [53] N. Arkani-Hamed, S. Dimopoulos, and G. R. Dvali, “Phenomenology, astrophysics and cosmology of theories with sub-millimeter dimensions and TeV scale quantum gravity,” *Phys. Rev.* **D59** (1999) 086004, [hep-ph/9807344](#).
- [54] F. Leblond, “Geometry of large extra dimensions versus graviton emission,” *Phys. Rev.* **D64** (2001) 045016, [hep-ph/0104273](#).
- [55] J. Q. Zhong and H. C. Yang, “On the estimate of the first eigenvalue of a compact Riemannian manifold,” *Sci. Sinica Ser. A* **27** (1984), no. 12, 1265–1273.
- [56] S. Y. Cheng, “Eigenvalue comparison theorems and its geometric applications,” *Math. Z.* **143** (1975), no. 3, 289–297.
- [57] M. Berger, *A panoramic view of Riemannian geometry*. Springer-Verlag, Berlin, 2003.
- [58] G.-M. Greuel, V. Levandovskyy, and H. Schönemann, “SINGULAR::PLURAL 2.1,” A Computer Algebra System for Noncommutative Polynomial Algebras, Centre for Computer Algebra, University of Kaiserslautern, 2003. <http://www.singular.uni-kl.de/plural>.